Nonfluoroscopic electromechanical mapping of the left ventricle

To Zoé, Sam and Ben

To Anneke

To my mother

And of course to you, papa

Nonfluoroscopic electromechanical mapping of the left ventricle

Evaluation of the technique as diagnostic tool and as guidance for novel therapeutic strategies

Zonder röntgendoorlichting in kaart brengen van de electromechanische eigenschappen van de linker kamer

Evaluatie van de techniek als diagnostisch middel
en als begeleiding van nieuwe therapeutische strategieën

PROEFSCHRIFT

Ter verkrijging van de graad van doctor
aan de Erasmus Universiteit Rotterdam
op gezag van de
Rector Magnificus
Prof. dr. ir. J.H. van Bemmel
en volgens besluit van het college voor promoties

De openbare verdediging zal plaats vinden op
woensdag 6 december 2000 om 15.45 uur

door

Glenn van Langenhove

geboren te Gent, België

Promotie commissie

Promotor:	Prof. dr. P.W. Serruys
Overige leden :	Prof. dr. A.J.J.C. Bogers Prof. dr. S. Ben-Haim Prof. dr. V. Legrand
Copromotor :	Dr. P. C. Smits

Financial support from the Netherlands Heart Foundation (NHS) for the publication of this thesis is gratefully acknowledged

ISBN: 90-73235-91-X

Contents

Introduction

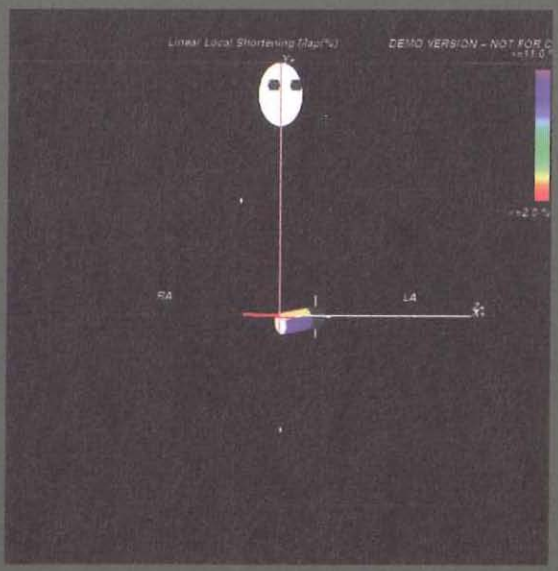

Introduction and outline of the thesis

With his landmark paper in Nature Medicine in 1996, Shlomo Ben-Haim and coworkers introduced a novel technique into the clinical arena.[1] Indeed, this initiated the possibility of on-line, real-time, in-cathlab 3-dimensional (3-D) assessment of the function of the left ventricle. Through a dedicated system they were able to exactly locate a catheter in 3-D space, to follow its excursions during ventricular contraction, and while making contact with the ventricular wall, also acquire electrical data. From the initial introduction of the technique, several investigators have shown its possibilities in assessing the quality of the human left ventricle, in evaluating possible recovery of diseased myocardium and in guiding therapies that may treat such conditions.[2-15]

The importance of the assessment of left ventricle dysfunction, its causes and potential treatment strategies cannot be underestimated. Indeed, in addition to about 3000 people per million that die annually from acute myocardial infarction in industrialized countries, an even bigger number suffers from heart failure, mainly due to advanced coronary heart disease.[16] Also, the continuous increase in life expectancy adds substantially to this problem. It is of uttermost importance to assess therapeutic possibilities for this patient group, as it has been shown that even a small gain in left ventricle ejection fraction (LVEF) may improve life quality and reduce mortality. One of the major therapeutic goals for the prevention of the consequences of ischemic heart disease should therefore be the preservation of LV function through the limitation of infarct size during the acute event, and by improvement of chronic ischemic LV dysfunction. While the prognosis of acute myocardial infarction has greatly improved with the advent of aggressive reperfusion strategies as thrombolysis and primary percutaneous coronary angioplasty (PTCA), chronic ischemic LV dysfunction may be more difficult to master.

Revascularization – with both established (coronary artery bypass surgery (CABG), PTCA) and experimental (direct myocardial revascularization (DMR), protein or gene injection therapy) techniques - of myocardium in jeopardy has been advocated to reduce the impact of chronic ischemic heart disease on morbidity and mortality.

As revascularization of necrotic tissue is unnecessary and may even prove to be hazardous, it is essential that injured myocardial tissue with potential for recovery is identified, so that patients who will actually benefit from the revascularization, are selected.

Several methods to assess myocardial function and detect viability are currently available. Positron emission tomography (PET) with 18F-fluorodeoxyglucose uptake is currently the gold standard. However, this technique is expensive, and is not readily available. Other techniques as single photon emission computed tomography (SPECT) and dobutamine stress echocardiography are clinically attractive, widely available and more cost-effective than PET, but are confronted with varying sensibility and specificity figures in predicting recovery of injured myocardium. Also, none of these techniques can be easily performed on-line, inside the cathlab.

Nonfluoroscopic electromechanical mapping with the NOGA™ system (Biosense-Webster, a Johnson&Johnson company) may fill this gap. Also, its unique 3-dimensional abilities to locate specific myocardial regions is able to guide local intramyocardial therapy with high specificity. Although very interesting research has been performed, the system still needs to find its place within common clinical interventional practice.

The *aim of this thesis* can be summarized as follows: in the first part of the thesis (chapters 1-5) we will explain the technical background of the system, and compare the diagnostic

capacities of the system to standard accepted methods to assess baseline left ventricular function. In the second part (chapters 6-8) we will evaluate the ability of the system to detect and to define myocardial viability. In the third part (chapters 9-12), we describe the use of the NOGA™ system as guidance for novel intramyocardial therapies. In the last part (chapter 13) we reflect on the future applications of nonfluoroscopic mapping.

References

1. Ben-Haim SA, Osadchy D, Schuster I, Gepstein L, Hayam G, Josephson ME. Nonfluoroscopic, in vivo navigation and mapping technology. Nat Med 1996;2(12):1393-5.
2. Kornowski R, Hong MK, Leon MB. Comparison between left ventricular electromechanical mapping and radionuclide perfusion imaging for detection of myocardial viability. Circulation 1998;98(18):1837-41.
3. Fuchs S, Kornowski R, Shiran A, Pierre A, Ellahham S, Leon MB. Electromechanical characterization of myocardial hibernation in a pig model. Coron Artery Dis 1999;10(3):195-8.
4. Gepstein L, Goldin A, Lessick J, Hayam G, Shpun S, Schwartz Y, et al. Electromechanical characterization of chronic myocardial infarction in the canine coronary occlusion model. Circulation 1998;98(19):2055-64.
5. Gepstein L, Hayam G, Ben-Haim SA. A novel method for nonfluoroscopic catheter-based electroanatomical mapping of the heart. In vitro and in vivo accuracy results. Circulation 1997;95(6):1611-22.
6. Gepstein L, Hayam G, Shpun S, Ben-Haim SA. Hemodynamic evaluation of the heart with a nonfluoroscopic electromechanical mapping technique. Circulation 1997;96(10):3672-80.
7. Kornowski R, Bhargava B, Leon MB. Percutaneous transmyocardial laser revascularization: an overview [see comments]. Catheter Cardiovasc Interv 1999;47(3):354-9.
8. Kornowski R, Fuchs S, Tio FO, Pierre A, Epstein SE, Leon MB. Evaluation of the acute and chronic safety of the biosense injection catheter system in porcine hearts. Catheter Cardiovasc Interv 1999;48(4):447-53; discussion 454-5.
9. Kornowski R, Hong MK, Gepstein L, Goldstein S, Ellahham S, Ben-Haim SA, et al. Preliminary animal and clinical experiences using an electromechanical endocardial mapping procedure to distinguish infarcted from healthy myocardium. Circulation 1998;98(11):1116-24.
10. Kornowski R, Hong MK, Shiran A, Fuchs S, Pierre A, Collins SD, et al. Electromechanical Characterization of Acute Experimental Myocardial Infarction. J Invasive Cardiol 1999;11(6):329-336.
11. Kornowski R, Leon MB. Left ventricular electromechanical mapping: current understanding and diagnostic potential. Catheter Cardiovasc Interv 1999;48(4):421-9.
12. Kornowski R, Leon MB, Fuchs S, Vodovotz Y, Flynn MA, Gordon DA, et al. Electromagnetic guidance for catheter-based transendocardial injection: a platform for intramyocardial angiogenesis therapy. Results in normal and ischemic porcine models. J Am Coll Cardiol 2000;35(4):1031-9.
13. Van Langenhove G, Hamburger J, Smits P, Foley D, Albertal M, Serruys P. Improved regional wall motion 6 months after direct myocardial revascularization (DMR) with the NOGA DMR system. Circulation 2000, 102;7:e44-e45.
14. Van Langenhove G, Hamburger J, Albertal M, Smits P, Onderwater E, Serruys P. Comparison of mechanical properties of the left ventricle in patients with severe coronary artery disease by nonfluoroscopic mapping versus two dimensional echocardiograms. Am J Cardiol 2000:In Press.
15. Van Langenhove G, Smits P, Serrano P, Kozuma K, Kay I, Albertal M, et al. Assessment of regional wall motion: a comparison between computerized LV angiography and nonfluoroscopic electromechanical mapping (Abstract). Circulation 1999;100(18 (suppl)):I-725.
16. Boersma H, Doornbos G, Bloemberg B, Wood D, Kromhout D, Simoons Me. Cardiovascular diseases in Europe. European registries of cardiovascular diseases and patient management. Sophia Antipolis, France: European Society of Cardiology; 1999.

Chapter 1

Nonfluoroscopic real-time endoventricular three-dimensional mapping. A novel catheter-based technique to assess mechanical and electrophysiological properties of the heart.

Part I. NOGA™.

Glenn Van Langenhove, MD; Peter C. Smits, MD. PhD; J.N. Hamburger, MD, PhD; Mariano Albertal, MD; Emile Onderwater, MSc; Jos R.T.C. Roelandt, MD, PhD; Patrick W. Serruys, MD, PhD. Thoraxcenter Rotterdam, Academic Hospital Dijkzigt, Erasmus University, The Netherlands

INTRODUCTION

Nonfluoroscopic electromechanical mapping is a novel technique that enables the investigator to acquire on-line information on electrical and mechanical endoventricular functioning of myocardial tissue. Although the system has only very recently been developed, it is already implied in the clinical arena in both the interventional cardiology (NOGA™) and electrophysiology (CARTO™) settings. The decision of the company that introduced the system (Biosense, Cordis-Webster, Johnson and Johnson) to subdivide NOGA™ and CARTO™ into two separate systems was a political one, based on the fact that in the United States interventional cardiology and interventional electrophysiology are two entirely separated branches of clinical cardiology. The basic concepts of the two systems are however the same. In this first of two parts, we shall review the NOGA™ system components, the left ventricular mapping technique, the initial experimental and clinical data available, the ongoing trials and the future applications of this technique. In the second part, an overview of the CARTO™ system will be presented.

The rationale of a new technique

Percutaneous interventional techniques such as catheter-based ablation of cardiac arrhythmia's, direct myocardial revascularization (DMR) or intramyocardial gene-injection are becoming widespread in clinical medicine. Previously these techniques needed surgical interventions, implying higher risks, cost and discomfort for the patient. The navigation of the minimally invasive tool in the body can be performed using standard imaging techniques such as echocardiography or fluoroscopy. This may prove cumbersome, as multiple views providing only two-dimensional projections are currently available on-line[1]. A major pitfall in the methods presently used in electrophysiology is indeed the inability to accurately associate the intracardiac electrogram with a specific endocardial site. Thus, the localization of the recording sites with fluoroscopy is inaccurate, cumbersome, and associated with high x-ray exposure for both the patient and the physician[2].

Although clinical application of on-line 3D echocardiography and magnetic resonance imaging are underway, until recently no technique for real-time 3D guiding of intervention tools and assessment of myocardial electromechanical functioning was available. Indeed, nonfluoroscopic electromechanical mapping has become the first navigation technique to accurately determine the trajectory of a tool inside the human heart, to guide the interventional device to a specific site, and to meticulously couple functional and anatomical properties[1].

The system

The system is composed of a miniature passive magnetic field sensor incorporated in a catheter, an external ultralow magnetic field emitter (location pad), and a processing unit (NOGA™, Biosense). The deflectable-tip catheter (NOGA-STAR, Cordis-Webster) contains both a location sensor just proximal to its tip, and standard electrodes that allow recording of unipolar (unipolar voltages, UPV) and bipolar (BPV) electrical signals (figure 1a).

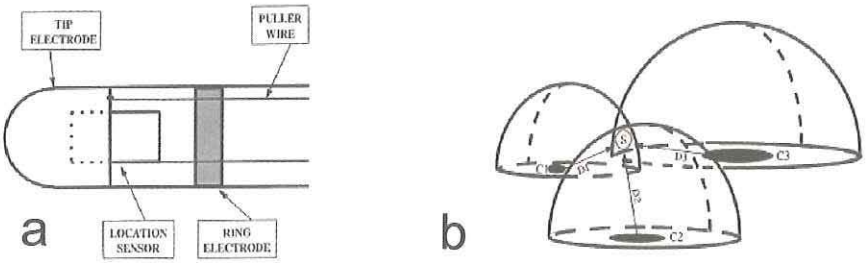

Figure 1

1a. Tip of mapping catheter, showing the location of the sensor and the electrodes. 1b. Three coils originating from the location pad (C 1,2 and 3) that is placed under the patient. Every point s is locatable in 3D space by its reference to the different magnetic field strengths (distances D1, 2 and 3).

The locator pad placed beneath the operating table consists of three radiators that generate ultralow magnetic fields ($5x10^{-5}$ to $5x10^{-6}$ Tesla) (figure 1b) that contain the information necessary to resolve the location and orientation of the sensor in 6 degrees of freedom. Indeed, the amplitude, phase and frequency of the emitted magnetic signals recorded by the location sensor allow the computer algorhitm to solve a number of complicated algebraic equations yielding the location (x, y and z) and orientation (roll, pitch and yaw) of the sensor. The NOGA™ processing unit consists of a computer that updates the acquired information in real-time and a Silicon Graphics workstation that displays the 3D left ventricular endocardial reconstruction. The operator can choose whatever view he wishes to work with during point acquisition, can add a second view in a separate window, and can change both views whenever he wishes to do so, during the mapping procedure. Besides electroanatomical activation maps, minimum voltage maps (showing uni- or bipolar voltages), local shortening maps, and bull's eyes views (figure 2),

Figure 2

(a) Electroanatomical map in LAO view showing activation times of the myocardium at the different sites. Color-coding is from very early (blue) to late (red). (b) Maximum voltage map showing unipolar voltages at the different measurement points. Color-coding is from high (blue-purple) to very low voltages (red). (c) Local linear shortening (LLS) map, with colors going from akinetic (red) to normal (blue-purple). (d) Bull's eye view of the LLS map, with basal (outer segments), mid and apical (inner segments) regions of A (anterior), L (lateral), P (posterior) and S (septal) segments. The average value of LLS is automatically given by the system.

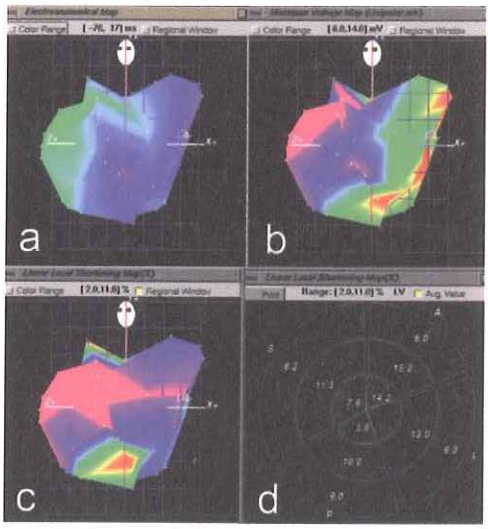

a variety of other features are provided by the system. A full-length description however would lead us too far.

Definitions

Point loop stability: measures the maximum of distances between the locations of the selected point in two consecutive heart cycles. Low point loop stability indexes indicate a good point.

Cycle length (CL) stability: the difference between the length of the current cycle and the average of the last 100 cycles recorded.

Local activation time (LAT) stability: measure of how stable the LAT is between cycles. Reliable points show a LAT variation of <3ms.

Location stability: a measure of the variability in position of the catheter tip on the endoventricular wall during two consecutive cardiac cycles.

Triangle fill threshold: by setting a "triangle fill threshold" value, the operator chooses the minimum triangle size for which the program will close a face on the reconstructed chamber (figures 3a and b).

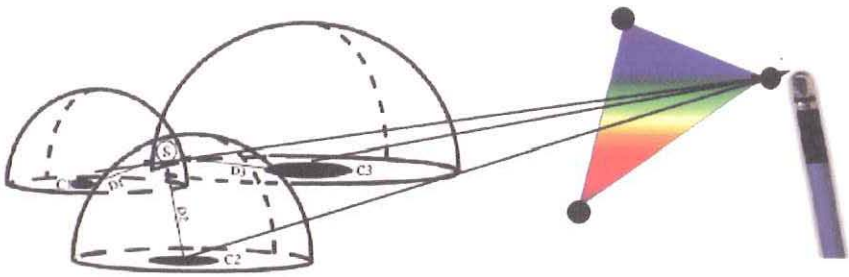

Figure 3

(a) Catheter tip while taking a third point, accurately located in space through distances relative to the different coils of the location pad; (b) the triangle threshold allows the triangle between the three points to be filled.

This feature allows the operator to determine the degree to which the system will interpolate between actual data points and will ensure that a minimal level of point density will be met at each mapped region. Usually an interpolation threshold of 30 mm between adjacent points is taken[3].

Inner points filtering: computer algorithm that removes points thought to be located inside the ventricular lumen (and not on the ventricular wall) or on a papillary muscle. The algorithm calculates relative position of points as compared to at least three neighboring ones and is therefore able to remove these contending points.

Local linear shortening (LLS): The local linear shortening assessment is based on the assumption that in healthy myocardium any two points move closer to each other during contraction. Measurement of distances between neighboring points is therefore the basis

for calculation of myocardial shortening. The computer algorithm takes into account the density of points around a point p, and gives a negligible weight to points too close (sampling noise) and points too far (of no influence as they provide non-local information). The algorithm for regional linear shortening is calculated as follows: for any two points on the map, i and j, LLS is calculated as the change in distance between these two points from end-diastole to end-systole, normalized for the length at end diastole:

$LLS_{ij} = (L(ED)_{ij} - L(ES)_{ij})/ L(ED)_{ij}$

For any point p LLS is calculated as a function of the LLS_{pj}, for all points j=1 to n on the map, so that

$LLS_p = (S_{j=1..n} W_{pj} (L(ED)_{pj}) x LLS_{pj}) / S_{j=1..n} W_{pj},$

where W is the weight of a certain point as a function of the distance Lij between two points i and j, the average distance D around point p (D is defined in the computer algorithm as the average distance of the ten closest points to p) (figure 4)

Figure 4

Local linear shortening is defined as the average distance that points move relative to each other during systole. The computer algorhitm takes the ten most neighboring points, but discards points to close or to far from the point under study, thereby confining a region of interest (orange in picture).

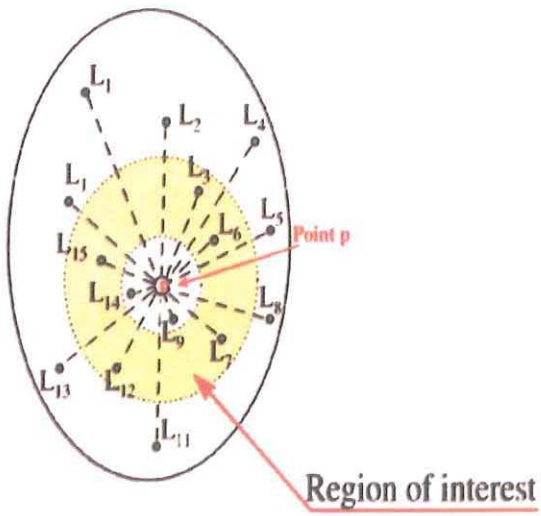

and the volume V at end-diastole. The weight is therefore function of the point density in a defined region, the volume of the heart and the distances between points at end-diastole.

The mapping procedure

The mapping catheter is introduced through a 7F or 8F femoral sheath. Prior to the actual mapping procedure, heparin is given intravenously (10,000 IU); additional heparin is given to maintain an activated clotting time (ACT) above 200s. A reference catheter can be inserted into the coronary sinus or RV apex or can be applied to the back of the patient. A mapping catheter is then inserted into the mapped chamber. The location of the tip of the mapping catheter while inside the heart is gated to end diastole and is recorded relative

to the fixed reference catheter, thus compensating for subject or cardiac motion[3]. As the catheter tip is dragged over the LV endocardial surface (figure 5),

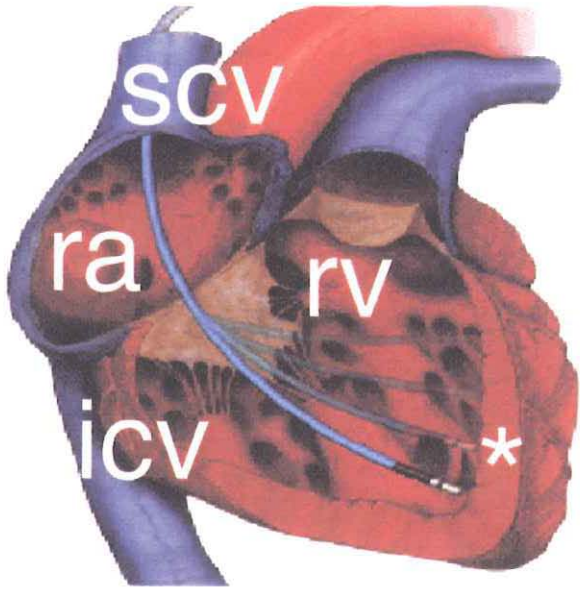

Figure 5

Dragging of the catheter over the endocardium, in this case of the right ventricle. (*) denotes the different positions of the catheter during the procedure. SCV= superior caval vein, ICV= inferior caval vein, RA= right atrium, RV= right ventricle. The procedure in the left ventricle is essentially the same; the approach is retrograde through the aortic valve; some investigators use a transseptal approach.

the system continuously analyzes its location in 3-dimensional space without the use of fluoroscopy. The set of points thus collected comprises an irregularly sampled data set of location points that are members of the endocardial surface. Chamber geometry is then reconstructed, in real time, using the set of sampled location points. The endocardial surface is presented as a set of polygons (triangles) whose vertices are the sampled points. The local activation time (LAT) at each site is determined as the time difference between a selected fiducial point on the body-surface ECG and the steepest negative intrinsic deflection in the unipolar intracardiac electrogram (filtered at 0.5 to 400 Hz) recorded from the tip of the mapping catheter. The activation map is color coded and superimposed on the 3D chamber geometry. The center of mass of the reconstructed chamber is automatically calculated from the set of the surface points. The volume of the chamber can be calculated from the sum of the volumes of all tetrahedrons constructed when connecting the center of mass to all triangles forming the reconstructed surface[2]. Thus, left ventricular end-diastolic (LVEDV) and end-systolic (LVESV) volumes, stroke volume (LVEDV-LVESV) and ejection fraction (LVEF, SV/LVEDV) can be calculated and displayed (figure 6).

Figure 6

(a) Volume-time curve. Minimum and maximum volumes are marked with blue crosses. (b) Electroanatomical map of the same patient. (c) Point displacement curve. Point displacement on the ventricular wall is a function of the local wall motion. The displacement bar graph shows the maximum distance between two locations of each point within the recorded period. (d) Loop stability graph. Shows maximum distances between the location of a specified point at a specified time during different heart cycles.

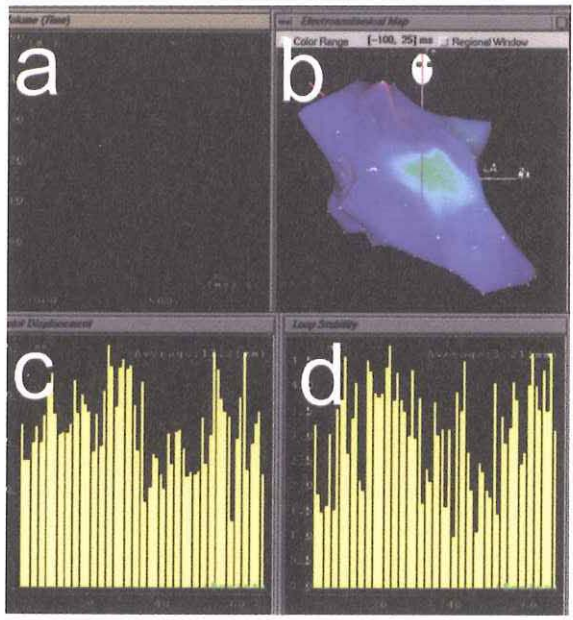

The stability of the catheter-to-wall contact is evaluated at every site in real time, and points are manually deleted from the map if 1 of the following criteria is met: (1) a premature beat or a beat after a premature beat; (2) location stability, defined as a difference of >4 mm in end-diastolic location of the catheter at 2 sequential heartbeats; (3) loop stability, defined as an average distance of >4 mm between the location of the catheter at 2 consecutive beats at corresponding time intervals in the cardiac cycle; (4) cycle length that deviated >10% from the median cycle length; (5) different morphologies of the local ECG at 2 consecutive beats, or severe ST-elevation of the intracardiac electrogram depicting excessive myocardial impression by the mapping catheter; (6) local activation time differences of >3 ms between 2 consecutive beats; (7) different QRS morphologies of the body surface ECG; (8) inner point location; (9) adjacent points closer than 5 mm (local linear shortening data proved to be unreliable if measured under these conditions) and (10) points not related to the left ventricle (such as atrial location)[3].

Experimental and clinical validation studies

The initial validation studies of the mapping system were reported by Gepstein et al.[4] These authors first tested the in vitro accuracy of the locatable-catheter capabilities. By using a test jig with several holes at precise known distances from each other, they showed that repeated measurements of the location of one specific site differed 0.16 mm maximally, and that distances between specific points were equally highly reproducible (mean error 0.42 mm). Also, the intracardiac electrical signal from the locatable catheter was found to correlate highly with the signal acquired using a standard nonlocatable electrophysiological catheter placed in the immediate vicinity of the mapping catheter (cross-correlation = 0.96 ± 0.01). In the same study, they tested the reproducibility of

measurements performed on the beating pig's heart. Again, standard deviation (SD) for measurements at the same site were low (0.74 ± 0.13 mm), and the overall mean error of distances measured inside the body (through the use of a long sheath with markers every 10 mm) proved to be low (0.73 ± 0.03 mm)[4]. Furthermore, Gepstein and colleagues found a consistent activation pattern of the left ventricle in pigs. During ventricular pacing, the earliest site of activation was at the site of pacing. During sinus rhythm, the earliest site of activation was on the superior part of the septum. Invariably, the latest site of activation in both rhythms was on the left lateral wall close to the mitral valve annulus. The total activation time of the left ventricle varied between 40 and 80 ms during sinus rhythm and between 57 and 87 ms during paced rhythm[4].

In a second series of validation studies by the same group, volumetric measurements of test jigs and pig ventricles were analyzed[2]. Phantom objects with known volumes showed that the measured volumes were very close to the actual volumes, with an average deviation of about 2.7%. Measurements of LV casts (with a more difficult anatomy) showed an average deviation of 9.6%. , with a correlation r=0.94 with the actual volumes. Measurements of volumes in a dynamic test jig showed high accuracy with known volumes, deviating only 1.4, 0.7, 6.0 and 5.2% for maximal volume, minimal volume, SV and EF respectively[2]. In 12 pigs tested in this study, the intra- and interobserver variability proved to be very low. Also, SV measurements acquired with the mapping system proved to be highly correlated with thermodilution cardiac output measurements (figure 7)[2].

Figure 7

Graph showing the correlation between NOGA™ mapping derived stroke volumes (NFM, Non fluoroscopic mapping, calculated SV) and thermodilution measured SV in pigs. A very good correlation of r2 = 0.93 was found.

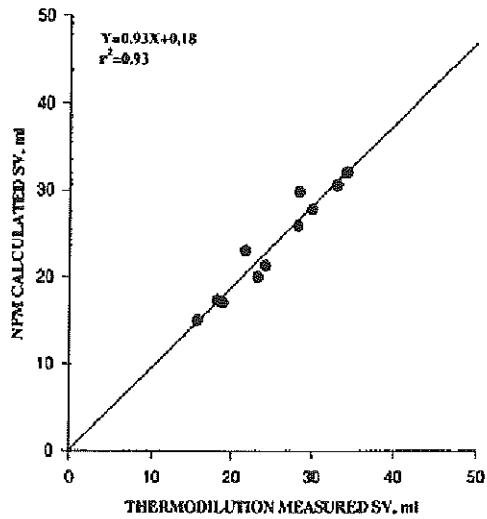

As further validation of the system as a tool for the assessment of local left ventricular function, Gepstein et al. acquired the left ventricular electromechanical regional properties in 11 dogs with chronic infarction (4 weeks after ligation of the proximal LAD) and 6 controls and compared them to the pathology results. Average endocardial local shortening (LS, measured at end systole and normalized to end diastole) and intracardiac bipolar electrogram amplitude were quantified at 13 LV regions. Endocardial LS was significantly lower at the infarcted area (1.2+/-0.9%, P<0.01) compared with the noninfarcted regions (7.2+/-1.1% to 13. 5+/-1.5%) and with the same area in controls

(15.5+/-1.2%, P<0.01). Average bipolar amplitude was also significantly lower at the infarcted zone (2.3+/-0.2 mV, P<0.01) compared with the same region in controls (10.3+/-1.3 mV) and with the noninfarcted regions (4. 0+/-0.7 to 10.2+/-1.5 mV, P<0.01) in the infarcted group. Also, the electrical maps could accurately delineate both the location and extent of the infarct, as demonstrated by the high correlation with pathology (Pearson's correlation coefficient=0.90) and by the precise identification of the infarct border. The authors concluded that chronic myocardial infarcted tissue could be accurately characterized and quantified by abnormal regional mechanical and electrical functioning[5] (figure 8).

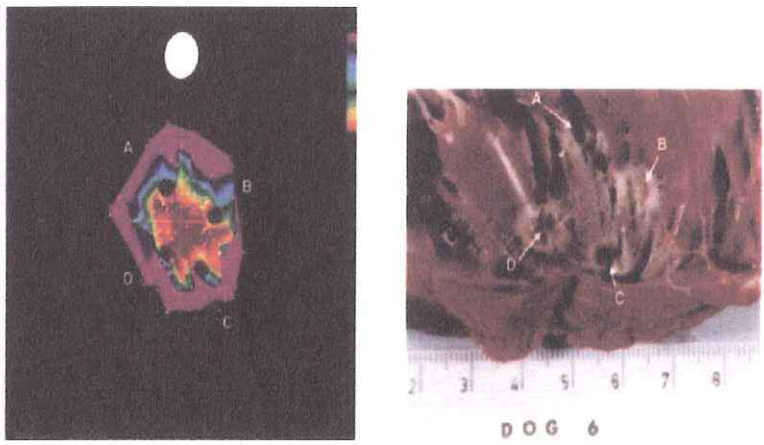

Figure 8

Local shortening map (left) showing a clear delineation of the infarct zone (in red) in a dog, with four (1-4) brown tags, revealing the places where ablation was performed. As one can clearly see, the ablation sites correlated pretty good with the sites of necrosis on authopsia (right picture). It also becomes clear from the picture that NOGA™ can accurately delineate myocardial infarction zones. From Gepstein L, Goldin A, Lessick J, et al. Electromechanical characterization of chronic myocardial infarction in the canine coronary occlusion model. Circulation 1998;98:2055-64.

The first human studies with the NOGA™ system were reported by Kornowski et al.[3] In 24 patients (12 patients with prior myocardial infarction (MI) and 12 control patients) LV endocardial mapping was performed to assess electromechanical function in infarcted versus healthy myocardial tissue. In patients with prior MI, the average voltage was 7.2+/-2.7 mV (UP)/1.4+/-0.7 mV (BP) in MI regions, 17.8+/-4.6 mV (UP)/4.5+/-1.1 mV (BP) in healthy zones remote from MI, and 19.7+/-4.4 mV (UP)/5.8+/-1.0 mV (BP) in control patients without prior MI (P<0.001 for MI values versus remote zones or control patients). They clearly showed that both UPV and local endocardial shortening were significantly impaired in MI zones compared with controls. Also, concordance with echocardiographic wall motion analysis was good[3](figure 9, figure 10).

Figure 9

Example of a normal NOGA™ map. Both the voltage map (a) as well as the local shortening map (b) are predominantly green-blue-purple-pink, showing high unipolar voltages and local shortening values. The respective bull's eye maps (c and d) show consistently high values of UPV and LLS, underlying the normal nature of this ventricle. Note again the low regional contractility and the low voltages in the vicinity of the mitral valve annulus.

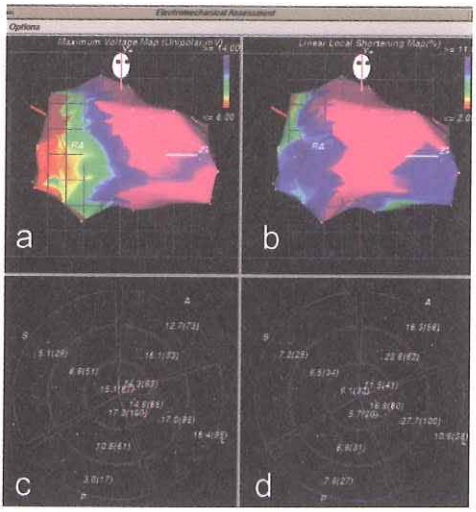

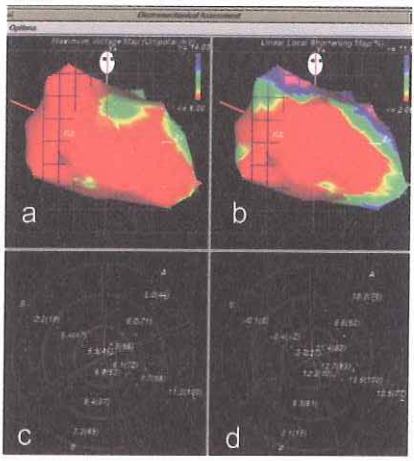

Figure 10

RAO view of a patient that suffered an anteroseptal infarction 3 years ago. The red zones in (a) and (b) delineate a zone with akinesia and absence of electrical activity. The respective bull's eye views show negative values for local shortening (d) in the septal and anterobasal segments, suggestive of wall a- to dyskinesia. The voltage map (c) shows UPV below 6 mV in the same region.

Kornowski et al. later reported on a comparison between NOGA™ mapping and radionuclide perfusion imaging[6]. They showed that UPV (14.0+/-2.0 mV) and LLS values (12.5+/-2.8%) were highest when measured in myocardial segments (n=56) with normal perfusion and lowest (7.5+/-3.4 mV and 3.4+/-3.4%) when measured in myocardial segments with fixed perfusion defects (n=20) (P0.0001) on single photon emission computed tomography imaging studies using ^{201}Tl at rest and 99mTc-sestamibi after adenosine stress. A significant difference in UPV and LLS values was found between groups (P<0.001 for each comparison by ANOVA). Myocardial segments with reversible perfusion defects (n=66) had intermediate UPV (12.0+/-2.8 mV, P=0.048 versus normal and P=0.005 versus fixed segments) and LLS values (10.3+/-3.7%, P=0.067 versus normal and P=0.001 versus fixed segments). From these results it was concluded that NOGA™ mapping might allow the detection of myocardial viability.

Van Langenhove et al. compared enddiastolic (EDV) and endsystolic volumes (ESV), stroke volume (SV) and ejection fraction in 44 patients with both LV angiogram and NOGA™ mapping. Although a strong correlation (r=0.78, p<0.001) for EF measurement

between the two techniques was found, the Bland-Altman analysis (figure 11)

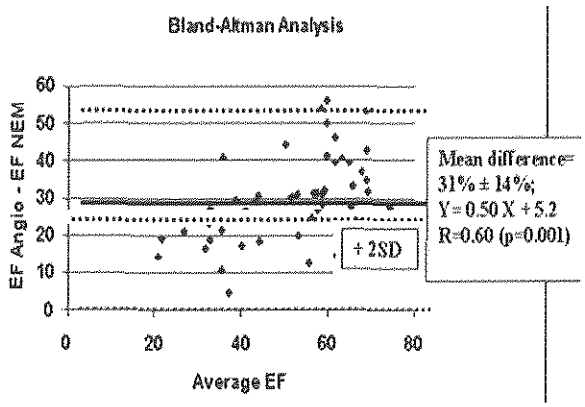

Figure 11

Bland-Altman analysis showing the non interchangeability of NEM (nonfluoroscopic electromechanical mapping) derived ejection fraction (EF) measurements, and LVEF calculated with LV angiogram. SD= Standard Deviation.

demonstrates the disagreement and the absence of interchangeability between both methods. Indeed, on average, a difference of about 30% in LVEF was found[7].
The same authors described moderate correlations between regional wall motion assessment using LV angiography as compared to LLS data acquired in the same segments($p<0.001$)[8] (figure 12).

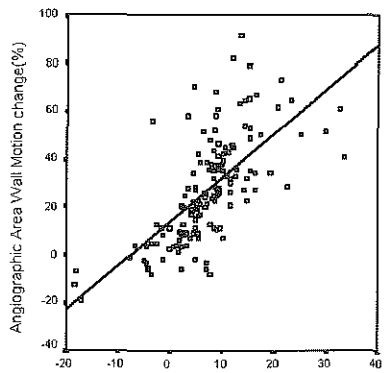

Figure 12

Comparison of area change as derived from the biplane left ventricular angiogram derived in 7 segments, analyzed using the area-length method. Area change is% change of a specified segment in diastole versus systole.

Finally, dobutamine stress echo was compared to LLS and UPV data for comparable segments in patients with a previous myocardial infarction. ROC curves showed significant cut-off values for myocardial viability of UPV=9.0 mV (sens 56%, spec 81%, $p<0.0001$) and LLS=6.8% (sens 56%, spec 92%, $p<0.0001$)[9].
Fuchs et al. assessed in-vivo electromechanical changes following gradual coronary artery occlusion in a pig ameroid constrictor model using NOGA™(10). UPV and LLS were measured in the ischemic lateral and non-ischemic anterior zones in animals at rest (n = 9) and 5 weeks after the implantation of ameroid constrictors around the left circumflex artery. Echocardiography was used to assess regional contractility (% myocardial thickening), and an echo-contrast perfusion study was performed using acoustic densitometry methods. The ischemic lateral zone showed reduced myocardial perfusion at rest (peak intensity; 3.4 +/- 1.7 versus 20.7 +/- 14.8, P = 0.005), impaired mechanical

function (percentage wall thickening 22 +/- 19% versus 40 +/- 11%, P = 0.03; local endocardial shortening 2.9 +/- 5.5% versus 11.7 +/- 2.1%, P = 0.002), and preserved electrical activity (unipolar voltage 12.4 +/- 4.7 versus 14.4 +/- 1.9 mV, P = 0.25; bipolar voltage 4.1 +/- 1.1 versus 3.8 +/- 1.5 mV, P = 0.62), compared with the anterior region. The authors concluded that gradual coronary artery occlusion resulting in regional reduced perfusion and function at rest (i.e. hibernating myocardium) is characterized by preserved electrical activity. Electromechanical left ventricular mapping may be of diagnostic value for identifying the hibernating myocardium[10].

Recently, Vale et al. showed feasibility and safety of percutaneous, catheter-based, nonfluoroscopic mapping guided myocardial gene transfer[11]. In six pigs in which the injection catheter was used to deliver plasmid using cytomegalovirus promoter/enhancer, encoding nuclear-specific LacZ gene (pCMV-nlsLacZ) (50 microg/ml) to a single LV myocardial region, peak beta-galactosidase activity after five days was documented in the target area of myocardial injection in each pig. As all pigs survived until sacrifice, and no complications were observed with either the mapping or the injection procedures, the authors concluded that percutaneous myocardial gene transfer can be successfully achieved in normal and ischemic myocardium without significant morbidity or mortality[11]. It is furthermore important to underline the importance of the 3D mapping technique for gene application procedures, as exact delineation of the area to be treated seems mandatory.

Ongoing clinical investigations

Some burning questions related to the clinical usability of the NOGA™ mapping system in clinical practice still are unanswered:

Is the local shortening function (LLS) really a reflection of the local wall motion?

Does direct myocardial revascularization (DMR), for which this system seems to be an ideal guiding tool, really improve the clinical status of the patient?

Is local gene application, again for which this system seems an optimal platform, going to be applied clinically?

Is the system able to detect true viability?

Is there need for this expensive technique for in-cathlab detection of viability/ischemia – when other techniques have already proven their value?

Some of these questions will be answered by ongoing investigations. The DIRECT and EURO-DIRECT trials are currently enrolling patients in the USA and Europe; these trials (single blinded, randomized NOGA™ mapping without versus with DMR in patients not suitable for any other type of revascularization) are aiming to answer the question if the presumed benefit with DMR is simply a placebo effect, or does really improve the patient's clinical and functional status (figure 13).

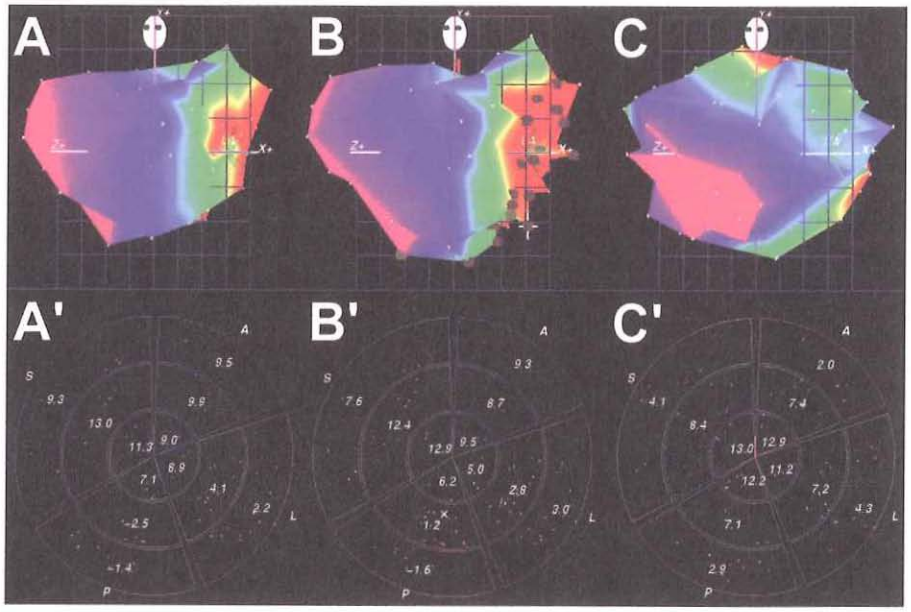

Figure 13

Local shortening maps before DMR (a), after DMR (b) and at 6 month follow-up (c). The posterolateral wall motion has clearly improved, as witnessed by the increase in local shortening in the mid- and basal zones of both the posterior and the lateral segments (see bull's eye view, a' through c').

Studies assessing "true viability" in patients scheduled for bypass surgery will answer the question if NOGA™ can predict recuperation of myocardial segments with wall motion abnormalities after revascularization. A study assessing the possible additional benefit of low-dose dobutamine during NOGA™ mapping is currently performed at the Thoraxcenter. Future investigations will evaluate the possible value of adenosine in the detection of ischemic segments, the diagnostic value of NOGA™ mapping as compared to magnetic resonance imaging (MRI) in myocardial viability, the efficacy of growth factors to induce myocardial angiogenesis and additional comparisons with radionuclide perfusion imaging studies[12-16].

Conclusions

Left endoventricular 3D real-time electromechanical mapping is a new, intriguing technique for in-cathlab assessment of mechanical and electrical functioning of the left ventricle. Although initial studies have shown safety, feasibility and reproducibility of this technique, and have provided similar results as compared to established techniques in the quest for viability, data on the additional clinical value of the system are still scarce. Ongoing trials on DMR and intramyocardial gene injection may definitely establish its place among currently used techniques in interventional cardiology.

References

1. Ben-Haim SA, Osadchy D, Schuster I, Gepstein L, Hayam G, Josephson ME. Nonfluoroscopic, in vivo navigation and mapping technology. Nat Med 1996;2(12):1393-5.
2. Gepstein L, Hayam G, Shpun S, Ben-Haim SA. Hemodynamic evaluation of the heart with a nonfluoroscopic electromechanical mapping technique. Circulation 1997;96(10):3672-80.
3. Kornowski R, Hong MK, Gepstein L, Goldstein S, Ellahham S, Ben-Haim SA, et al. Preliminary animal and clinical experiences using an electromechanical endocardial mapping procedure to distinguish infarcted from healthy myocardium. Circulation 1998;98(11):1116-24.
4. Gepstein L, Hayam G, Ben-Haim SA. A novel method for nonfluoroscopic catheter-based electroanatomical mapping of the heart. In vitro and in vivo accuracy results. Circulation 1997;95(6):1611-22.
5. Gepstein L, Goldin A, Lessick J, Hayam G, Shpun S, Schwartz Y, et al. Electromechanical characterization of chronic myocardial infarction in the canine coronary occlusion model. Circulation 1998;98(19):2055-64.
6. Kornowski R, Hong MK, Leon MB. Comparison between left ventricular electromechanical mapping and radionuclide perfusion imaging for detection of myocardial viability. Circulation 1998;98(18):1837-41.
7. Van Langenhove G, Hamburger J, Smits P, Serrano P, Albertal M, Onderwater E, et al. Nonfluoroscopic Electromechanical Mapping for Evaluation of Left Ventricular Hemodynamics. A Comparison with Contrast Ventriculography. Acta Cardiologica 1999:(In publication).
8. Van Langenhove G, Smits P, Serrano P, Kozuma K, Kay I, Albertal M, et al. Assessment of regional wall motion: a comparison between computerized LV angiography and nonfluoroscopic electromechanical mapping (Abstract). Circulation 1999;100(18 (suppl)):I-725.
9. Van Langenhove G, Smits P, Albertal M, Serrano P, Kay I, Poldermans D, et al. NOGA mapping for the detection of viable and ischemic myocardium: a comparison with dobutamine stress echocardiography (Abstract). Circulation 1999;100(18 (suppl)):I-23.
10. Fuchs S, Kornowski R, Shiran A, Pierre A, Ellahham S, Leon MB. Electromechanical characterization of myocardial hibernation in a pig model. Coron Artery Dis 1999;10(3):195-8.
11. Vale PR, Losordo DW, Tkebuchava T, Chen D, Milliken CE, Isner JM. Catheter-based myocardial gene transfer utilizing nonfluoroscopic electromechanical left ventricular mapping. J Am Coll Cardiol 1999;34(1):246-54.
12. Vale P, Tkebuchava T, Milliken C, Chen D, Symes J, Isner J. Percutaneous electromechanical mapping demonstrates efficacy of pVGI.1(VEGF2) in an animal model of chronic myocardial ischemia (Abstract). Circulation 1999;100(18 (Suppl)):I-22.
13. Kornowski R, Baim D, Moses J, Laham R, Hong M, Kuntz R, et al. Six month results following percutaneous direct myocardial revascularization guided by Biosense left ventricular mapping in patients with refractory coronary ischemic syndromes. (Abstract). Circulation 1999;100(18 (Suppl)):I-22.
14. Laham R, Pearlman J, Datta R, Gao L, Baim D. Biosense-guided laser myocardial revascularization improves 30-day and 6-month regional wall motion, perfusion and collateralization of the treated zone(s) (Abstract). Circulation 1999;100(18 (Suppl)):I-22.
15. Botker H, Lassen J, Bottcher M, Sygehus S, Hermansen F, Sogaard P, et al. Left ventricular electromechanical mapping for detection of myocardial viabilityin patients with impaired left ventricular function due to chronic ischemic heart disease (Abstract). Circulation 1999;100(18 (Suppl)):I-22.
16. Fuchs S, Hendel R, Kuntz R, Pierre A, Wallace D, Bonow R, et al. Left ventricular electromechanical mapping reflects resting myocardial perfusion and viability: comparative analysis with SPECT radionuclide myocardial imaging (Abstract). Circulation 1999;100(18 (Suppl)):I-22.

Chapter 2

Electromechanical properties of the normal human left ventricle: assessment with nonfluoroscopic 3-D real-time mapping

Glenn van Langenhove, MD; Irenee Bossi, MD; Jaap N. Hamburger, MD, PhD; Peter C. Smits, MD, PhD; Leonidas Diamantopoulos, MD, PhD; Dirk Stockman, MD; Paul Van den Heuvel, MD; Emile Onderwater, BSc; Jean Fajadet, MD; Jean Marco, MD; Patrick W. Serruys, MD, PhD; From the Thoraxcenter Rotterdam, Dijkzigt Hospital, Erasmus University, Rotterdam, The Netherlands (GVL, JNH, PCS, LD, EO, PWS), the Department of Interventional Cardiology, Clinique Pasteur, Toulouse, France (IB, JF, JM), the Department of Interventional Cardiology, Middelheim Hospital, Antwerp, Belgium (DS, PVDH) and Dipartimento Cardiologico A. De Gasperis - Ospedale Ca' Granda Niguarda, Milano, Italy (IB).

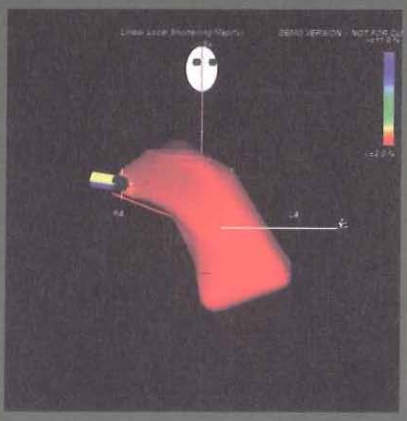

Abstract

Electromechanical properties of the normal human left ventricle: assessment with nonfluoroscopic 3-D real-time mapping

Background: Nonfluoroscopic electromechanical mapping (NEM) has been introduced as a novel technique for the evaluation of electrical and mechanical functioning of the myocardium. In this system, local linear shortening (LLS) is the parameter used for assessment of local mechanical properties; unipolar (UPV) and bipolar (BPV) voltages represent the electrical properties of the left ventricle. Studies concerning the possible detection of viable or ischemic regions using this system are currently being performed. Also, the system is being used as guidance tool to direct new interventional modalities as direct myocardial revascularization (DMR) and injection therapy. As the normal left ventricle should be used as a reference model, and a paucity of data on this issue exist, we analyzed electromechanical maps in normal left ventricles.

Methods: Patients were included in this study if they met all three following criteria: 1) Negative history of myocardial infarction or hospitalization for acute coronary syndrome; 2) Normal baseline ECG; 3) Absence of abnormal regional wall motion on contrast left ventricle angiogram and 4) Absence of objective signs of ischemia on stress testing. Nonfluoroscopic maps and left ventricle angiograms were analyzed by independent observers. Ejection fraction (LVEF), end-diastolic (LVEDV), end-systolic (LVESV) and stroke volumes (SV) were calculated, and compared to the same parameters of patients in the database that did not meet the aforementioned criteria. LLS, UPV and BPV were defined for the different ventricular segments.

Results: Of the 110 patients in our database, 24 met the criteria for normal left ventricular function. LVEF and SV were consistently higher, LVEDV and LVESV were lower than in ventricles that did not match the criteria for normal function. LLS and UPV were high throughout all segments, except for posterior and septal basal segments, that showed consistently lower values. Finally, large variations in LLS, UPV and BPV for normal myocardial segments were noted.

A strong correlation between angiography and NEM for the measurement of LVEF was found (R=0.73). However, the Bland-Altman analysis performed clearly showed the clinical non-interchangeability between the two techniques.

Conclusion: NEM is a powerful tool for invasive electromechanical assessment of myocardial function. Normal left ventricles show consistently lower values for both UPV and LLS for the posterior and septal basal regions, probably caused by mitral and aortic valve ring fibrous tissue. These facts should be taken into account in future evaluations of these regions. Also, underlying clinical conditions may account for the large variations between different normal segments in LLS, UPV and BPV. Finally, LVEF value for the same patients differ strongly when comparing NEM and angiographic assessments, despite their strong correlation.

List of acronyms

NEM:	nonfluoroscopic electromechanical mapping
UPV:	unipolar voltage
BPV:	bipolar voltage
LLS:	local linear shortening
LVA:	left ventricle angiogram
RAO:	right anterior oblique
LAO:	left anterior oblique
LVEDV:	left ventricle end diastolic volume
LVESV:	left ventricle end systolic volume
LVEF:	left ventricle ejection fraction
SV:	stroke volume

INTRODUCTION

Nonfluoroscopic mapping (NOGA™, Biosense-Webster, Waterloo, Belgium) is a new technique for in-cathlab on-line assessment of electromechanical properties of the left ventricle[1]. Research with this technique is now focusing on the future use for the in-cathlab detection of myocardial viability[2], and as a guidance tool to direct novel therapeutic modalities as direct myocardial revascularization (DMR)[3] and direct myocardial injection.[4,5] Although the system has shown its possibilities in distinguishing infarcted from normal myocardial tissue and from myocardium with reversible perfusion defects[6-10], there is still little information on the electromechanical properties of the normal human ventricle. Also, the currently available data on the normal canine and pig ventricle may not be easily applied to the human situation.[9] We therefore assessed the electrical, mechanical and volumetric properties in 24 patients with normal left ventricles.

METHODS

Patients

Patients were included in this study if they met all of the following criteria: 1) Negative history of myocardial infarction or hospitalization for acute coronary syndrome; 2) Normal baseline electrocardiogram, including the absence of left or right bundle branch block; 3) Absence of myocardial ischemia on stress test and 4) Normal left ventricle angiography as assessed by an independent investigator. All patients signed an informed consent.

Left ventricular angiography

Left ventricle angiograms (LVA) in RAO 30° and LAO 60° were performed using standard techniques (11). LVA's were first analyzed visually. Only the angiograms with a normal contraction pattern were included in the study. Angiograms were then analyzed using the centerline method (CAAS II system, PIE Medical, Maastricht, The Netherlands). The 5F diagnostic pig tail catheters were used for computerized calibration. The left ventricle boundaries at end-diastole and end-systole were traced manually with a digitizing device. The frame showing the largest ventricular volume was chosen as the end-diastole, the frame with the smallest volume as the end-systole. Care was taken that measurements were not performed during or immediately after an extrasystole. The CAAS system algorithm automatically provides end-diastolic, end-systolic and stroke volumes, and left ventricle ejection fractions. Patients were excluded from the study if any myocardial segment showed reduced regional functioning (any value <-1.0 SD/chord).

Nonfluoroscopic electromechanical mapping:

The NEM system has been described previously.[1,6-8,10] In short, a reference catheter was taped securely to the patient's back. The mapping catheter (NOGA-STAR™, Biosense-Webster, a Johnson & Johnson company), also with a tip sensor, was introduced through a femoral sheath and placed through the aortic valve in the left ventricle. The location pad fixed beneath the catheterization table generates a low magnetic field ($5x10^{-6}$ to $5x10^{-5}$ Tesla) which allows that at all times, the tip of the catheter can be located with six degrees of freedom (x, y, z, pitch, yaw and roll). The catheter was then dragged along the

endocardial surface of the left ventricle in order to acquire electromechanical data. When a stable signal was obtained a "point" was added to a three-dimensional map as shown on the NEM unit. Electrophysiological data (UPV, BPV, and local activation time) and mechanical data (LLS) were displayed three-dimensionally, while the images obtained could be viewed from different angles as chosen by the operator. A bull's eye view showing average voltages and LLS for 12 segments (basal, mid and apical parts of anterior, lateral, posterior and septal segments) was visualized on the NEM screen (figure 1).

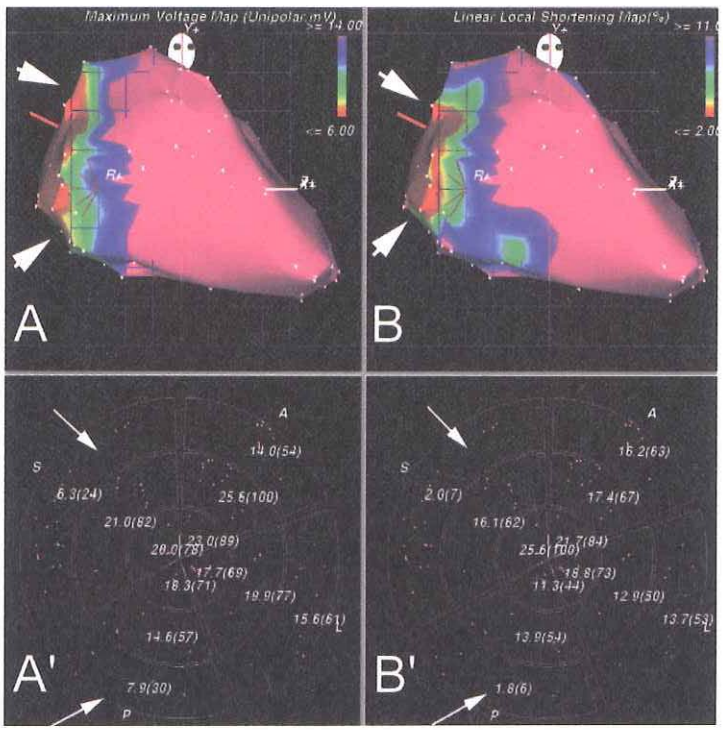

Figure 1

Electromechanical assessment using nonfluoroscopic electromechanical mapping. Panel A shows unipolar voltages (UPV) of the left ventricle in 30° RAO view, with the color bar in the upper right corner. Color-coding goes from red (<6 mV) to blue-purple (>14 mV), with purple zones being normal. The arrowheads delineate a zone of low voltages in the vicinity of the mitral valve area. Panel A' shows a bull's eye view of the same UPV map, with –clockwise from upper right A (anterior), L (lateral), P (posterior) and S (septal) regions. Every region is subdivided into a basal (outer), mid and apical (inner) segment. The two arrows show the basal septal and basal posterior segments that clearly present lower voltages. Also, the large inter-segment variations can be appreciated. Panel B shows the linear local shortening (LLS) map of the same ventricle. The arrowheads delineate the ventricular segment with low LLS, located in the mitral valve area. Panel B' shows the bull's eye view of the LLS map, with the arrows directed at the basal septal and basal posterior segments with lower values as compared to the other segments. Again, large inter-segment differences can be noted.

The LLS assessment is based on the assumption that in healthy myocardium any two points move closer to each other during contraction. Measurement of distances between neighboring points is therefore the basis for calculation of myocardial shortening. The computer algorithm takes into account the density of points around a point p, and gives a negligible weight to points too close (sampling noise) and points too far (of no influence as they provide non-local information). The algorithm for LLS is calculated as follows [12]: for any two points on the map, i and j, LLS is calculated as the change in distance between these two points from end-diastole to end-systole, normalized for the length at end diastole:

$$LLS_{ij} = (L(ED)_{ij} - L(ES)_{ij}) / L(ED)_{ij}$$

For any point p LLS is calculated as a function of the LLS_{pj}, for all points j=1 to n on the map, so that

$$LLS_p = (S_{j=1..n} W_{pj} (L(ED)_{pj}) x LLS_{pj}) / S_{j=1..n} W_{pj},$$

where W is the weight of a certain point as a function of the distance Lij between two points i and j, the average distance D around point p (D is defined as the average distance of the ten closest points to p) and the volume V at end-diastole. The weight is then function of the point density in a defined region, the volume of the heart and the distances between points at end-diastole. We used the revised NOGA 4.0 software version (Biosense-Webster, Johnson&Johnson, June 2000) with (1) a new weight function so that very close neighboring points within the range of noise are not given any weight and do not influence the LLS value of the investigated point, and that very distant points do not influence LLS for a certain point; (2) changing the arithmetic mean by the geometric mean which is better suited for location validation because it is virtually unaffected by the density of points; (3) very careful determination of the apical point, either defined automatically by the system or manually by the user. If such a point it is not meeting the criteria of the various filters a "Location-only" (where its value is not used to determine the LLS in this particular region) comment will appear on the Point List. The user can then decide if another near point in the apical region should be defined as Apex. If the original point is kept then the LLS will not be computed but will rather represent the average of its neighbors. The changes in the new software have been validated (Biosense-Webster, personal communication).

Statistics

Statistical analysis was performed using SPSS, version 9.0 (SPSS Inc., Chicago, Illinois, USA). Data are expressed as mean ± SD. Correlations were performed using Pearson's test. LVEDV, LVESV, LVEF and SV were compared using an independent Student's t-test. LVEF values measured using NOGA and LV angiogram were compared with the Bland-Altman test. Means of nominal values for LLS, UPV and BPV were compared between all segments by the Wilcoxon signed ranks test. A Friedman nonparametric test was used where appropriate. A value of $P<0.05$ was considered statistically significant.

RESULTS

Between June 1997 and April 2000, 110 patients were studied. Of these, 24 met the criteria for normal left ventricular function. Clinical characteristics of both groups are shown in the table.

	Normal LV function (n=24)	Abnormal LV function (n=86)
Age (years ± SD)	61 ± 12	57 ± 9
Male	21 (88%)	73 (85%)
Previous MI (n)	0	80 (93%)
Previous PCI (n)	0	68 (79%)
Previous CABG (n)	0	46 (53%)
Signs of ischemia on non-invasive testing (n)	0	54 (63%)
Congestive heart failure (n)	0	23 (27%)
Hypertension (n)	6 (25%)	46 (53%)
Diabetes (n)	1 (4%)	13 (15%)
Smoking history (n)	7 (29%)	44 (51%)
Hypercholesterolemia (n)	8 (33%)	53 (62%)
Family history (n)	1 (4%)	21 (24%)

Table

Clinical parameters of patients with normal and abnormal left ventricular function. LV=left ventricle, MI=myocardial infarction, PCI=percutaneous coronary intervention, CABG=coronary artery bypass graft.

The average procedure time for the acquisition was 49 ± 18 minutes for normal maps versus 44 ± 22 minutes for NEM maps of the diseased ventricles (p=0.4). All 110 patients remained in stable hemodynamic conditions during the respective procedures, as confirmed by continuous in-cathlab heart rate and blood pressure monitoring data. One patient suffered a stroke after diagnostic catheterization, before introduction of the NOGA-catheter. Four patients had a pericardial effusion after the procedure, two of which required pericardial drainage. One patient died of a large intramyocardial effusion with subsequent heart arrest that could not be corrected despite urgent surgical treatment. No complications however occurred in the last 40 procedures, and no complications were seen in the "normal" group. NOGA-derived LVEDV (90±33ml versus 107±42ml, p=0.04), LVESV (51±22ml versus 77±37ml, p=0.001), SV (38±13ml versus 30±12ml, p=0.003) and LVEF (44±8% versus 29±10%, p<0.0005) differed significantly for the normal versus the diseased ventricles. Average LLS for all segments of the normal ventricles was 15.6±7.4%; average UPV was 15.1±5.6mV, average BPV was 4.5±2.9mV. LLS however varied consistently throughout the left ventricle: LLS of apical segments was higher than that in all other segments (18.0±6.5% versus 14.4±4.8%, p=0.001). LLS of the posterior basal (9.0±6.8%) and the septal basal (6.0±5.7%) segment were also consistently lower than all other segments (p<0.0005 for all comparisons). Average UPV for all segments was 15.1±5.6mV. UPV's were higher in all apical and mid-segments as

compared to all basal segments (17.2±5.4mV and 10.8±3.5mV respectively, p<0.0005). Again, values were lowest in the posterior basal and septal basal segments (9.6±3.1mV and 8.4±3.2mV respectively, p<0.0005 for all comparisons).
Pearson correlation graph between UPV and BPV for the same segments is shown in figure 2.

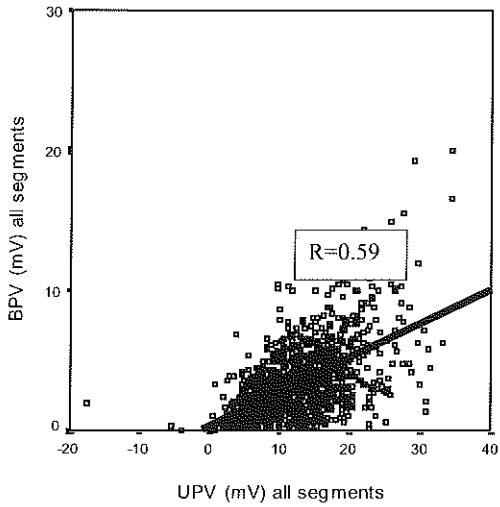

Figure 2

Correlation graph of unipolar (UPV) and bipolar voltages (BPV) for all segments

Correlation was only moderate (R=0.59), albeit highly significant. BPV's were lower in the basal septal region as compared to all other regions (2.3±1.3mV versus 4.8±2.8mV, p<0.0005 for all comparisons), but not consistently for the posterior basal region. Bipolar voltages differed importantly amongst segments, ranging from 6.3±3.8mV in the apical septal segment to 3.5±2.5mV in the mid anterior segment.
LVEF measured by NOGA mapping correlates with LVEF calculated using the LV angiogram (R=0.73, p<0.0005) (see figure 3).

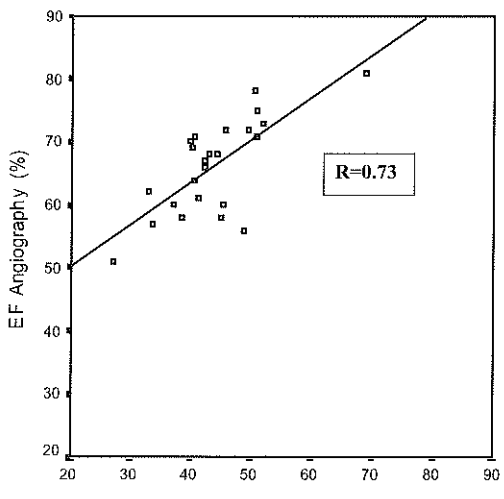

Figure 3

Correlation of left ventricular ejection fraction (EF) as assessed by angiography versus nonfluoroscopic mapping.

The Bland-Altman graph however demonstrates the difference of ±25% in LVEF between the two methods (see figure 4).

Figure 4

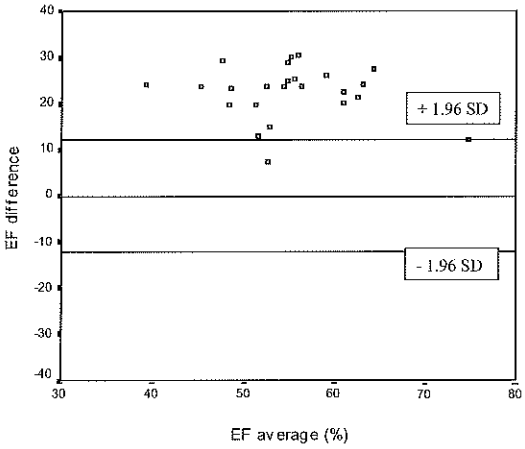

Bland-Altman comparison of left ventricular ejection fraction assessed by angiography versus nonfluoroscopic mapping. The Bland-Altman analysis maps the differences between the two techniques and the averages of the values obtained by the two techniques. Ideally, all points would be on the zero reference line (when the two techniques show no difference in the absolute value obtained). The other two reference lines demonstrate the + and – 1.96 standard deviations of the differences. As most of the values shown, appear outside of these borders, it can be concluded that the two methods are clinically not interchangeable.

Large variations for LLS, UPV and BPV between normal segments were noted. LLS ranged from 3.7% up to 30.4%, UPV from 3.0 up to 34.5, and BPV from 0.3 up to 16.5. The study however was not powered to detect possible clinical parameters predictive for differences in electromechanical parameters.

Discussion

The main finding of this study is that UPV and LLS are consistently high throughout the normal left ventricle. Regions surrounding the aortic, but mostly the mitral valve area (posterior and septal basal regions) however both show lower UPV as well as LLS, when compared to all other regions. These findings are explained by the presence of dens fibrous tissue in the valve region, that shows both a limited movement and a limited amount of functional myocardial cells, accounting for the lower voltages measured.

The correlation between UPV and BPV was significant, albeit very moderate. Also, BPV did not consistently show lower values in the entire valve area, although significantly lower BPV was seen in the basal septal area. Although it has been shown that BPV recordings may be less influenced by contact stability, and far-field potentials, it is also known that the orientation of the catheter tip towards the mapping area may influence the magnitude of the BPV signal. The difficulties in mapping the area very close to valves and the sometimes awkwardly curled catheter profiles in these areas may therefore account for the lack of strong correlation of BPV with UPV in some of the basal myocardial segments.

Only one study has previously described nonfluoroscopic mapping in normal, healthy myocardium in human volunteers[8]. In that study, mean values for all myocardial segments were 19.7±4.4 mV for UPV, 5.8±1.0mV for BPV and 14.3±2.7% for LLS. The findings in

our study are consistent with these results: UPV=15.1±5.6mV, BPV=4.5±2.9mV, LLS=15.6±7.4%. Although Kornowski et al. mention the trend towards lower voltages in the mitral annulus area, no measurements are set forward. Our study is therefore the first to clearly delineate areas that show physiologically altered electromechanical properties. When defining electromechanical properties of posterior and septal areas, these findings should be taken into account.

Although not the main purpose of our study, we compared LVEF as assessed by electromechanical mapping using the new NOGA 4.0 software and compared these data with angiographically measured LVEF. We found a strong correlation, albeit with important absolute differences, as shown by the Bland-Altman analysis. Previously we have shown that in diseased ventricles, the two methods were not interchangeable for EF measurement [13]. In that study however, the use of a previous software version and the limited mapping experience may in part have accounted for the large differences in EF found. In the present study, although the differences are still important, EF measurements come in the range of echocardiographic and magnetic resonance measurements, which in previous studies have also shown differences in EF as compared to angiography that may reach up to 20-30%[14, 15]. The differences may be caused by the differences in volume calculation of the two methods, the fact that the pig tail catheter is used for calibration in the angiography method, which may induce significant absolute faults, the possibility that the mapping catheter may not reach all relevant areas, and also the fact that the effects of a sudden contrast injection into the left ventricle are not clear[16-18].

Limitations. The ventriculogram is a two-D reconstruction of a three-D structure, and may therefore not constitute the optimal technique for wall motion abnormality detection. Also, the computer-assisted centerline method is subject to interobserver variability, as choosing of the respective digitized cine frames and manual tracing of the endocardial border is operator-dependent. However, also a negative history and the absence of ECG abnormalities were necessitated to enter the study, so that it is probable that these were indeed normal left ventricles. The limitations concerning LV angiography may however influence the value of the EF measurements. Also, the importance of accurate apex positioning is of cornerstone importance. Indeed, the whole segmental division performed by the computer's algorithm is based on the initial choice of the apex by the operator. Although in all patients we carefully checked for defining the true apex, there is no absolute certainty that in all cases this was effectively accomplished.

Last, although high values for LLS and UPV were found in these normal ventricles, there still are important differences amongst patients (as there were in the study by Kornowski et al.[8]): differences for UPV reached from as low as 3mV to as high as 34mV, and for LLS from as low as 0% to as high as 33%. Although we performed a regression analysis model, no predicting clinical factor (such as gender, age, diabetes, use of beta-blockade, use of anti-arrhythmic medication...) could be isolated. The current study was not powered to find such differences. It remains to be seen if certain clinical characteristics may alter baseline voltages and local shortening function.

In conclusion, our study showed consistently high LLS, UPV and BPV throughout most of the left ventricle in patients with normal myocardial function. Only the basal septal and the basal posterior segments in the mitral annulus area showed lower LLS and UPV, with respect to the rest of the left ventricular segments. These findings have to be taken into account when assessing the myocardial function in this area. Secondly, NEM-derived

LVEF differs significantly from angiographic measurements, and may therefore necessitate comparison with other accepted techniques. Third, large differences in LLS, UPV and BPV of normal myocardial segments exist between patients and between normal segments in the same patient.

References

1. Ben-Haim SA, Osadchy D, Schuster I, Gepstein L, Hayam G, Josephson ME. Nonfluoroscopic, in vivo navigation and mapping technology. Nat Med 1996;2(12):1393-5.
2. Van Langenhove G, Smits P, Albertal M, Serrano P, Kay I, Poldermans D, et al. NOGA mapping for the detection of viable and ischemic myocardium: a comparison with dobutamine stress echocardiography (Abstract). Circulation 1999;100(18 (suppl)):I-23.
3. Kornowski R, Baim D, Moses J, Laham R, Hong M, Kuntz R, et al. Six month results following percutaneous direct myocardial revascularization guided by Biosense left ventricular mapping in patients with refractory coronary ischemic syndromes. (Abstract). Circulation 1999;100(18 (Suppl)):I-22.
4. Kornowski R, Fuchs S, Tio FO, Pierre A, Epstein SE, Leon MB. Evaluation of the acute and chronic safety of the biosense injection catheter system in porcine hearts. Catheter Cardiovasc Interv 1999;48(4):447-53; discussion 454-5.
5. Vale PR, Losordo DW, Tkebuchava T, Chen D, Milliken CE, Isner JM. Catheter-based myocardial gene transfer utilizing nonfluoroscopic electromechanical left ventricular mapping. J Am Coll Cardiol 1999;34(1):246-54.
6. Gepstein L, Hayam G, Ben-Haim SA. A novel method for nonfluoroscopic catheter-based electroanatomical mapping of the heart. In vitro and in vivo accuracy results. Circulation 1997;95(6):1611-22.
7. Gepstein L, Hayam G, Shpun S, Ben-Haim SA. Hemodynamic evaluation of the heart with a nonfluoroscopic electromechanical mapping technique. Circulation 1997;96(10):3672-80.
8. Kornowski R, Hong MK, Gepstein L, Goldstein S, Eliahham S, Ben-Haim SA, et al. Preliminary animal and clinical experiences using an electromechanical endocardial mapping procedure to distinguish infarcted from healthy myocardium. Circulation 1998;98(11):1116-24.
9. Gepstein L, Goldin A, Lessick J, Hayam G, Shpun S, Schwartz Y, et al. Electromechanical characterization of chronic myocardial infarction in the canine coronary occlusion model. Circulation 1998;98(19):2055-64.
10. Kornowski R, Hong MK, Leon MB. Comparison between left ventricular electromechanical mapping and radionuclide perfusion imaging for detection of myocardial viability. Circulation 1998;98(18):1837-41.
11. Slager CJ, Hooghoudt TE, Serruys PW, Schuurbiers JC, Reiber JH, Meester GT, et al. Quantitative assessment of regional left ventricular motion using endocardial landmarks. J Am Coll Cardiol 1986;7(2):317-26.
12. Biosense-Webster. NOGA Cardia Electromechanical Mapping System. User's Manual. Software Revision 2 ed; June 1998.
13. Van Langenhove G, Hamburger J, Smits P, Albertal M, Onderwater E, Kay I, et al. Evaluation of Left Ventricular Volumes and Ejection Fraction Using a Nonfluoroscopic Endoventricular Three- Dimensional Mapping Technique. A Comparison with Contrast Ventriculography. Am Heart J 2000:In Press.
14. Dilworth L, Aisen A, Mancini G, Lande I, Buda A. Determination of left ventricular volumes and ejection fraction by magnetic resonance imaging. Am heart J 1987;113:24-32.
15. Folland ED, Parisi AF, Moynihan PF, Jones DR, Feldman CL, Tow DE. Assessment of left ventricular ejection fraction and volumes by real- time, two-dimensional echocardiography. A comparison of cineangiographic and radionuclide techniques. Circulation 1979;60(4):760-6.
16. Beier J, Wellnhofer E, Oswald H, Fleck E. Accuracy and precision of angiographic volumetry methods for left and right ventricle. Int J Cardiol 1996;53(2):179-88.
17. Kaku K, Hirota Y, Shimizu G, Kita Y, Saito T, Kawamura K. Depressed myocardial contractility in mitral stenosis—an analysis by force-length and stress-shortening relationships. Jpn Circ J 1988;52(1):35-43.
18. Jehle J, Pehle R, Neuhaus KL, Schmiel FK, Spiller P. [Experimental studies of the effects of contrast medium on left ventricular function (author's transl)]. Z Kardiol 1981;70(9):670-7.

Chapter 3

Evaluation of Left Ventricular Volumes and Ejection Fraction Using a Nonfluoroscopic Endoventricular Three- Dimensional Mapping Technique. A Comparison with Contrast Ventriculography.

Glenn Van Langenhove, MD; Jaap N. Hamburger, MD; Peter C. Smits, MD; Mariano Albertal, MD; Emile Onderwater, BSc; I. Patrick Kay, MD; Patrick W. Serruys, MD. Thoraxcenter Rotterdam, Dijkzigt Hospital, Erasmus University, The Netherlands

Structured Abstract

Background: Recently, a novel non-fluoroscopic three-D electromechanical mapping technique was introduced in the clinical arena. Although initial in vitro and in vivo studies suggested the reliability of the system in volumetric and hemodynamic evaluation of the left ventricle, no validation in humans has been performed.

Methods: A nonfluoroscopic electromechanical mapping (NOGA™, Biosense-Webster) procedure was performed in 44 patients. All patients received a contrast left ventriculogram during the same session. Volumetric (end-diastolic (EDV) and end-systolic volumes (ESV)) and hemodynamic (LVEF and stroke volume (SV)) parameters using both systems were compared.

Results: Two uncomplicated pericardial effusions occurred with the first-generation mapping catheters. Using the new-generation mapping catheters, no procedural complications were noted. Significant correlations were found between mapping-derived and ventriculography-based measurements for both ESV ($r=0.67$, $p<0.001$) and LVEF ($r=0.78$, $p<0.001$). Absolute volumes, however, were only comparable for ESV (46.6 ml ±25.3 vs 48.8±37.0 resp, $p=0.13$), but differed greatly for LVEF (35%±13 vs 65±19 resp, $p<0.001$), EDV (69.1ml±28.6 vs 125.9±53.4 resp, $p<0.001$) and SV (22.4±9.9 vs 77.1±33.7 resp, $p<0.001$). Moreover, Bland-Altman analysis showed the clinical non-interchangeability between these techniques for the measurement of hemodynamic parameters.

Conclusion: Measurement of hemodynamic parameters using nonfluoroscopic mapping of the left ventricle is feasible and safe. The system provides data that strongly correlate, but that are in clinical disagreement with angiographic data. Therefore, the interchangeability of these techniques may be questioned.

Short title:

Three-D mapping for evaluation of LV volumes and EF

INTRODUCTION

The acquisition of hemodynamic data and the assessment of the left ventricular function remain of cornerstone importance in clinical cardiology. These parameters may play a role in the assessment of the severity of several cardiac disorders, may direct therapeutic options, and can evaluate the efficacy of measures taken[1-4]. Changes in left ventricular volumes during the various stages of the cardiac cycles and hence the left ventricular ejection fraction, have been measured by a variety of techniques, such as two-dimensional (two-D) echocardiography[5,6], two-D echocardiography with automated border detection[7,8], three-D echocardiography[9,10], radionuclide ventriculography[11-13], left ventricular contrast angiography[14], computed tomography[15] and magnetic resonance imaging (MRI)[16-18]. Most of these techniques however may have limitations. Two-D echocardiographic as well as angiographic techniques are based on geometric assumptions; this can be particularly hazardous when confronted with distorted ventricular anatomy. Three-D reconstruction of left ventricle dynamic volumes is time-consuming and can not be performed on-line, and -as in all echocardiographic techniques- depends on a good precordial image quality. Isotope-scanning techniques are expensive, while exact volume calculation is difficult. Furthermore computed tomography and MRI are not readily available.

Recently, a novel technique using a non-fluoroscopic electromechanical mapping (NEM) system has been proposed[19]. This technique utilizes a miniature locatable sensor that is incorporated in a 7 or 8 F (first generation) flexible catheter. Through the induction of a low magnetic field and with the use of a reference catheter that is placed on the back of the patient, the precise three-D location of the catheter-tip can be determined on-line. At the same time, electrodes located in the tip of the catheter measure typical electrophysiological data. The use of this technique in the assessment of volumetric measurements and of hemodynamic parameters has recently been validated in vitro and in the animal model[20]. In the present study we compared left ventricle (LV) volumes and ejection fraction (EF) measured by the NEM system to LV angiogram derived measurements.

METHODS

Definitions

Point loop stability (LS): measures the maximum of distances between the locations of the selected point in two consecutive heart cycles. Low absolute LS values indicate a good point.

Cycle length (CL) stability: the difference between the length of the current cycle and the average of the last 100 cycles recorded.

Local activation time (LAT) stability: measure of how stable the LAT is between cycles. Reliable points show a LAT variation of <3ms.

Location stability: a measure of the variability in position of the catheter tip on the endoventricular wall during two consecutive cardiac cycles.

Triangle fill threshold: this parameter, which can be altered by the operator, defines the minimum triangle size for which the computer algorithm will close a space between adjacent points, and thus will make an interpolation between actual data. For our data set

we used a uniform value of 40 mm.

Inner points filtering: computer algorithm that removes points thought to be located inside the ventricular lumen (and not on the ventricular wall) or on a papillary muscle. The algorithm calculates relative position of points as compared to at least three neighboring ones and is therefore able to remove these contending points.

System components and mapping technique

The system and its various components have been described previously [19-23]. In short, a low magnetic field (10^{-5} to 10^{-6} Tesla) is generated around the patient. A catheter securely taped to the patient's back serves as a reference to compensate for subject or heart motion during the procedure. A 7 or 8 French catheter containing a locatable sensor and recording electrodes in its deflectable tip is inserted through an 8 F femoral sheath and is then moved along the left ventricular endocardium. Acquired signals are then send through the catheter shaft and processed by the NOGA processing unit (Biosense-Webster). The system can determine the location (with an accuracy of <1mm) 24 and orientation of the catheter in six degrees of freedom (x, y, z, roll, pitch, and yaw). Electromechanical information is obtained using a combination of data gathered by the electrodes and the location sensor. Thus unipolar and bipolar endocardial potentials and local linear shortening data for every contact point are acquired, and can be displayed in bull's eye maps. Chamber geometry can then be accurately reconstructed using three-D endocavital information.

The computer algorithm directly calculates three-D volumes. Acquired points are synchronized using the intracardiac electrocardiogram provided by the system. At any specific point in the cardiac cycle, the system is able to calculate volumes by connecting all available points in a three-dimensional polyhedron. The computer algorhitm addresses the largest volume as the enddiastolic volume (EDV), and the smallest as the endsystolic volume (ESV). Ejection fraction is calculated as (EDV – ESV)/ EDV; stroke volume (SV) is calculated as EDV – ESV.

Post-processing of data was performed to eliminate points suggestive for catheter tip instability, as evidenced by catheter point loop stability, cycle length stability, local activation time and location stability data. A triangle fill threshold of 40 mm was chosen for our data set. This setting allows the system to fill triangles between acquired points using an interpolation algorithm; distances between points larger than 40 mm were left blank until points in between were captured.

After applying an inner point filtering by the computer algorithm, points were manually deleted when they did not fit standard stability criteria (location stability <4mm, cycle length stability < 10% and loop stability <4mm), if they were taken during ST-segment elevation (suggestive for severe wall impression), if adjacent points were closer than 5 mm (local linear shortening data proved to be unreliable if measured under these conditions) and if the points were not related to the left ventricle (such as atrial location).

Contrast left ventricular angiogram

Prior to the electromechanical mapping, biplane left ventricular angiograms in a 30° right anterior oblique and 60° left anterior oblique view using 7 F pig tail catheters were performed. Calibration was performed using non contrast-filled catheters. Measurements of ventricular volumes were calculated during sinus rhythm only . Measurements of

ventricular volumes during or after an extrasystole were avoided. LV angiograms were made with the patient in a stable position and during maximal inspiration. The measurements were performed on the CAAS II system (PIE medical, Maastricht, The Netherlands) by an independent investigator, who was blinded for the left ventricular mapping data. This system calculates left ventricular volumes using the area length method of Dodge for single plane angiography, modified by Kennedy et al[25,26]. Ejection fraction was then calculated through the above mentioned formula EF=(EDV-ESV)/EDV.

Patients and mapping procedure

The study protocol was approved by the ethics committee of the hospital, and all patients signed an informed consent prior to the procedure.

Coronary angiography was performed in all patients using standard 6F diagnostic and 7F pig tail catheters. A 7 or 8F mapping catheter was then introduced through an 8 F femoral sheath and placed in the left ventricle. The apex of the left ventricle and the aortic and mitral valves were located using fluoroscopic guidance, to ensure the exact location of these important anatomical landmarks, which could then be used as reference points. Further mapping was done solely using the mapping system, unless repositioning of the catheter in the left ventricle was necessary.

The volume-time curves were examined to make sure that smallest and largest volumes along the cardiac cycle were chosen by the computer algorithm to calculate the hemodynamic parameters (figure 1).

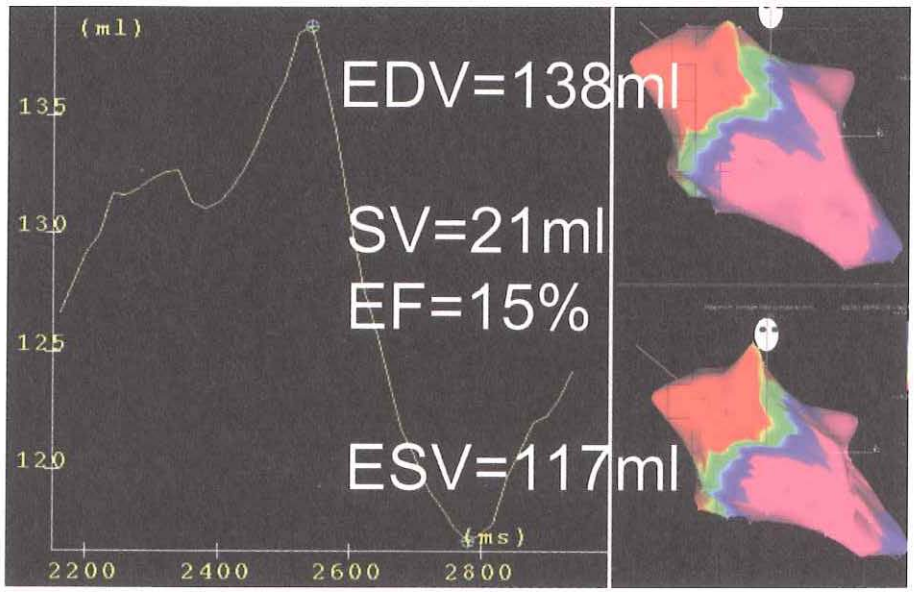

Figure 1

Example of volume-time curves displayed by the non-fluoroscopic electromechanical mapping (NOGA™) system. The blue + marks in the left-side picture show the points of minimal and maximal volumes, respectively. Electromechanical maps showing maximal and minimal volumes are shown to the right.

To ensure hemodynamic stable conditions during the mapping procedure, heart rate and blood pressure were monitored continuously.
A representative map of the left ventricle in end-diastole and end-systole, and its corresponding RAO and LAO ventriculographic views are shown in figure 2.

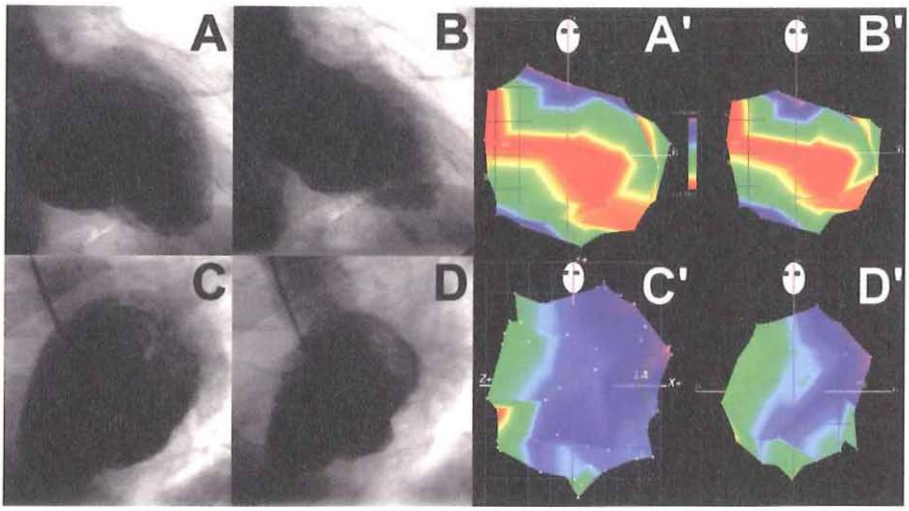

Figure 2

Example of ventriculographic (A-D) and corresponding unipolar voltage (UPV) maps using the NOGA™ system (A'-D'). A=RAO at end-diastole with A' as its corresponding view using the mapping system in the same patient; B (B') =RAO end-systole; C (C') = LAO end-diastole; D (D') =LAO end-systole. The color code shown in A' shows regions with UPV < 6 mV in red, and zones with high UPV in blue-purple (>14 mV). Enddiastolic (EDV) and endsystolic (ESV) volumes, stroke volume (SV) and left ventricular ejection fraction (LVEF) are shown for both techniques. The most distal apical part is possibly not entirely mapped, explaining in part why end diastolic measurements may be underestimated using the mapping technique.

Statistics

Data are reported as mean ± SD. Means of values acquired with both techniques were compared using an unpaired Student's t-test. Correlation coefficients are reported as R2 and were calculated with a Pearson test. The techniques used for volumetric data acquisition and ejection fraction calculation were compared using a Bland-Altman test[27]. A value of $p<0.05$ was considered significant.

Results

A mapping procedure was performed in 44 patients. Mean age of the patients (39 males, 89%) was 59.2 ± 9.7 years. Twenty-nine patients (66%) had a previous myocardial infarction with wall motion abnormalities on the LV angiogram. Twenty-four patients (55%) had a history of coronary artery bypass surgery, 29 patients (66%) were previously treated with a percutaneous coronary intervention. Maps were performed with an average

procedure time of 45 ± 15 minutes. On average, 89 ± 42 (range 77-165) points were taken. After editing, 62 ± 30 (range 51-113) points remained as the basis for our analysis. With the 8F first generation catheter there were two incidents of pericardial effusion necessitating pericardial drainage. With the new 7F catheter (n=18) there were no procedural complications. Average fluoroscopy time was 3.2 ± 2.4 minutes. The catheter was re-introduced into the left ventricle 4 ± 2 times.
Mean values of angiographic and endoventricular mapping EDV, ESV, SV and LVEF data are shown in the table. Except for the ESV values, the absolute values as measured by the two different methods were significantly different between individual patients. As the ESV values were comparable for both methods, the higher enddiastolic volumes measured by contrast ventriculography account for the higher values of LVEF measured with this technique. The Pearson test (see table)

Table. Comparison between LV angiography and NOGA™ mapping for the assessment of hemodynamic parameters

NEM-parameters		**Angiographic parameters**		**Comparison of the means**	**Correlation (Pearson) R^2**	**p-value of correlation**
MaxVolume (ml ± SD)	69.1 ± 28.6	EDV Angio (ml ± SD)	125.9 ± 53.4	<0.001	0.09	0.1
MinVolume (ml ± SD)	46.6 ± 25.3	ESV Angio (ml ± SD)	48.8 ± 37.0	0.13	0.45	<0.001
SV (ml ± SD)	22.4 ± 9.9	SV Angio (ml ± SD)	77.1 ± 33.7	<0.001	0.014	0.52
LVEF (% ± SD)	35 ± 13	LVEF Angio (%± SD)	65 ± 19	<0.001	0.61	<0.001

The table shows the respective volumes of the left ventricle and the derived parameters LVEF and SV measured by the two methods; NEM =Nonfluoroscopic Electromechanical Mapping, SD=Standard Deviation, Max= maximum, Min =minimum, LVEF=Left Ventricular Ejection Fraction, EDV =Enddiastolic Volume, ESV =Endsystolic Volume, Angio =Angiographic. Columns 5 to 7 show the p-value for the comparison of the means, correlation R2 (Pearson) and the p-value for correlation, respectively.

shows the correlation coefficients between measurement techniques. A significant correlation between NOGA™ and angiography for ESV and EF is shown, where no such correlation was found for EDV and SV. When we divided the patients in groups without versus with regional wall motion abnormalities, correlations for EF, EDV, ESV and SV were 0.08 (not significant (NS)), 0.14 (NS), 0.50 (p=0.04), and 0.1 (NS) respectively for the normal ventricles, versus 0.69 (p=0.005), -0.38 (NS), 0.15 (NS) and 0.54 (p=0.03) respectively for the ventricles with wall motion abnormalities.
The correlation between the two methods is shown in figure 3.

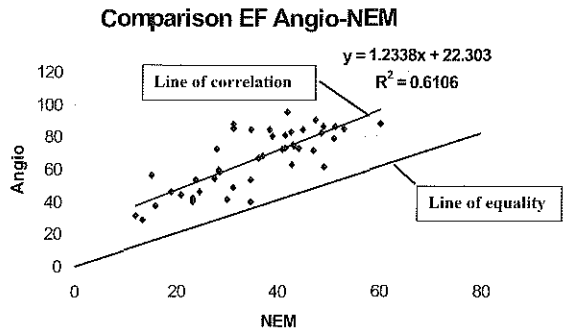

Figure 3

Scatterplot for the left ventricular ejection fraction (LVEF) obtained with angiographic (Angio) and nonfluoroscopic (NEM) measurements of LVEF.
A line of equality is drawn in the picture. This line shows the optimal situation in which the values of a parameter measured by two different methods would not only correlate perfectly, but in which the measurement techniques would also be interchangeable. The line of correlation, the correlation equation and the value of correlation are also shown.

Although this method of comparison may not provide a correct interpretation of the data[27], the figure however provides an idea of the general correlation between the methods. The line of equality and the line of correlation approach each other in the area of lower ejection fractions, suggesting a better correlation between the two methods for patients with worse ejection fractions.

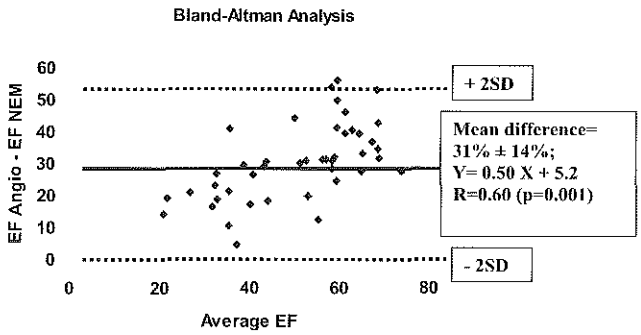

Figure 4

Bland-Altman plot for angiographic and mapping technique measurements of left ventricular ejection fraction (LVEF). The analysis demonstrates the large mean difference in LVEF between the two techniques, with values measured by left ventricular angiography being on average 31% higher. EF = Ejection Fraction; Angio = Angiographic; NEM = Nonfluoroscopic Electromechanical Mapping; SD = Standard Deviation

Figure 4 shows a Bland-Altman analysis comparing angiographic measurements of LVEF and nonfluoroscopic electromechanical mapping measurements.

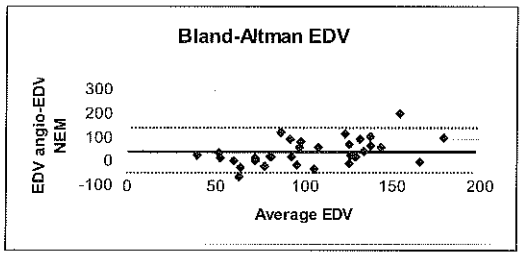

Figure 5a. Bland-Altman comparison of EDV measurements.
Mean difference = 43.8 ± 53.8 ml

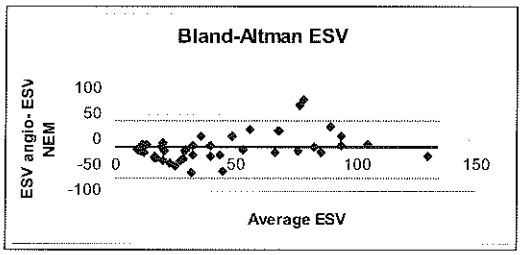

Figure 5b. Bland-Altman comparison of ESV measurements.
Mean difference = -14.2 ± 27.7 ml

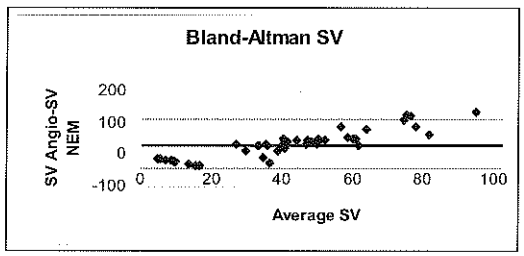

Figure 5c. Bland-Altman comparison of SV measurements.
Mean difference = 33.3 ± 44.7 ml

Figure 5

The different Bland-Altman plots for End-Diastolic Volumes (EDV), End-Systolic Volumes (ESV) and Stroke Volume (SV) respectively. Only measurements of ESV are in relatively close agreement with one another. Measurements of EDV and SV differ on average 33 ml and 44 ml respectively, and therefore do not seem to be interchangeable in the clinical setting.

Figure 5 shows Bland-Altman analyses for ESV, EDV and SV measured by the two techniques. These figures demonstrate the disagreement and absence of interchangeability between all measured parameters, even for those measurements that showed the strongest correlations. Indeed, the average difference mounts up to 44±54 ml, -14±28 ml, 33±45 ml and 31±37% for EDV, ESV, SV and LVEF respectively.
Also, a bivariate Pearson's correlation test showed a significant correlation between the

total amount of points acquired and of points edited, and the maximum diastolic volume measured by NEM (correlation R2 0.40, p<0.001 and 0.50, p<0.001 respectively).

Discussion

The current study showed that the absolute values of LVEF and ESV provided by the mapping technique are correlated to the volumetric measurements using angiography. However, the Bland-Altman analysis showed an important disagreement and thus a clinical non-interchangeability between the two measuring techniques. As shown in the table, end-systolic volumes had a good correlation, but end-diastolic volumes differed greatly. Moreover, ventricles with regional wall motion abnormalities seemed to have better correlations for both LVEF and SV than did normal ventricles. The explanation for these findings is not straightforward. One possible explanation is that spaces between chordae, or around the papillary muscles, are filled with contrast, but are not easily reached with the mapping catheter. In the end-systolic phase these spaces are cleared of contrast through the muscular contractions, and the end-systolic volumes recorded were indeed in better agreement for both techniques. Also, careful review of the angiograms acquired in our patients suggested a considerable movement of the apex towards the base of the ventricle; earlier studies using implanted markers however clearly showed the remarkable stationary behavior of the apex[28-30]. This may account for a difference of the volumetric changes. Thirdly, there is no certainty that at the end of a mapping procedure, all myocardial areas are covered. As the three-D reconstruction is based on points collected by the mapping catheter, the LV volumes can be underestimated if not all regions of the LV were covered by the catheter. It is furthermore clear that within these non-covered regions anatomical variations may occur. We used the area-length method for the angiographic measurements. Although minor differences between measuring techniques may exist, Kussmaul et al. recently found that all methods correlate well and do not show important differences in volumetric analysis.[44]

Nonfluoroscopic electromechanical mapping is a novel technique that enables the investigator to acquire on-line information on electrical and mechanical endoventricular functioning of myocardial tissue. Previously, investigators have found this technique to be easy, safe, reliable and reproducible[31]. Kornowski et al. showed the reliability of the system in differentiating normal from infarcted myocardial tissue[23]. Gepstein et al. found a strong correlation of hemodynamic parameters in the animal model acquired with NEM and stroke volume measured through the Fick method[20]. This study however was performed on only 12 pigs with a normal left ventricular function, so that the drawing of definite conclusions from this experience may be hazardous. Another issue that may interfere with our findings, is the inter- and intra-observer variability. Gepstein et al however showed a low intra- (8% for EDV, 12% for ESV, 5% for SV and 7% for EF) and inter-observer variability (6% for EDV, 8% for ESV, 11% for SV and 7% for EF). Again, the study refers to only 12 pigs[20].

The number of points acquired and the number of points retained in the manually edited maps in the present study correlated strongly with the EDV measured. This finding confirms the first results of Gepstein et al., where he stated that volume measurements can be performed accurately after acquisition of 40 points in the animal model [20]. Possibly a much higher amount of points is needed in the ischemic and distorted left ventricle. The

low end diastolic volumes obtained by electromechanical mapping may indeed reflect incomplete endocardial sampling.

Although the LV angiogram is considered a "gold standard", the literature on the value of measurements of ventricular volumes using angiography is somewhat contradictory. Volumes calculated by the different angiographic volume calculation methods regularly exceed known volumes[32].This might be explained by the fact that all current methods apply an ellipsoid reference, which might not be truly representative of the irregularly shaped LV. Previous studies have shown lower absolute values by other techniques such as radionuclide tomography (25% difference)[33], echocardiography (35%)[34], or computed tomography studies(40%)[35], measuring LVEF as compared to ventriculography, while others showed good correlations between the different methods [36,37]. Starling et al. showed that standard orthogonal projections (RAO 30° and LAO 60°) as used in our study, provide accurate determinations of left ventricular volumes and hence ejection fractions[38]. Rogers et al. found a highly accurate volume determination using biplane angiocardiography in the RAO/LAO method[39]. Beier et al. recently found that manual contour detection for left ventricle angiographic volumetry results in an over-estimation of the measured volumes. These authors stated that these measurements are case dependent and should only be seen as an estimate of the actual values[40]. A second observation is that the ancillary structures inside the left ventricle are not taken into account when calculating the size of the left ventricle with angiography. Indeed, structures as the papillary muscle are obscured by contrast on two-dimensional films, and volumes are calculated as if these structures were not present. Furthermore, it has not been shown what the precise effect is of a sudden injection of a volume of contrast material on the left ventricular function. Possibly the hyperacute (i.e. within seconds) effect is negligible, as previously shown.[41,42] Erbel et al. however showed comprehensively that 10 minutes after contrast injection the ischemic ventricle shows a pronounced alteration (increase as well as decrease, depending on amount and duration of injection and baseline hemodynamic characteristics) of the systolic and diastolic function[43]. It is therefore possible that during the mapping procedure (performed immediately after the contrast ventriculogram) left ventricular volumes and hemodynamic properties are influenced by a previous injection of contrast.

It could be of relevance that non-fluoroscopic measurements are made during a time period of circa 30-40 minutes. Although hemodynamic stability was present in all patients during the procedure, it is possible that in this time frame, some minor changes in the LV function occurred. Also, as this technique is not easy to master, and has only recently been developed, increased operator experience may improve the agreement between the two methods.

In conclusion, our study showed that LVEF measurement using nonfluoroscopic mapping of the left ventricle is feasible and safe. The system however provides data that are in strong correlation but clinical disagreement with LV angiographic data. Therefore, the interchangeability of these techniques may be questioned. Announced improvements of the computer algorithm (with smoothening of the contours detected by the mapping catheter) may rectify this shortcoming.

References

1. McGhie AI, Willerson JT, Corbett JR. Radionuclide assessment of ventricular function and risk stratification after myocardial infarction. Circulation. 1991;84(suppl I):167- 76.
2. Becker LC, Silverman KS, Bulkley BH, Kallman CH, Mellits ED, Weisfeldt M. Comparison of early thallium-201 scintigraphy and gated blood pool imaging for predicting mortality in patients with acute myocardial infarction. Circulation. 1983;67:1272-82.
3. Cintron G, Johnson G, Francis G, Cobb F, Cohn JN, for the V-HeFT VA Cooperative Studies Group. Prognostic significance of serial changes in left ventricular ejection fraction in patients with congestive heart failure. Circulation. 1993;87(suppl VI):17-23.
4. Pfeffer MA, Braunwald E, Moye LA, Basta L, Brown EJ, Cuddy TE, Davis BR, Geltman EM, Goldman S, Flaker GC, Klein M, Lamas GA, Packer M, Rouleau J, Rouleau JL, Rutherford J, Wertheimer JH, Hawkins CM. Effect of captopril on mortality and morbidity in patients with left ventricular dysfunction after myocardial infarction. N Engl J Med 1992;327:669-77.
5. Gueret P, Meerbaum S, Wyatt HL, Uchiyama T, Lang TW, Corday E. Two-dimensional echocardiographic quantitation of left ventricular volumes and ejection fraction. Circulation 1980;62:1308-18
6. Wyatt HL, Heng MK, Meerbaum S, Gueret P, Hestenes J, Dula E, Corday E. Cross-sectional echocardiography. Analysis of mathematic models for quantifying volume of the formalin-fixed left ventricle. Circulation 1980; 61: 1119-25
7. Chandra S, VK Bahl, SCB Reddy, B Bhargava, A Malhotra, HS Wasir. Comparison of echocardiographic acoustic quantification system and radionuclide ventriculography for estimating left ventricular ejection fraction: Validation in patients without regional wall motion abnormalities. Am Heart J 1997;133:359-63
8. Van Langenhove G, Vaerenberg M, Oei F, Van den Branden F ; Estimating Left Ventricular Ejection Fraction : a Comparison Between Acoustic Quantification, Contrast Ventriculography and Radionuclide Ejection Fraction. Eur Heart J 1998;19:375.
9. Nosir YFM, Fioretti PM, Vletter WB, Boersma E, Salustri A, Postma JT, Reijs AEM, Ten Cate FJ, Roelandt JRTC. Left Ventricular Ejection Fraction by 3D Echocardiography. Circulation 1996; 94:460-66
10. Nosir YFM, Salustri A, Kasprzak JD, Breburda CS, Ten Cate FJ, Roelandt JRTC. Left ventricular ejection fraction in patients with normal and distorted left ventricular shape by two three-dimensional echocardiographic methods; a comparison with radionuclide angiography. J Am Soc Echocardiogr 1998;11:620-30
11. Hains AD, Khawaja IA, Lahiri A, Raftery FB. Radionuclide left ventricular ejection fraction: a comparison of three methods. Br Heart J 1987;57:232-6
12. Shah PK, Picher M, Berman DS, Singh BN, Swan HJC. Left ventricular ejection fraction determined by radionuclide ventriculography in early stages of first transmural myocardial infarction. Am J Cardiol 1980;45:542-6
13. Nichols K, De Pucy EG, Gooneratne N, Saledsky H, Friedman M, Cochoff S. First-pass ventricular ejection fraction using a single-crystal nuclear camera. J Nucl Med. 1994;35:1292-1300
14. Dodge HT, Sandler H, Baxley WA, Hawley RR. Usefulness and limitations of radiographic methods for determining left ventricular volume. Am J Cardiol 1966;18:10-24
15. Reiter SJ, Rumberger JA, Feiring AJ, Stanford W, Marcus ML. Precision of measurements of right and left ventricular volume by cine computed tomography. Circulation 1986;74:890-900
16. Dilworth LR, Aisen AM, Mancini GBJ, Lande I, Buda AJ, Determination of left ventricular volumes and ejection fraction by magnetic resonance imaging. Am Heart J 1987;113:24-32
17. Benjelloun H, Granney GB, Kirk KA, Blackwell GG, Lotan CS, Pohst GM. Interstudy reproducibility of biplane cine nuclear magnetic resonance measurements of left ventricular function. Am J Cardiol 1991;1413-20
18. Sakuma H, Fujita N, Foo TKF, Caputo GR, Nelson SJ, Hartiala J, Shimakawa A, Higgins CB. Evaluation of left ventricular volume and mass with breath-hold cine MR-imaging. Radiology 1993;188:377-80

19. Ben-Haim SA, Osadchy D, Schuster I, Gepstein L, Hayam G, Josephson ME. Nonfluoroscopic, in vivo navigation and mapping technology. Nat Med. 1996;2:1393-5
20. Gepstein L, Hayam G, Shpun S, Ben-Haim SA. Hemodynamic Evaluation of the Heart With a Nonfluoroscopic Electromechanical Mapping Technique. Circulation 1997;96:3672-80
21. Shpun S, Gepstein L, Hayam G, Ben-Haim SA. Threedimensional Magnetic Guidance of radiofrequency Ablation. Circulation 1997; 96: 2016-21
22. Kornowski R, Hong MK, Leon MB. Comparison Between Left Ventricular Electromechanical Mapping and Radionuclide Perfusion Imaging for Detection of Myocardial Viability. Circulation 1998; 98:1837-41
23. Kornowski R, Hong MK, Gepstein L, Goldstein S, Ellahham S, Ben-Haim SA, Leon MB. Preliminary animal and clinical experiences using an electromechanical endocardial mapping procedure to distinguish infarcted from healthy myocardium. Circulation 1998;98:1116-24
24. Gepstein L, Hayam G, Ben-Haim SA. A novel method for nonfluoroscopic catheter-based electroanatomical mapping of the heart: in vitro and in vivo accuracy results. Circulation 1997;95:1611-22
25. Dodge HT, Sandler H, Baxley WA, Hawley RR. Usefulness and limitations of radiographic methods for determining left ventricular volume. Am J Cardiol 1966,18:10-24
26. Kennedy JW, Trenholme SE, Kasser IS. Left ventricular volume and mass from single-plane cineangiocardiogram. A comparison of anteroposterior and right anterior oblique methods. Am Heart J 1970;80:343-52
27. Bland JM, Altman DG. Statistical methods for assessing agreement between two methods of clinical measurement. Lancet 1986;1:307-10
28. Ingels NB, Mead CW, Daughters GT, Stinson EB, Alderman EL. A new method for assessment of left ventricular wall motion. In: Computers in cardiology. Long Beach, CA: IEEE Computers Society, 1978:57-61
29. McDonald IG. The shape and movements of the human left ventricle during systole. Am J Cardiol 1970;26:221-30
30. Slager CJ, Hooghoudt TEH, Serruys PW, Schuurbiers JCH, Meester GT, Verdouw PD, Hugenholtz PG. Quantitative assessment of regional left ventricular motion using endocardial landmarks. J Am Coll Cardiol 1986;7:317-26
31. Smeets JLRM, Ben-Haim SA, Rodriguez LM, Timmermans C, Wellens HJJ. New method for nonfluoroscopic endocardial mapping in humans: accuracy assessment and first clinical results. Circulation 1998;97:2426-32
32. Dodge HT, Sandler H, Ballew DW, Lord JD. The use of biplane angiocardiography for measurement of left ventricular volume in man. Am Heart J 1960;60:762.
33. Nusynowitz ML, Benedetto AR, Walsh RA, Starling MR. First-pass Anger camera radiocardiography: biventricular ejection fraction, flow, and volume measurements. J Nucl Med 1987;28:950–9
34. Folland ED, Parisi AF, Moynihan PF, Jones DR, Feldman CL, Tow DE. Assessment of left ventricular ejection fraction and volumes by real-time, two-dimensional echocardiography. A comparison of cineangiographic and radionuclide techniques. Circulation 1979;60:760-6
35. Foster CJ, Brownlee WC, Griffin JF, Yates J, Love HG, Isherwood I. A comparison of angiographic and electrocardiographically gated computed tomography measurements of left ventricular function. Br J Radiol 1987;60:969-74
36. Williams KA and Taillon LA. Left Ventricular Function in Patients With Coronary Artery Disease Assessed by Gated Tomographic Myocardial Perfusion Images: Comparison With Assessment by Contrast Ventriculography and First-Pass Radionuclide Angiography. J Am Coll Cardiol 1996;27:173-81
37. Gueret P, Meerbaum S, Zwehl W, Wyatt HL, Davidson RM, Uchiyama RM, Corday E.. Two-dimensional echocardiographic assessment of left ventricular stroke volume: experimental correlation with thermodilution and cineangiography in normal and ischemic states. Cathet Cardiovasc Diagn 1981;7:247-58
38. Starling MR, Walsh RA. Accuracy of biplane axial oblique and oblique cineangiographic left ventricular cast volume determinations using a modification of Simpson's rule algorithm. Am Heart J 1985;110(6):1219-25

39. Rogers WJ, Smith LR, Hood WP Jr, Mantle JA, Rackley CE, Russell RO Jr. Effect of filming projection and interobserver variability on angiographic biplane left ventricular volume determination. Circulation 1979;59: 96-104
40. Beier J, Wellnhofer E, Oswald H, Fleck E. Accuracy and precision of angiographic volumetry methods for left and right ventricle. Int J Cardiol 1996;53(2):179-88
41. Kaku K, Hirota Y, Shimizu G, Furubayashi K, Kawamura K. Sequential changes of left ventricular function after cineangiography in normal heart and coronary artery disease. Jpn Circ J 1984;48:552-8
42. Jehle J, Pehle R, Neuhaus KL, Schmiel FK, Spiller P. Experimental studies of the effects of contrast medium on left ventricular function. Z Kardiol 1981;70:670-7
43. Erbel R, Neuhaus KL, Spiller P, Benn M, Kreuzer H. The effect of contrast medium injection into the left ventricle on systolic and diastolic ventricle function. Z Kardiol 1976;65:305-18

Chapter 4

Mechanical properties of the left ventricle in patients with severe coronary artery disease. A comparison between nonfluoroscopic mapping and two-dimensional echocardiograms.

Glenn Van Langenhove[a], MD; Jaap N. Hamburger[a], MD; Jos R.T.C. Roelandt[b], MD; Peter C. Smits[a], MD; Emile Onderwater[a], BSc; Mariano Albertal[a], MD; Alex J. Wardeh[a], MD; AH Marco Knook[a], MD; Patrick W. Serruys[a], MD.

From the Departments of [a]Interventional Cardiology and [b]Echocardiography, Thoraxcenter Rotterdam, Dijkzigt Hospital, Erasmus University, Rotterdam, The Netherlands

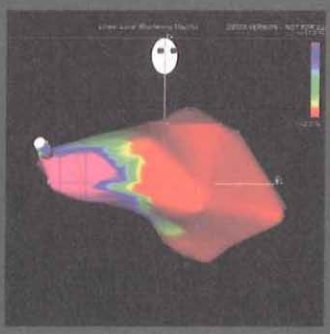

Two-sentence summary for the table of contents

In 40 patients, we compared local linear shortening assessed with nonfluoroscopic electromechanical mapping (NEM) as a function of regional wall motion with echocardiographic data in a subset of patients with severe coronary artery disease and subsequently decreased LV-function. Our study showed that NEM mapping can accurately assess regional wall motion. In addition, this study showed a significant decrease in unipolar voltages amongst segments with declining regional function.

Running Head:

Nonfluoroscopic mapping for left ventricle evaluation

Key words:

Nonfluoroscopic mapping
Echocardiography
Regional wall motion

Text

Recently, a novel nonfluoroscopic electromechanical (NEM) three-dimensional on-line in-cathlab mapping device for assessment of left ventricle electrical and mechanical function has been introduced[1]. The mapping system has proven its accuracy in the exact delineation of infarcted myocardium when compared to radionuclide and pathology studies[2,3]. Recent reports have suggested its value in the detection of viability in myocardium with reduced function.[4] The current study compared the mechanical properties (local linear shortening, LLS) of diffusely diseased myocardium in patients with severe coronary artery disease assessed with the NEM system, with echocardiography data for comparable segments. In addition, unipolar voltages (UPV) for segments with different contractility patterns were compared.

The NEM system has been described previously.[1-7] It is composed of a miniature passive magnetic field sensor incorporated in a catheter, an external ultralow magnetic field emitter (location pad), and a processing unit (NOGA™, Biosense-Webster, Cordis, Johnson&Johnson). The deflectable-tip catheter contains both a location sensor just proximal to its tip, and standard electrodes that allow recording of unipolar (UPV) and bipolar (BPV) electrical signals.

The locator pad placed beneath the operating table consists of three radiators that generate ultralow magnetic fields ($5x10^{-5}$ to $5x10^{-6}$ Tesla) that contain the information necessary to resolve the location and orientation of the sensor in 6 degrees of freedom.[1] As the catheter tip is dragged over the LV endocardial surface, the system continuously analyzes its location in 3-dimensional space without the use of fluoroscopy. The set of points thus collected comprises a data set of location points that are members of the endocardial surface. Chamber geometry is then reconstructed, in real time, using the set of sampled location points. Electrical (through the incorporation of standard electrodes in the catheter's tip) and mechanical (through LLS measurement, see further) function of the myocardium can thus be assessed.[1,2,5,6] The LLS assessment is based on the assumption that in healthy myocardium any two points move closer to each other during contraction. Measurement of distances between neighboring points is therefore the basis for calculation of myocardial shortening. The computer algorithm takes into account the density of points around a point p, and gives a negligible weight to points too close (sampling noise) and points too far (of no influence as they provide non-local information).[8] LLS is the average of the change in distance between any point p and its ten closest surrounding points of interest from end-diastole to end-systole, normalized for the length at end diastole.[8]

Electrical data (UPV, BPV and local activation time) and mechanical data (LLS) can be displayed in a three-dimensional way, and the images obtained can be viewed from any angle chosen by the operator. A bull's eye view showing average voltages, activation time or LLS for 12 segments (basal, mid and apical parts of anterior, lateral, posterior and septal segments) can be seen in an extra window on the NOGA™ screen (figure 1).

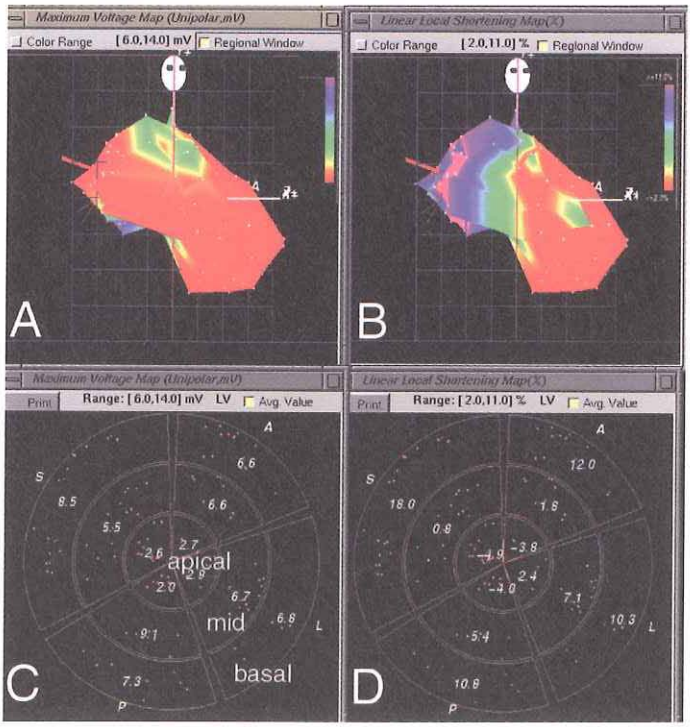

Figure 1

Example of a nonfluoroscopic electromechanical map in a patient with a large apical aneurysm. Figure A shows the unipolar voltage (UPV) map in RAO view. The color bar on the right shows the color coding ranging from red (≤ 6.0 mV) to blue-purple (≥ 14.0 mV). Clearly, a large apical aneurysmal sac with very low voltages – suggesting scar tissue - can be seen (white arrowheads). Figure B shows the local linear shortening (LLS) map in the same RAO view. The color bar ranges from red (LLS ≤ 2.0%) to blue-purple (≥ 11.0%). Again, the extent of the apical aneurysm becomes clear. Figure C shows the bull's eye view of the unipolar voltage map as displayed by the system. Four regions (clockwise from top: anterior (A), lateral (L), posterior (P) and septal (S)) are each divided in 3 segments (apical, mid and basal), dividing the whole map in twelve segments. The low UPV's of all apical segments are shown (white arrow). Figure D shows the bull's eye view of the LLS map, again with very low LLS values for the entire apex, with the akinesia extending towards the mid septal (LLS = 0.8%) and mid anterior region (LLS = 1.8%).

Between March 1998 and November 1999, we performed nonfluoroscopic mapping on 40 patients (34 male, 85%). Of these patients, 38 (95%) previously underwent percutaneous or surgical revascularization, 31 (78%) had suffered a myocardial infarction. Prior to the mapping procedure, an echocardiogram was performed in all patients. Two-dimensional echocardiograms were obtained at rest with a commercially available system (Hewlett Packard Sonos 5500; HP Company, Palo Alto, Cal,USA) with the patients lying in the left lateral decubitus position. Standard views, including conventional parasternal short and long axes, and apical 2- and 4-chamber views were used. Segmental wall motion was visually evaluated and scored as normal, hypokinetic or akinetic. The echocardiographic

data were obtained by 3 experienced cardiologists who were unaware of the mapping results. To produce a comparable data set, the 16-segment division used for the echocardiographic analysis was reduced to 12 segments as shown in figure 2.

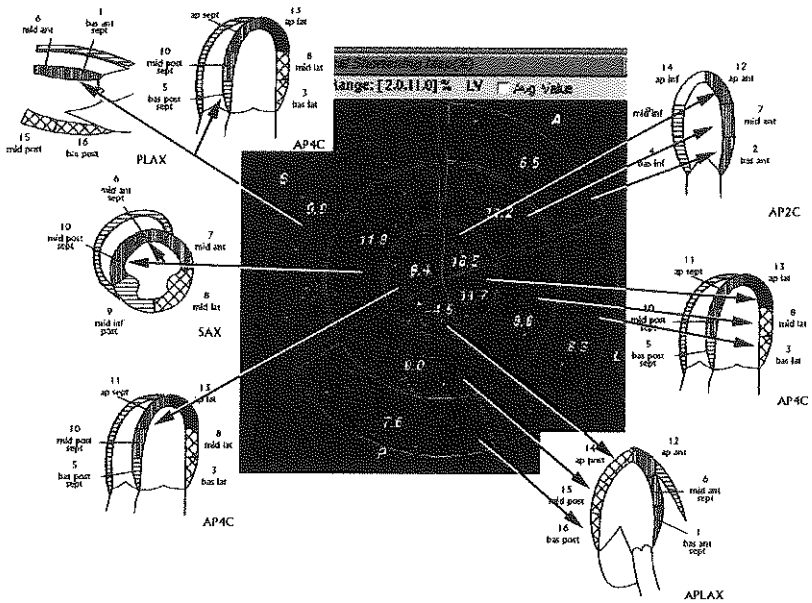

Figure 2

Reduction of the 16- segment division of the echocardiographic images to 12 segments to produce a data set comparable with the 12-segment division of the bull's eye LLS map shown in color. (A) shows the 3 anterior segments in the echocardiographic apical two-chamber view with the corresponding segments on the bull's eye, (B) the 3 lateral segments, (C) the 3 posterior segments, and (D) the 3 septal segments. From (D) one can appreciate the fact that for both the mid and basal septal segments on the bull's eye, 2 echocardiographic segments were taken into account. If these segments were in disagreement, the worst evaluation was chosen.
Abbreviations for each echocardiographic view (from upper right (A), clockwise): AP2C= apical two-chamber view, AP4C= apical four-chamber, APLAX= apical long axis, SAX= short axis, PLAX= parasternal long axis.

The study was approved by the local ethics committee, and all patients signed an informed consent.
Data are presented as mean ± SD. Means of nominal values (UPV and LLS) were compared between segments with normal wall motion, mild or severe hypokinesia or akinesia by one-way analysis of variance (ANOVA). Comparison between groups was made by independent t-test with Bonferroni correction. A value of $p < 0.05$ was considered statistically significant.
Of 480 segments, 46 (10%) could not be assessed because less than 3 points were taken during the mapping procedure (n=13), or because of insufficient image quality for proper

echocardiographic assessment (n=33). Of the remaining 434 segments, 136 were normal, 210 were hypokinetic, and 88 were akinetic. The average values of LLS and UPV, the results of the ANOVA and of the unpaired t-tests are shown in the table.

	Normal	p-values	Hypokinesia	p-values	Akinesia	Overall ANOVA
N	136		210		88	434
UPV (mV ± SD)	14.86 ± 5.42	<0.0005*	9.23 ± 3.62	<0.0005 †	6.95 ± 3.83	<0.0005
LLS (% ± SD)	13.15 ± 5.89	<0.0005*	7.56 ± 4.36	<0.0005 †	3.26 ± 7.16	<0.0005

**for the comparison with hypokinetic and akinetic segments ; † for the comparison with akinetic segments. UPV= Unipolar Voltage, LLS= Linear Local Shortening, SD= Standard Deviation, ANOVA= Analysis Of Variance.*

Table

Unipolar voltages and local linear shortening for normal, hypokinetic or akinetic segments, the results of the different independent t-tests with Bonferroni correction, and the result of the overall ANOVA.

Our study showed highly significant differences in LLS as assessed through NEM mapping for segments scored as normal, hypokinetic or akinetic on echocardiography. Also, UPV proved to be significantly different amongst these segments.
Kornowski et al. recently demonstrated concordances in regional wall motion assessment between NEM mapping and echocardiography ranging from 58% to 100%, depending on the segment analyzed. The power of these findings however were hampered by the low number of patients included in this substudy (n=12).[3]
The absolute values for normal and akinetic segments reported in our study are in close agreement with previously published data.[4] It must be stressed however that segments that are akinetic on echocardiography do not necessarily all reflect scarred tissue, as viability may be present in some of these segments.
Limitations: Assessment of regional wall motion through echocardiography is strongly operator-dependent. Furthermore, although at least three points per segment were taken, this may not be enough to cover the complete segment. Also, the reduction of the echocardiographic assessment from 16 to 12 segments is not validated.
In conclusion, our study showed that NEM mapping –through its LLS-function- can accurately assess regional wall motion in a subset of patients with severe coronary artery disease and subsequently decreased LV-function. In addition, this study shows a significant decrease in UPV amongst segments with declining regional function .

References

1. Ben-Haim SA, Osadchy D, Schuster I, Gepstein L, Hayam G, Josephson ME. Nonfluoroscopic, in vivo navigation and mapping technology. Nat Med. 1996;2:1393-5.
2. Gepstein L, Goldin A, Lessick J, Hayam G, Shpun S, Schwartz Y, Hakim G, Shofty R, Turgeman A, Kirshenbaum D, Ben-Haim SA. Electromechanical characterization of chronic myocardial infarction in the canine coronary occlusion model. Circulation. 1998;98:2055-64.
3. Kornowski R, Hong MK, Gepstein L, Goldstein S, Ellahham S, Ben-Haim SA, Leon MB. Preliminary animal and clinical experiences using an electromechanical endocardial mapping procedure to distinguish infarcted from healthy myocardium. Circulation. 1998;98:1116-24.
4. Kornowski R, Hong MK, Leon MB. Comparison between left ventricular electromechanical mapping and radionuclide perfusion imaging for detection of myocardial viability. Circulation. 1998;98:1837-41.
5. Gepstein L, Hayam G, Ben-Haim SA. A novel method for nonfluoroscopic catheter-based electroanatomical mapping of the heart. In vitro and in vivo accuracy results. Circulation. 1997;95:1611-22.
6. Gepstein L, Hayam G, Shpun S, Ben-Haim SA. Hemodynamic evaluation of the heart with a nonfluoroscopic electromechanical mapping technique. Circulation. 1997;96:3672-80.
7. Vale PR, Losordo DW, Tkebuchava T, Chen D, Milliken CE, Isner JM. Catheter-based myocardial gene transfer utilizing nonfluoroscopic electromechanical left ventricular mapping. J Am Coll Cardiol. 1999;34:246-54.
8. Biosense-Webster. NOGA Cardiac Electromechanical Mapping System. User's Manual. Software Revision 2 ed; June 1998.

Chapter 5

Validation of the local shortening function as assessed by nonfluoroscopic electromechanical mapping: a comparison with computerized left ventricular angiography

Glenn Van Langenhove, MD; Jaap N. Hamburger, MD, PhD; Leonidas Diamantopoulos, MD, PhD; Peter C. Smits, MD, PhD; Emile Onderwater, BSc; Patrick W. Serruys, MD, PhD. Thoraxcenter Rotterdam, Dijkzigt Hospital, Erasmus University, The Netherlands

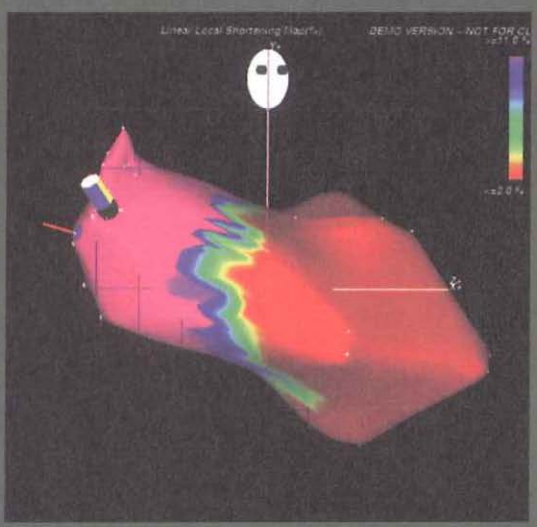

ABSTRACT

Background: Nonfluoroscopic electromechanical mapping (NEM) has been proposed as a new technique for the evaluation of electrical and mechanical functioning of the myocardium. In this system, linear local shortening (LLS) is the parameter used for assessment of local mechanical properties. To validate this parameter, we compared LLS with regional wall motion (RWM) data derived from contrast left ventriculograms acquired in the same patients.

Methods and results: Twenty-six patients were included. Twenty patients (77%) patients suffered a previous myocardial infarction, 19 (73%) had undergone 1 or more revascularisation procedures (CABG or PTCA). The majority of the patients suffered stable angina (22 patients, 85%) at the time of catheterization. Angiographic left ventricular RWM was analyzed using the area-length method. The right anterior oblique view was divided in 5 segments, the left anterior oblique view in 2. Through a comparison of enddiastolic and endsystolic areas drawn from a computer- defined central point to the respective wall delineation, RWM was calculated as change in area. In the first approach, we compared area changes to comparable NEM segments. In the second part of the study, LLS values for normokinetic, hypokinetic, akinetic and dyskinetic segments were correlated to the change in angiographic RWM. In the first approach, the overall comparison of segments yielded a correlation coefficient of 0.67 ($p<0.0005$). In the second part of the study, differences in LLS values between dyskinetic (LLS= -3.68% ± 8.86), akinetic (2.84% ± 3.96), hypokinetic (9.35% ± 4.27) and normokinetic (13.66% ± 7.98) segments were highly significant (overall ANOVA: $p<0.0005$).

Conclusion: NEM is a powerful tool for invasive electromechanical assessment of myocardial function.

Key Words
Ventricles
Myocardial contraction
Imaging
Angiography
Nonfluoroscopic mapping

List of acronyms

NEM:	nonfluoroscopic electromechanical mapping
UPV:	unipolar voltages
LLS:	linear local shortening
LVA:	left ventricle angiogram
RWM:	regional wall motion
RAO:	right anterior oblique
LAO:	left anterior oblique
ANOVA:	analysis of variance
CCS:	Canadian Cardiovascular Society
NYHA:	New York Heart Association
CABG:	Coronary Artery Bypass Graft
PTCA:	Percutaneous Transluminal Coronary Angioplasty

INTRODUCTION

Recently, a new nonfluoroscopic electromechanical mapping (NEM) system was introduced into the clinical arena. Using a locatable sensor positioned in a magnetic field, the endocardial border can be traced and local information on electrical (unipolar and bipolar voltages) and mechanical (linear local shortening, LLS) properties of the myocardium can be assessed[1-5]. The local myocardial shortening function has been validated with techniques as radionuclide perfusion imaging and echocardiography[1-3, 5], but clinical data remain scarce. Because left ventricle angiography remains an important tool in the assessment of regional wall motion.[6, 7], we compared regional wall motion (RWM) contractility assessed by computerized left ventricular angiography (LVA) with LLS data provided by the NEM system.

METHODS

Patients

Patients were included if wall motion abnormalities were present on the left ventricular angiogram, whatever the reason for their referral for coronary angiography. Exclusion criteria were presence of left ventricular thrombus, unstable angina, atrial fibrillation, severe ventricular instability that did not allow for ensuring stable catheter positions, aortic valve prosthesis and severe aortic valve stenosis. The study was approved by the Erasmus University Hospital medical ethics committee, and all patients signed an informed consent.

Left ventricular angiography

LVA's in RAO 30° and LAO 60° were performed using standard techniques[8]. Angiograms were analyzed using the CAAS II system (PIE Medical, Maastricht, The Netherlands). The catheters (5- 7 French) were used for computerized calibration. The left ventricle boundaries at end-diastole and end-systole were traced manually with a digitizing device by an observer blinded for the mapping results. The frame showing the largest ventricular volume was chosen as the end-diastole, the frame with the smallest volume as the end-systole. By using a simultaneously recorded ECG signal measurements related to an extra-systole were eliminated prior to the analysis. Then, the RWM was analyzed through a comparison of enddiastolic and endsystolic areas drawn from a computer- defined central point to the respective wall delineation. Regional wall motion was expressed as change in area: (enddiastolic area - endsystolic area)/enddiastolic area. Seven segments were identified: 5 in the RAO view (anterobasal, anterolateral, apical, inferior, posterobasal) and 2 in the LAO view (posterolateral, septal) (figures 1 and 2).

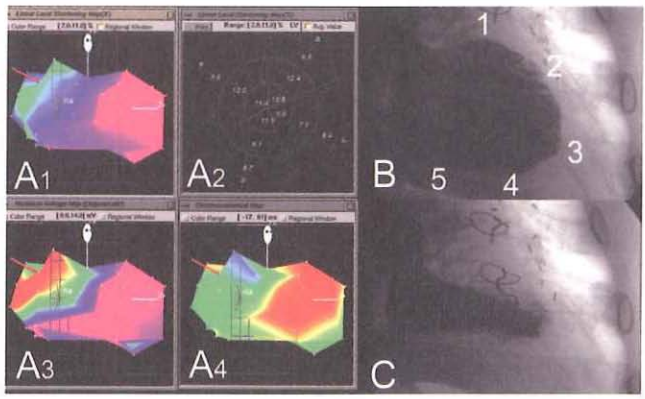

Figure 1

Nonfluoroscopic and angiographic view of a normal left ventricle. A1 to 4 show a nonfluoroscopic mapping- derived linear local shortening map in a 30 degrees RAO view (A1), a bull's eye view of the same map (A2), a unipolar voltage map in RAO view (A3), and an electroanatomical map, showing time to activation relative to a reference point. The same RAO view of the left ventricle angiogram in end-diastole is shown in B. Numbers B1 to 5 show the anterobasal, anterolateral, apical, inferior and posterobasal segments, respectively. C shows the left ventricular angiogram in end-systole in the same RAO view.

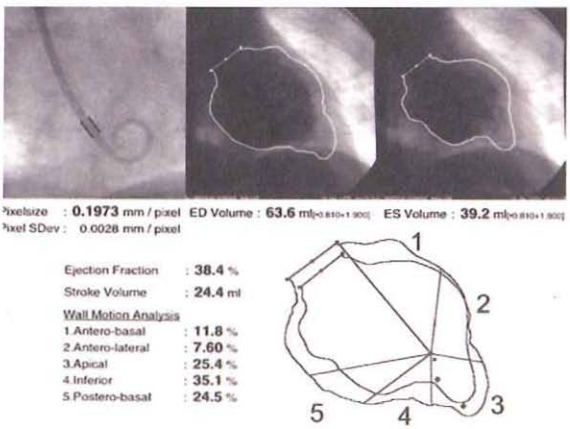

Figure 2

Angiographic assessment of wall motion using the area-length method (CAAS II system, PIE Medical, Maastricht, The Netherlands). The top left picture shows the catheter calibration. Top middle and top right are the RAO views of the left ventricle at end-diastole and end-systole, respectively, with the manually outlined contour, and the calculated volumes shown below the respective pictures. The bottom shows the calculations of ejection fraction and stroke volume, and the regional wall motion analysis for the different segments (with segments numbered from 1 to 5, with the antero-basal segment (segment 1) beginning as first clockwise from the straight aortic valve delineation), expressed as a percentage change in area.

Nonfluoroscopic electromechanical mapping

The NEM system has been described previously.[1-3, 5, 9] In short, a reference catheter, with a location sensor in its tip, was taped securely to the patient's back. The mapping catheter (NOGA-STAR™, Biosense-Webster, Cordis, Johnson & Johnson), also with a tip sensor, was introduced through an 8F femoral sheath and placed retrogradely through the aortic valve in the left ventricle. The location of the mapping catheter was gated to end diastole and recorded relative to the location of the fixed reference catheter at that time, thus compensating for subject motion. The location pad was fixed beneath the operating table generating an ultralow magnetic field ($5x10^{-6}$ to $5x10^{-5}$ Tesla) which codes the mapping space around the chest with both temporal and spatial distinguishing characteristics. Thus, at all times, the tip of the catheter could be located with six degrees of freedom (x, y , z, pitch, yaw and roll). The catheter was dragged along the endocardial surface of the left ventricle in order to acquire electromechanical data. When a stable signal was obtained (see definition section) a "point" was added to a three-dimensional map as shown on the NEM unit. Electrophysiological data (UPV, bipolar local voltages, and local activation time) and mechanical data (LLS) were displayed three-dimensionally, while the images obtained were viewed from different angles as chosen by the operator. A bull's eye view showing average voltages, activation time or LLS for 12 segments (basal, mid and apical parts of anterior, lateral, posterior and septal segments) was visualized in an extra window on the NEM screen (figure 3).

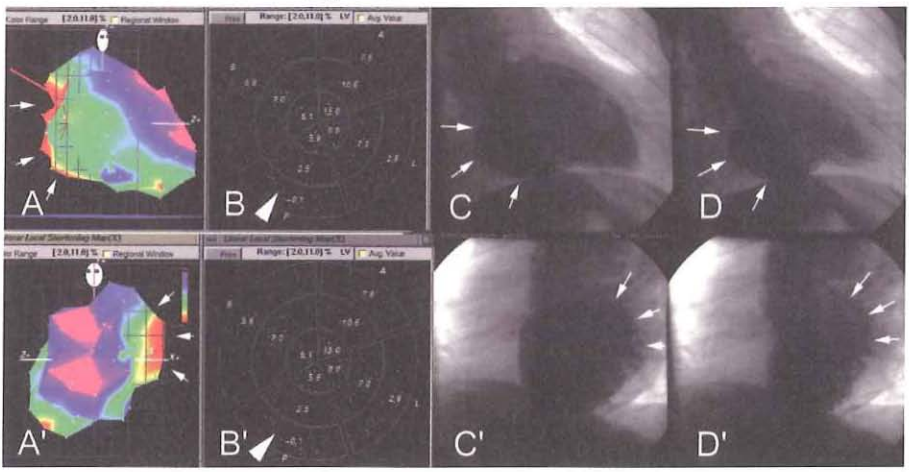

Figure 3

Nonfluoroscopic and angiographic image of the left ventricle with bull's eye view of LLS data in another patient (than fig 1). C-D show 30∞ RAO views at ED and ES respectively. C'-D' show the 60∞ LAO views at ED and ES respectively. The arrows delineate the posterobasal (C-D) and posterolateral (C'-D') segments showing akinesia. Figures A-A' show the 30∞ RAO (fig A) and 60∞ LAO (fig A') NEM- images with the bull's eye map (of course the same for both projections) (B-B') of the same patient, showing the linear local shortening (LLS) data. Again color coding is from low LLS (<2%, red) to high (>11%, blue-purple). The same akinesia can be easily appreciated as the red zone in A-A' (see small arrows), and through the very low and even negative LLS values in the posterobasal (-0.1%, see arrowhead in B-B'), mid posterior (2.5%) and lateral (2.8%, see large arrow) segments seen in the bull's eye map.

The LLS assessment is based on the assumption that in healthy myocardium any two points move closer to each other during contraction. Measurement of distances between neighboring points is therefore the basis for calculation of myocardial shortening. The computer algorithm takes into account the density of points around a point p, and gives a negligible weight to points too close (sampling noise) and points too far (of no influence as they provide non-local information). The algorithm for LLS is calculated as follows[10]: for any two points on the map, i and j, LLS is calculated as the change in distance between these two points from end-diastole to end-systole, normalized for the length at end diastole:

$$LLSij = (L(ED)ij - L(ES)ij)/ L(ED)ij$$

For any point p LLS is calculated as a function of the LLSpj, for all points j=1 to n on the map, so that

$$LLSp= (Sj=1..n\ Wpj\ (L(ED)pj)x\ LLSpj\ ) / Sj=1..n\ Wpj,$$

where W is the weight of a certain point as a function of the distance Lij between two points i and j, the average distance D around point p (D is defined in the computer algorithm as the average distance of the ten closest points to p) and the volume V at end-diastole. The weight is therefore function of the point density in a defined region, the volume of the heart and the distances between points at end-diastole.

Definitions

Point loop stability (PLS): measures the maximum of distances between the locations of the selected point in two consecutive heart cycles. Low PLS indicate a reproducible catheter movement trajectory.

Cycle length (CL) stability: the difference between the length of the current cycle and the average of the last 100 cycles recorded by the system. Number has to be as small as possible.

Location stability: a measure of the variability in position of the catheter tip on the endocardial wall during two consecutive cardiac cycles.

Comparison of angiographic and NEM data

Although the NEM system allows for viewing the three-D images in any angle chosen by the operator, we analyzed the mapping data in the 30° RAO and 60° LAO views, in order to create comparable data sets. The respective angiographic segments related to the bull's eye map results were as follows:

Angio	Bull's eye mapping
Anterobasal segment	A1
Anterolateral	A2, L1, L2
Apical	A3, L3, P3, S3
Inferior	P2

Posterobasal	P1
Septal	S1, S2
Posterolateral	P2, P3, L2, L3

For every segment, the average local linear shortening was calculated. These results were compared to the regional wall motion changes in the same angiographic segments. Averages were not calculated if fewer than 5 points were obtained in any one segment.
In the second part of the study, we defined LLS values for normokinetic, hypokinetic, akinetic and dyskinetic segments respectively. A segment was defined as normokinetic when the area change was > 40%, hypokinetic between 20 and 40%, akinetic between 0 and 20% and dyskinetic when <0%.6, 11 The change in angiographic RWM was compared to the corresponding LLS of the predefined segments on the NEM bull's eye map.

Statistics

Statistical analysis was performed using SPSS, version 9.0 (SPSS Inc., Chicago, Illinois, USA). Data are expressed as mean ± SD. Correlations were performed using Pearson's test. Means of nominal values for LLS were compared between myocardial segments with normokinetic, hypokinetic or akinetic wall motion by ANOVA. Intergroup comparison was made using Student's t-test with Bonferroni correction. A value of $P<0.05$ was considered statistically significant.

Results

Between March 1998 and November 1999, 26 patients were studied. In this study, male gender was predominant (23/26, 88%). Mean age was 61 ± 8 years. Twenty patients (77%) patients suffered a previous myocardial infarction. Nineteen (73%) had undergone 1 or more revascularisation procedures (CABG or PTCA). Five patients (19%) were in NYHA heart failure class II, 7 (27%) in NYHA class I, the remainder having no signs of heart failure. Reasons for referral for cardiac catheterization were stable angina (CCS class 1 in 11 patients (42%), CCS class 2 in 6 patients (23%), class 3 in 5 patients (20%)) or coronary assessment following myocardial infarction (4 patients, 15%). Of 30 patients initially screened, 4 were excluded (1 for atrial fibrillation, 1 for stable angina that became unstable during admission, 1 for aortic valve prosthesis, and 1 for unwillingness to sign an informed consent). Risk factors were hypercholesterolemia (18 patients, 69%), hypertension (13 patients, 50%), smoking history (16 patients, 62%), diabetes (5 patients, 19%) and family history (9 patients, 35%).
The average procedure time for the acquisition of NEM maps was 41 ± 27 minutes. All patients remained in stable hemodynamic conditions during the respective procedures, as confirmed by continuous in-cathlab heart rate and blood pressure monitoring data. There were no procedural complications. In the first part of the study, 162 (out of 182, 89%) angiographic segments were analyzed. Twenty segments could not be compared due to insufficient (less than 5) number of points taken during the NEM procedure. The overall comparison of angiographic and NEM segments yielded a Pearson correlation coefficient of 0.67 ($p<0.0005$) (figure 4).

Figure 4

Correlation between angiographic wall motion analysis per segment and the corresponding local linear shortening (LLS) data.

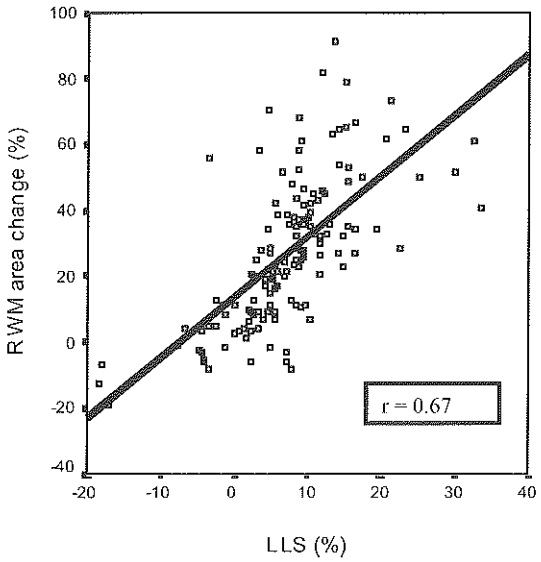

The Pearson correlation differed among segments, as shown in table 1.

Table 1. Local linear shortening (LLS), average wall motion change on angiography, Pearson correlation and p-values of the different segments. SD= standard deviation.

Angiographic Segment	*Average LLS of corresponding segment (%±SD)*	*Average Wall motion change (%±SD)*	*Pearson Correlation r*	*p-value*
Anterobasal (segment 1)	6.9±7.4	31.1±20.2	0.55	0.04
Anterolateral (segment 2)	9.7±7.1	27.4±23.1	0.63	<0.001
Apical (segment 3)	7.9±7.2	30.4±19.8	0.61	0.01
Inferior (segment 4)	7.5±8.3	34.0±18.7	0.54	0.02
Posterobasal (segment 5)	8.7±9.2	33.1±14.7	0.68	<0.001
Posterolateral (segment 6)	9.7±6.5	28.4±15.6	0.74	<0.0005
Septal (segment 7)	8.2±7.7	29.2±17.4	0.72	<0.0005
All segments	8.7±5.5	30.1±13.4	0.67	0.008

From this table it is clear that correlation was best for septal and posterolateral segments (r=0.72 and 0.74 respectively), and worst for anterobasal and inferior segments (r=0.55 and 0.54 respectively). However, all correlations reached statistical significance.
In the second part of the study, we compared RWM (assessed as normokinetic, hypokinetic, akinetic or dyskinetic) with the LLS value obtained for the same segments. Of the 162 segments, 18 were dyskinetic (LLS= −3.68% ± 8.86), 44 were akinetic (LLS=2.84% ± 3.96), 60 were hypokinetic (LLS= 9.35% ± 4.27) and 40 were normokinetic (LLS= 13.66% ± 7.98) (p<0.0005 by ANOVA, table 2).

Table 2. Mean local linear shortening (LLS) values for dyskinetic (-1), akinetic (0), hypokinetic (1) and normokinetic (2) segments. Number of segments (N), standard deviation, standard error, 95% confidence interval and p-value for the overall analysis of variance are also shown.

Segmental motion	N	Mean LLS (%)	Std. Deviation	Std. Error	95% Confidence Interval		ANOVA
					Lower Bound	Upper Bound	
-1	18	-3.69	8.86	2.29	-8.59	1.23	
0	44	2.84	3.96	0.65	1.52	4.16	
1	60	9.35	4.27	0.60	8.13	10.56	P<0.0005
2	40	13.66	7.98	1.33	10.96	16.36	
Total	162	7.31	8.10	0.69	5.95	8.68	

Table 3. Unpaired Student's t-test with Bonferroni correction for the comparison of local linear shortening (LLS) values between dyskinetic (-1), akinetic (0), hypokinetic (1) and normokinetic (2) segments. Mean differences, standard error, and statistical significance are shown.

Comparison of dys-, a-, hypo-, and normokinetic segments				
Segmental wall motion		Mean difference	Std Error	p-value
-1 (dyskinetic)	0	-6.52	1.83	0.003
	1	-13.03	1.76	<0.0005
	2	-17.34	1.84	<0.0005
0 (akinetic)	-1	6.52	1.83	0.003
	1	-6.50	1.30	<0.0005
	2	-10.82	1.40	<0.0005
1 (hypokinetic)	-1	13.03	1.76	<0.0005
	0	6.50	1.30	<0.0005
	2	-4.31	1.31	0.007
2 (normokinetic)	-1	17.34	1.84	<0.0005
	0	10.82	1.40	<0.0005
	1	4.31	1.31	0.007

Table 3 shows the results of the different unpaired t-tests with Bonferroni correction between LLS values for the different groups.

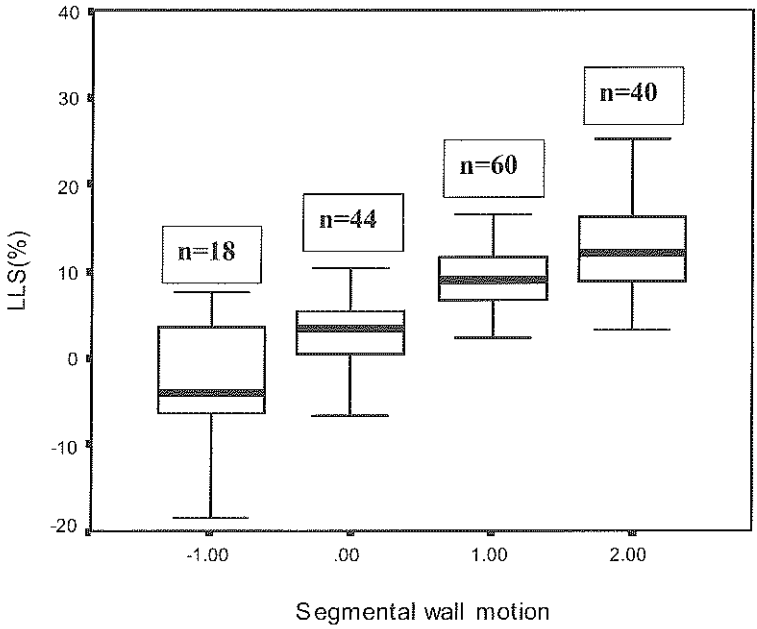

Figure 5 shows a box plot for comparison of LLS values for the different angiographic RWM analyses.

Discussion

Although the independent prognostic value on long-term outcome of indexes of regional function is still in debate,[12] it remains important that reliable observer-independent information on regional myocardial function can be obtained. Nonfluoroscopic electromechanical mapping has been proposed for on-line in-cathlab detection of myocardial viability.[5] However, the LLS function of the NEM system had not yet been validated as compared to standard angiographic techniques.[2, 3, 5] As NEM has been proposed for in-cathlab assessment of left ventricular function, we compared NEM data with RWM as assessed by computerized LVA. Our study showed that left ventricular regional wall motion measurements using NEM provide information comparable with computerized LVA assessment. In addition we showed highly significant (overall ANOVA: $p<0.0005$) differences in LLS values for dyskinetic (LLS= -3.68% ± 8.86), akinetic (2.84% ± 3.96), hypokinetic (9.35% ± 4.27) and normokinetic (13.66% ± 7.98) segments. The value of electromechanical mapping has been studied in the animal and in the human model. Kornowski et al. showed impaired local shortening in the anterior wall in dogs after ligation of the left anterior descending artery.[3] In the same study, the mapping data clearly delineated infarcted areas in patients, and a concordance of 78% between echocardiography and local shortening data was shown. The greatest discordance was seen in the posterior wall. Gepstein et al. showed a high correlation between mapping

data and pathology-confirmed infarcted areas in the canine coronary occlusion model.[4] Recently, a strong correlation between radionuclide perfusion and local shortening values was demonstrated [5], where normal and infarcted segments showed average LLS of 12.5% ± 2.8 and 3.4% ± 3.4 respectively. Our findings of LLS for normokinetic and akinetic segments (13.66% ± 7.98 and 2.84% ± 3.96 respectively) are in close agreement with these results.

The reason for some segments having better correlations (lateral and septal regions) than others is not clear. A possible explanation could be that effects such as differences in twisting motion and radial motion that have been described recently may not be demonstrated accurately by two-D left ventricular angiography of diseased left ventricles.[13,14] However, the number of points taken per segment may also have influenced these findings, as it indeed has been shown that a minimum number of points is mandatory to accurately assess segmental characteristics[2]. For this reason, areas with less than 5 points were omitted from our analysis.

Limitations. First, subjective interpretation of angiographic left ventricular regional wall motion is routinely performed with knowledge of the location and extent of coronary artery disease. Studies have shown that subjective interpretation of local wall motion may be biased through this knowledge.[15] In our study, the observer who calculated angiographic local wall motion was blinded for CAD severity. Second, the ventriculogram is a two-D reconstruction of a three-D structure, and may therefore not constitute the optimal technique for wall motion abnormality detection. Also, the computer-assisted area method is subject to interobserver variability, as choosing of the respective digitized cine frames and manual tracing of the endocardial border is operator-dependent. Recently, Natarajan and coworkers have found a time-related dependence of wall motion abnormalities, suggesting that ischemic ventricular segments may seem hypokinetic on angiography, but in fact appear to have normal absolute shortening due to a contraction delay. [16] In the left ventricular angiograms this temporal consideration was not taken into account for the assessment of regional function. Also, in this study, patients with atrial fibrillation and excessive ventricular ectopia were excluded. Indeed, these situations do not allow for adequate cycle length stability and loop stability, and may therefore confound regional electromechanical properties. It is therefore impossible to make definite statements on the use of electromechanical mapping in these clinical settings.

In conclusion, our study showed that LLS data are significantly correlated with angiographic wall motion for comparable segments. In addition, LLS is a reliable parameter for the evaluation of regional wall motion. Thus, NEM is a suitable technique for invasive assessment of regional left ventricular function.

References

1. Gepstein L, Hayam G, Ben-Haim SA. A novel method for nonfluoroscopic catheter-based electroanatomical mapping of the heart. In vitro and in vivo accuracy results. Circulation 1997; 95:1611-22.
2. Gepstein L, Hayam G, Shpun S, Ben-Haim SA. Hemodynamic evaluation of the heart with a nonfluoroscopic electromechanical mapping technique. Circulation 1997; 96:3672-80.
3. Kornowski R, Hong MK, Gepstein L, et al. Preliminary animal and clinical experiences using an electromechanical endocardial mapping procedure to distinguish infarcted from healthy myocardium. Circulation 1998; 98:1116-24.
4. Gepstein L, Goldin A, Lessick J, et al. Electromechanical characterization of chronic myocardial infarction in the canine coronary occlusion model. Circulation 1998; 98:2055-64.
5. Kornowski R, Hong MK, Leon MB. Comparison between left ventricular electromechanical mapping and radionuclide perfusion imaging for detection of myocardial viability. Circulation 1998; 98:1837-41.
6. Kussmaul WGd, Kleaveland JP, Zeevi GR, Hirshfeld JW, Jr. Accuracy of subjective and computer-assisted assessments of angiographic left ventricular regional wall motion. Cathet Cardiovasc Diagn 1990; 20:153-64.
7. Harrison JK, Califf RM, Woodlief LH, et al. Systolic left ventricular function after reperfusion therapy for acute myocardial infarction. Analysis of determinants of improvement. The TAMI Study Group. Circulation 1993; 87:1531-41.
8. Slager CJ, Hooghoudt TE, Serruys PW, et al. Quantitative assessment of regional left ventricular motion using endocardial landmarks. J Am Coll Cardiol 1986; 7:317-26.
9. Ben-Haim SA, Osadchy D, Schuster I, Gepstein L, Hayam G, Josephson ME. Nonfluoroscopic, in vivo navigation and mapping technology. Nat Med 1996; 2:1393-5.
10. Biosense-Webster. NOGA Cardia Electromechanical Mapping System. User's Manual., June 1998.
11. Nissen SE, Booth D, Waters J, Fassas T, DeMaria AN. Evaluation of left ventricular contractile pattern by intravenous digital subtraction ventriculography: comparison with cineangiography and assessment of interobserver variability. Am J Cardiol 1983; 52:1293-8.
12. Mancini GB, Bourassa MG, Williamson PR, et al. Prognostic importance of quantitative analysis of coronary cineangiograms. Am J Cardiol 1992; 69:1022-7.
13. Fogel MA, Gupta K, Baxter BC, Weinberg PM, Haselgrove J, Hoffman EA. Biomechanics of the deconditioned left ventricle. Am J Physiol 1996; 271:H1193-206.
14. Fogel MA, Weinberg PM, Gupta KB, et al. Mechanics of the single left ventricle: a study in ventricular-ventricular interaction II. Circulation 1998; 98:330-8.
15. Diamond GA, Vas R, Forrester JS, et al. The influence of bias on the subjective interpretation of cardiac angiograms. Am Heart J 1984; 107:68-74.
16. Natarajan A, Bove AA. Comparison of shortening with timing of wall motion in detecting regional abnormalities of the left ventricle in coronary disease. Cathet Cardiovasc Diagn 1993; 28:106-13.

Chapter 6

Electromechanical properties of myocardium supplied by coronary collateral circulation

Glenn Van Langenhove[1], MD; Irenee Bossi[2], MD; Jean Fajadet[2], MD; Paul Van den Heuvel[3], MD; Jaap N. Hamburger[1], MD; Dirk Stockman[3], MD; Mariano Albertal[1], MD; Peter C. Smits[1], MD; Emile Onderwater[1], BSc; Marc Vaerenberg[3], MD; Jean Marco[2], MD; Patrick W. Serruys[1], MD.

From the Departments of [1]Interventional Cardiology, Thoraxcenter Rotterdam, Dijkzigt Hospital, Erasmus University, Rotterdam, The Netherlands, the Department of Interventional Cardiology, Clinique Pasteur, Toulouse, France[2] and the Department of Cardiology, Middelheim Hospital Antwerp, Belgium[3].

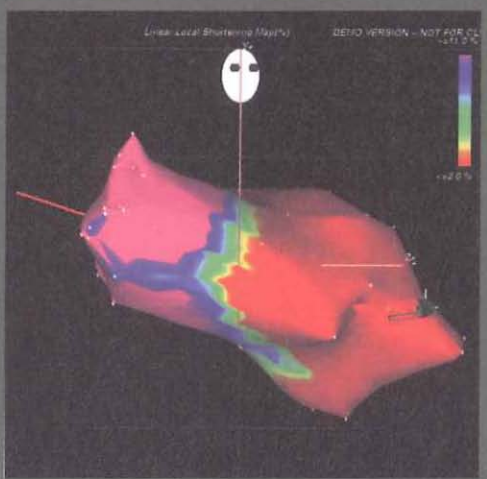

Introduction

The quality of coronary collateral formation may decide on the amount of residual functional myocardium after coronary occlusion.[1] It has been shown that the presence of an efficient microvascular collateral network can maintain viability in the myocardial region previously perfused by the occluded coronary artery.[2] Coronary angiography however only assesses the anatomical quality of these collaterals.[3]

NEM is a novel technique for in-cathlab on-line assessment of the functional mechanical and electrical properties of the myocardium.[4-10] The electromechanical properties thus assessed may predict the presence of viability in previously injured segments, and may therefore reflect the functionality of the collateral formation.[8]

We therefore assessed the correlation between the presence and the extent of coronary collaterals in patients with one native total coronary occlusion with the electromechanical properties of the target myocardium of the occluded coronary artery.

Methods

Patients

All consecutive patients that underwent NEM in our centers were entered in a database. Patients were elected for the present study if they met the following criteria:

No more than one occluded native coronary artery, but at least one.

Coronary angiography and biplane left ventriculogram during the index procedure

No previous bypass surgery

Successful NEM mapping

Informed consent signed

Coronary angiography and collateral grading

Angiography was performed before NEM using the right femoral approach according to standard techniques. Left and right 6F diagnostic catheters were used to engage the coronary ostia, and all images were recorded on a digital recording system. Coronary collateral grading was performed by an investigator blinded for the mapping results. Collateral grading was scored according to the Rentrop classification (0= no opacification ; 1= filling of the side branches of the occluded artery without visualization of the epicardial segment ; 2= partial filling of the epicardial segment but not up to the original occlusion ; 3= complete retrograde filling of the occluded coronary artery up to the original occlusion).

Left ventricle angiography

Left ventricle (LV) angiography was performed with 5, 6 or 7F pigtail catheters, according to the preference of the operator. Angiograms were recorded in a 30° right anterior oblique and 60° left anterior oblique view. LV angiograms were made with the patient in a stable position and during maximal inspiration. The angiograms were analyzed on the CAAS II system (PIE medical, Maastricht, The Netherlands) by an independent investigator, who was blinded for the left ventricular mapping data. Calibration was performed using non contrast-filled catheters. The extent of the myocardial region originally perfused by the occluded artery was defined on a visual basis. The myocardium involved was then analyzed

using the centerline method, dividing the involved areas into normal, hypokinetic or akinetic.[11,12]

Nonfluoroscopic electromechanical mapping (NEM)

The system and its various components have been described previously. In short, a low magnetic field (10^{-5} to 10^{-6} Tesla) is generated around the patient. A catheter securely taped to the patient's back is used as a reference to compensate for subject motion during the procedure. A 7 French catheter (NOGA-STAR™, Biosense-Webster, a Johnson&Johnson company) containing a locatable sensor and recording electrodes in its deflectable tip is inserted through an 8 F femoral sheath and is then dragged along the endocardium of the left ventricle. Acquired signals are then send through the catheter shaft and processed by the NOGA processing unit (Biosense-Webster). The system can determine the location (with accuracy of <1mm) and orientation of the catheter in six degrees of freedom (x, y, z, roll, pitch, and yaw). Electromechanical information is obtained using a combination of data gathered by the electrodes and the location sensor. Thus unipolar (UPV) and bipolar (BPV) endocardial potentials and local linear shortening (LLS) data for every contact point are acquired, and can be displayed in bull's eye maps. Chamber geometry can then be accurately reconstructed using three-D endocavital information.

Post-processing of data was performed to eliminate points suggestive for catheter tip instability, as evidenced by catheter point loop stability, cycle length stability, local activation time and location stability data (see definition section). A triangle fill threshold of 40 mm was chosen for our data set. This setting allows the system to fill triangles between acquired points using an interpolation algorithm; distances between points larger than 40 mm were left blank until points in between were captured.

After applying an inner point filtering by the computer algorithm, points were manually deleted when they did not fit standard stability criteria (location stability <4mm, cycle length stability < 10% and loop stability <4mm), if they were taken during ST-segment elevation (suggestive for severe wall impression) and if the points were not related to the left ventricle (such as atrial location).

Comparison of angiographic LV regions, coronary artery supply and NEM regions

To ascertain that comparisons of the same areas on angiography and on NEM were obtained, the location of the mapping catheter was verified with angiography in a subset of five patients. For every point sampled with NEM, the location of the mapping catheter at the same time was recorded with biplane angiography (30∞ RAO and 60∞ LAO). After the procedure, locations of these points on the NEM bull's eye map were compared to the location of the mapping catheter on the recorded angiographic session according to the 7-segment division of the biplane LV angiogram. Correlations between the area supplied by the coronary artery under study and the myocardial region of interest was performed as described previously by Sheehan and coworkers[12-15]:

LAD: anterobasal (segment 1), anterolateral (segment 2), apical (segment 3) and septal (segment 6)RCA: diaphragmatic (segment 4) and posterobasal (segment 5)

CX: diaphragmatic (segment 4), posterobasal (segment 5) and posterolateral segment (segment 7) After defining which angiographic segment correlated to which nonfluoroscopic segment, we were able to define the relationship between each coronary

artery and the NEM segments perfused by it. We then assessed the average LLS, UPV and BPV of segments originally perfused by the occluded coronary artery and compared them to the respective parameters of segments that were perfused by a patent coronary artery. Also, we compared the different parameters between segments with good collateral flow (defined as having collateral flow grade 2 or 3) to those with poor collateral flow (defined as having collateral flow grade 0 or 1).

Statistics:

All data are reported as mean value ± SD. Parametric comparisons were performed using the unpaired Students' t-test, nonparametric comparisons with the Wilcoxon signed ranks test. Proportional data were analyzed by the chi-square test, with the Yates correction if one of the frequencies in the 2X2 contingency table was <5. Collateral index was compared using the Wilcoxon signed ranks test. A value of $p<0.05$ was considered significant.

Results

One hundred twenty-two consecutive patients underwent NEM between June 1997 and May 2000. Of these, 67 had previous bypass surgery, 11 only had monoplane left ventricle angiography, 1 patient had 2 completely occluded coronary arteries and 5 patients had an incomplete data set. Finally, 38 (31%) patients were studied. Clinical parameters are shown in table 1.

	Poor collateral quality (collateral grading = 0 or 1)	Good collateral quality (collateral grading = 2 or 3)	p-value
N	13	24	
Age (years ± SD)	59±10	61±12	NS
Male n (%)	9 (69%)	22 (92%)	NS
Previous PCI	11 (85%)	18 (75%)	NS
Q-wave myocardial infarction	9 (69%)	15 (63%)	NS
Hypercholesterolemia	10 (77%)	18 (75%)	NS
Hypertension	8 (62%)	17 (71%)	NS
Smoking history	10 (77%)	16 (67%)	NS
Diabetes	1 (8%)	2 (5%)	NS

Table 1

Clinical characteristics. SD= standard deviation; PCI= percutaneous coronary intervention.

The first part of the study involved the defining of the NEM segments that correlated with the respective coronary arteries. In 5 patients, 320 points were assessed through biplane angiography and consequently every catheter position was correlated with the point on the NOGA map that was taken at exactly the same time. The results are shown in table 2.

Angiographic segment	NEM segments
Anterobasal	A1
Anterolateral	L1,L2,P2
Apical	A3,L3,P3,S3
Diaphragmatic	P1,P2,P3,S3
Posterobasal	P1,P2,S1
Septal	S1,S2,S3
Posterolateral	L1,L2,P2

Table 2

Correlation between angiographic segments and segments defined by the nonfluoroscopic electromechanical mapping (NEM) system. The left column shows the respective 7-segment subdivision on angiography, the right column shows the respective segments derived from NEM, with A=anterior, L=lateral, P=posterior, S=septal.

Following the coronary artery distribution correlated to biplane angiography as previously described by Sheehan et al., we constructed a similar model for the NEM bull's eye map, as shown in table 3.

Coronary artery	NEM segments involved
LAD	A1,A2,A3,L1,L2,L3,S3,P3
RCA	A1,P1,P2,S3,P3
CX	L1,L2,P1,P2,P3,S3

Table 3

Correlation between coronary artery and NEM-segments.

The comparison for all patients of LLS, UPV and BPV between injured segments and segments remote from the injured myocardium is shown in table 4.

	Injured segments	Remote segments	p-value
LLS (% ± SD)	8.0	13.7	<0.0005
UPV (mV ± SD)	10.5	14.9	<0.0005
BPV (mV ± SD)	2.8	4.9	<0.0005

Table 4

Average values for linear local shortening (LLS), unipolar (UPV) and bipolar voltages (BPV) for segments located in the initial target myocardial region of the occluded coronary artery (injured segments) as compared to the average values of the same parameters for segments in the non-affected areas (remote segments).

The results of the analysis of variance performed to detect differences between segments with good collateral perfusion and segments with poor collateral perfusion is shown in table 5.

	Poor collaterals	Good collaterals	p-value
LLS injured segments	3.8±4.7	10.3±3.5	<0.0005
LLS remote segments	11.9±2.6	14.7±4.5	0.07
UPV injured segments	6.0±2.5	13.0±3.4	<0.0005
UPV remote segments	13.1±4.0	15.8±3.7	0.07
BPV injured segments	1.6±1.9	3.5±1.7	<0.0005
BPV remote segments	3.8±1.9	5.4±2.2	0.06

Table 5

Comparison of linear local shortening (LLS), unipolar (UPV) and bipolar voltages (BPV) for regions both injured (injured segments) and non-affected (remote segments) in ventricles without versus those with good collateral formation.

Examples are shown in figures 1 and 2.

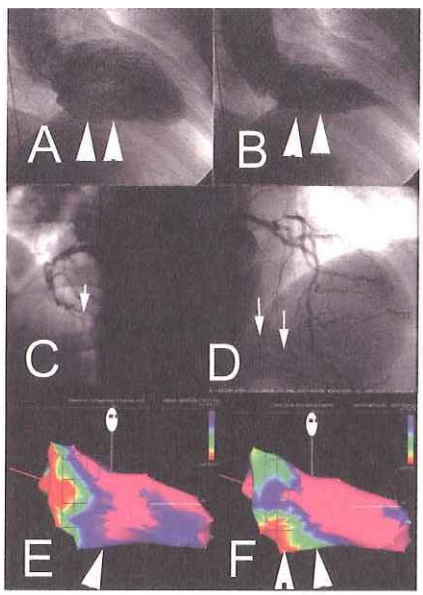

Figure 1

Patient with previous inferoposterior myocardial infarction. A and B show the right anterior oblique (RAO) view of the left ventricle angiogram in end-diastole and end-systole respectively. One can appreciate the inferior infarction (arrowheads in A and B). C shows the occluded right coronary artery (arrow) in RAO, D shows the left anterior oblique view of the left coronary artery tree. Collaterals (Rentrop class 3) can be clearly appreciated (arrows). E shows the RAO view of the nonfluoroscopic unipolar voltage map. The arrow indicates the high voltages in the inferior region, suggesting viable tissue. Color grading shows voltages from very high (>14 mV) in purple, to very low (<6mV) in red. F depicts the linear local shortening map, with the arrowheads showing decreased regional functioning as suggested by the red color. Color coding ranges from high (>11%) in purple, to very low (<2%) in red.

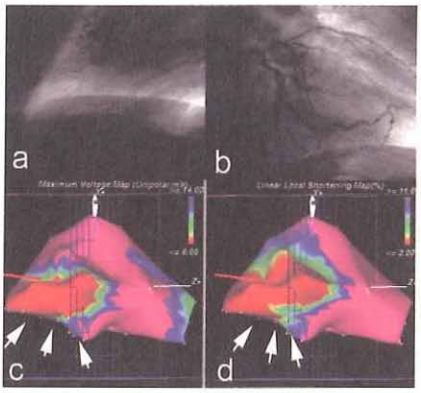

Figure 2

Patient with previous inferoposterior myocardial infarction due to an occluded right coronary artery. (a) shows the occluded RCA in the left anterior oblique (LAO) view, (b) shows the left coronary tree in LAO view. No collaterals are seen. (c) and (d) show unipolar voltage and linear local shortening maps in RAO view; the arrows delineate the inferoposterior region of low voltages and decreased linear local shortening.

Discussion

The most important finding from our study is that electromechanical properties of myocardial segments of which the perfusing native coronary artery has occluded and that are supplied by coronary collaterals of good quality, are better preserved than segments that do not have good coronary artery supply. From table 5 it becomes clear that in previously injured segments that are provided by a good collateral supply, higher LLS, UPV and BPV are found. On the other hand, remote segments of ventricles with poor collateral supply do not show statistically significant differences in LLS, UPV as well as BPV.

It has been previously shown that good collateral supply may be a sign of myocardial viability.[2] This finding can be supported by the current data set.

Limitations: The model created through LV angiographic determination of coronary artery perfusion is not validated. Also, our model is based upon 5 patients in which the correlation between angiographic location and NEM location was made. Further study may be necessary on this issue.

Conclusion

Nonfluoroscopic mapping data of previously injured myocardial segments are significantly correlated with the quality of collateral coronary artery supply to the target region of occluded coronary arteries. This further underscores the potential of nonfluoroscopic mapping in assessing myocardial viability.

References

1. Fukai M, Ii M, Nakakoji T, Kawakatsu M, Nariyama J, Yokota N, Negoro N, Kojima S, Ohkubo T, Hoshiga M, Nakajima O, Ishihara T. Angiographically demonstrated coronary collaterals predict residual viable myocardium in patients with chronic myocardial infarction: a regional metabolic study. J Cardiol. 2000;35:103-11.
2. Petronio AS, Baglini R, Limbruno U, Mengozzi G, Amoroso G, Cantarelli A, Vaghetti M, Distante A, Balbarini A, Mariani M. Coronary collateral circulation behaviour and myocardial viability in chronic total occlusion treated with coronary angioplasty [see comments]. Eur Heart J. 1998;19:1681-7.
3. van Liebergen RA, Piek JJ, Koch KT, de Winter RJ, Schotborgh CE, Lie KI. Quantification of collateral flow in humans: a comparison of angiographic, electrocardiographic and hemodynamic variables. J Am Coll Cardiol. 1999;33:670-7.
4. Ben-Haim SA, Osadchy D, Schuster I, Gepstein L, Hayam G, Josephson ME. Nonfluoroscopic, in vivo navigation and mapping technology. Nat Med. 1996;2:1393-5.
5. Fuchs S, Kornowski R, Shiran A, Pierre A, Ellahham S, Leon MB. Electromechanical characterization of myocardial hibernation in a pig model. Coron Artery Dis. 1999;10:195-8.
6. Gepstein L, Hayam G, Shpun S, Ben-Haim SA. Hemodynamic evaluation of the heart with a nonfluoroscopic electromechanical mapping technique. Circulation. 1997;96:3672-80.
7. Gepstein L, Goldin A, Lessick J, Hayam G, Shpun S, Schwartz Y, Hakim G, Shofty R, Turgeman A, Kirshenbaum D, Ben-Haim SA. Electromechanical characterization of chronic myocardial infarction in the canine coronary occlusion model. Circulation. 1998;98:2055-64.
8. Kornowski R, Hong MK, Leon MB. Comparison between left ventricular electromechanical mapping and radionuclide perfusion imaging for detection of myocardial viability. Circulation. 1998;98:1837-41.
9. Kornowski R, Hong MK, Gepstein L, Goldstein S, Ellahham S, Ben-Haim SA, Leon MB. Preliminary animal and clinical experiences using an electromechanical endocardial mapping procedure to distinguish infarcted from healthy myocardium. Circulation. 1998;98:1116-24.
10. Kornowski R, Hong MK, Shiran A, Fuchs S, Pierre A, Collins SD, Elahham S, Leon MB. Electromechanical Characterization of Acute Experimental Myocardial Infarction. J Invasive Cardiol. 1999;11:329-336.
11. Sheehan FH, Mathey DG, Schofer J, Krebber HJ, Dodge HT. Effect of interventions in salvaging left ventricular function in acute myocardial infarction: a study of intracoronary streptokinase. Am J Cardiol. 1983;52:431-8.
12. Sheehan FH, Mathey DG, Schofer J, Dodge HT, Bolson EL. Factors that determine recovery of left ventricular function after thrombolysis in patients with acute myocardial infarction. Circulation. 1985;71:1121-8.
13. Sheehan FH, Schofer J, Mathey DG, Kellett MA, Smith H, Bolson EL, Dodge HT. Measurement of regional wall motion from biplane contrast ventriculograms: a comparison of the 30 degree right anterior oblique and 60 degree left anterior oblique projections in patients with acute myocardial infarction. Circulation. 1986;74:796-804.
14. Kennedy J, Sheehan F. Ventriculography. In: Pepine C, ed. Diagnostic and therapeutic cardiac catheterization. 2nd ed. Baltimore, Md: Williams and Wilkins; 1994:221-237.
15. Sheehan FH, Bolson EL, Dodge HT, Mathey DG, Schofer J, Woo HW. Advantages and applications of the centerline method for characterizing regional ventricular function. Circulation. 1986;74:293-305.

Chapter 7

Left ventricular electromechanical endocardial mapping to assess myocardial viability: comparison with thallium radionuclide perfusion imaging

Irene Bossi, MD; Glenn Van Langenhove#, MD; Catherine Klersy*, MD; Remi Choussat, MD; Alexander J. Black MB BS†; Nicolas Fourquet, MD; Bruno Farah, MD; Jean-Pierre Laurent, MD; Bernard Cassagneau, MD; Jean Fajadet, MD; Jean Marco, MD.

Unité de Cardiologie Interventionelle, Clinique Pasteur, Toulouse, France

#Thoraxcenter Rotterdam, The Netherlands

*Biometry-Research Management Department – I.R.C.C.S. Policlinico S. Matteo, Pavia, Italy

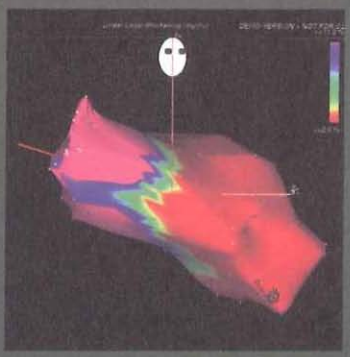

Structured abstract

Objectives. We sought to discriminate between normal, non viable and ischemic myocardium by comparing left ventricle (LV) electromechanical maps with redistribution perfusion thallium studies.

Background. The Biosense Noga is a catheter-based system for electromechanical mapping which uses magnetic technology to localize a sensor tip catheter reconstructs the 3D geometry of LV in real time.

Methods. In 29 patients with coronary artery disease, linear local shortening (LLS) and local intracardiac signals (unipolar voltage=UV) were compared with thallium redistribution images analyzed by single photon emission tomography, and myocardial regions were classified as normal (^{201}Tl uptake >75% of maximal), viable impaired (^{201}Tl uptake >50%) and non viable (^{201}Tl uptake< 50%).

Results. A total of 280 LV segments had adequate scintigraphic and electromechanical data for comparison. Overall UV and LLS values were significantly lower (UV: 6.1±2.6 versus 10.8±5.3 mV; p<0.001. LLS: 2.9±6.4 versus 6.5±5.8%; p<0.015) in regions with ^{201}Tl uptake<50% versus regions with impaired ^{201}Tl uptake (50-75%), and higher in regions with normal ^{201}Tl uptake (>75%). (UV:13.8±6.1 mV, and LLS: 8.9±7.6%; p<0.001 and p=0.0032 respectively versus viable impaired). Based on these data the UV threshold to distinguish non-viable myocardium was 6.5 mV, with a sensitivity of 68.2 (95% CI: 45.1 – 86.1) and a specificity of 84.9 (95% CI: 79.9 – 89.9).

Conclusions. Electromechanical maps distinguish normal, non viable and ischemic myocardium as assessed by thallium perfusion imaging studies.

Key words

Mapping, ischemia, ventricles, myocardium, viability,

Condensed abstract

The Biosense Noga is a catheter-based system for electro-mechanical mapping of the left ventricle (LV).

In 29 patients linear local shortening (LLS) and unipolar voltage (UV) potentials measured by this new left ventricular mapping system were compared to redistribution thallium activity. Overall a significant difference in LLS and UV was found between normal, viable impaired and non-viable myocardium as assessed by thallium perfusion imaging studies.

Abbreviations and Acronyms

BP:	Bipolar Voltage
DMR:	Direct myocardial revascularization
EMC:	Electromechanical coupling
FI:	Fragmentation Index
LLS:	Linear local shortening
LV:	Left ventricle

MI: Myocardial infarction
SPECT: Single photon emission computed tomography
^{201}Tl: Thallium -201
UV: Unipolar voltage

INTRODUCTION

Diagnostic testing to evaluate the presence and the extent of viable, but dysfunctional myocardium has become an important component of the clinical assessment of patients with chronic coronary artery disease and left ventricular dysfunction. Several noninvasive methods are currently used to identify physiological markers of myocardial viability in regions with contractile dysfunction, including PET imaging to assess myocardial metabolic activity, ^{201}Tl imaging to assess myocardial perfusion and membrane activity and dobutamine echocardiography to assess myocardial contractile reserve. Recently, a new non-fluoroscopic, catheter-based, mapping system (NOGA – Biosense) designed to acquire, analyze and display electro-anatomical maps of the human heart, has been developed and validated both in animal and human studies. Previous studies confirmed that such an LV mapping procedure in patients with myocardial ischemia allows to distinguish between infarcted, ischemic and normal myocardium according to the perfusion status in radionuclide SPECT imaging.
The purpose of this study was to compare LV electromechanical mapping data with ^{201}Tl perfusion imaging studies in the aim of discriminating between normal, non viable and ischemic myocardium. In addition we sought to evaluate if electro-mechanical coupling as assessed by NOGA may enable differentiation of hypocontractile viable myocardium.

METHODS

Patients

The study population is formed by 29 patients which underwent LV electromechanical assessment and ^{201}Tl perfusion imaging studies to detect myocardial viability as part of evaluation of chronic ischemic heart disease. Fourteen patient had a previous myocardial infarction. All the patients have significant coronary artery disease documented by coronary angiography. Informed consent was obtained from all patients before any diagnostic procedure.
Electromechanical mapping system. The nonfluoroscopic electromechanical mapping system (Noga, Biosense) has been described elsewhere. Briefly it comprised an external ultralow magnetic field emitter located under the operating table (triangular location pad), a 7F deflectable–tip electrophisiological catheter which incorporates a miniature passive magnetic location sensor (NOGA-STAR, Cordis-Webster), and a workstation for information processing and 3-dimensional LV reconstruction and display (Silicon Graphics).

Electromechanical mapping procedure. The fixed reference catheter was positioned under fluoroscopy externally on the back of the patients corresponding to the heart region. The accurate position (within 5 cm of location pad center) was verified with the reference catheter location check on the NOGA system. It is used to detect small changes in intracardiac position due to respiration or movement of the patient. After cannulating the femoral artery with an 8F sheath, the mapping catheter was advanced under fluoroscopy guidance to the descending aorta, its tip deflected to form a J shape, and introduced across the aortic valve. Once inside the LV cavity the catheter tip deflection was released and the first three points (apex, aortic outflow and mitral inflow) were acquired under fluoroscopic

guidance to generate the initial 3-D image of the LV. The "mapper" operator acquired subsequent points exploring different regions of the endocardium by dragging the catheter tip. The position of the catheter appears on the screen in real-time as an icon superimposed on the cardiac map being constructed. As the catheter moves on the endocardium, local electrograms and the catheter locations are reported simultaneously to the system which construct a 3-D geometrical representation of the cardiac LV chamber, using a triangular algorithm. Points were acquired as much homogeneously as possibly thorough the LV cavity, when the endocardial contact of the catheter tip was stable as evidenced by location stability, cycle length stability, local activation time stability, loop stability and good synchronization of the intracardiac electrograms of two consecutives heart cycles. The operator analyzed signals, and if the point based on the previous parameters is accepted as valid, it is brought into the 3-D map which is updated with every accepted point in real-time. A "triangle fill threshold" of 40 mm was chosen in order to provide a minimal level of points density at each mapped site. Validation of both intracardiac location accuracy and intracardiac signal recording have been previously established.

The post - processing of the data points was done automatically using the moderate points filter provided by the system, which deletes points based on the inner points filter (cone angle < 25°; relative depth > 10%) and the points stability filter (location displacement > 6 mm; trajectory instability > 6 mm; median cycle length ± 15%). Some more points were edited manually (visually inner points, points closer than 5 mm and points with prominent ST-segment elevation on the intracardiac electrogram), to assure a correct interpretation of the maps. Only segments with more than 3 sampled points were considered for the analysis.

Electromechanical map data definition

Unipolar voltage map: represents an electrical map displaying a map of maximum peak-to-peak voltage of the intracardiac signal measured by mapping catheter tip.

Bipolar voltage map: represents an electrical map displaying a map of maximum peak-to-peak voltage of the intracardiac signal measured by the difference measured between two unipolar channel placed at the mapping catheter tip and ring respectively.

Linear Local Shortening map: represents a mechanical map and displays the local shortening calculated on the linear distance from each point to its neighboring points.

Fragmentation Index map: represents a map which displays an estimation of the QRS complex fragmentation.

Electromechanical coupling: An estimate of EMC was provided based on LLS and UV values. A threshold of 6.5% for LLS for contractile myocardium derived from a comparison with left ventricular wall-motion at angiography and a threshold for UV of 6.5 mV for viable myocardium derived from the comparisons with ^{201}Tl perfusion studies were used. Electromechanical coupling index was defined as LLS x UV.

Myocardial perfusion ^{201}Thallium imaging

All patients were injected with ^{201}Tl (1.5 MBq/Kg).

Myocardial perfusion imaging was performed with a rotating 2-head gamma camera (SOPHY – DST) equipped with a low energy – High Resolution collimator and interfaced to a computer (SOPHA – Vision). Images were acquired with patient in prone position on a special dedicated scinti-bed. 32 projections (matrix 64*64; 40 seconds per projection) were acquired from 45° right anterior oblique view to 45° left posterior oblique view. Tomographic reconstruction was performed by standard filtered back projection with a hamming-Hann filter to generate transaxial tomograms. Reconstructed 6.4 mm slices were summed and reoriented in standard short axis, horizontal long-axis and vertical long-axis for visual analysis. For quantitative analysis, 2 consecutive short axis thick slices were considered from base to apex and sectorial profiles were generated using the John Hopkins/Frankfurt protocol. Apex was analyzed on long-axis slices and profiles were generated using the same protocol.

A ten segments model was used for this study: the short axis tomograms were divided into four segments representing the anterior, antero-septal, infero-posterior and lateral wall. The apex was divided into two regions: antero-septal and infero-lateral.

To asses myocardial viability in segments with fixed perfusion or partially reversible defect, the redistribution perfusion images were analyzed after nitrate administration and ^{201}Tl reinjection; myocardial regions were classified as normal (viable and not impaired) when ^{201}Tl uptake > 75% of maximal, viable impaired with ^{201}Tl uptake of 50% to 75% and non viable when ^{201}Tl uptake was < 50%. In addition the regions with very low ^{201}Tl uptake (< 50%) were subdivided in segments non viable with ^{201}Tl activity < 20% and regions with a ^{201}Tl fixation between 20 and 50%.

Statistical analysis

In the Tables and in the body of the text, continuous variables are expressed as mean ± standard deviation. Categorical variables are expressed as absolute or relative frequencies. Means of nominal values of LLS and UV were compared between myocardial segments non-viable, viable impaired and normal as assessed by rest/redistribution ^{201}Tl perfusion imaging by the non-parametric test of Kruskal-Wallis. Intergroup comparisons was made by Wilcoxon (Mann-Whitney test) with Bonferroni correction. A p value < 0.05 has been considered statistically significant. Statistical analysis was performed using Stata 6.0 for Windows (StataCorp, College Station, TX).

Results

Clinical patients' characteristics are shown in Table 1.

Table 1. Patient clinical and angiographic characteristics

Age (yrs)	63 (52-68)
Female gender	3 (15.8 %)
Ejection fraction (%)	55.8 ± 14.7
Multivessel disease	26 (89.6 %)
Previous MI	16
Previous PTCA	15
Previous CABG	10

MI : myocardial infarction.
PTCA : percutaneous transluminal coronary angioplasty.
CABG : coronary artery bypass graft.

The study population comprises 29 patients (3 females, mean age 61 ± 9.5 years) with documented coronary artery disease. No procedural complications were observed during or after the mapping procedure. The mean acquisition time was 53.2 ± 12.4 min, and 111 ± 23 data points (74 ± 16 after automatic post-processing and 56 ± 13 after manual editing) were obtained per patient.

Comparisons of electromechanical maps with redistribution thallium perfusion imaging

A total of 280 segments had adequate scintigraphic and NOGA electromechanical data for comparison. The distribution of mean ± SD LLS, UV, BP, FI values according to thallium activity is reported in Table 2.

Table 2. Distribution of mean ± SD local linear shortening, unipolar voltage, bipolar voltage and fragmentation index values according to redistribution ^{201}Tl activity.

	Normal N=192	**Viable impaired** N=68	**Non-viable** N=20	**P value***
LLS (%)	8.9 ± 7.6	6.5 ± 5.8	2.9 ± 6.4	0.0021
UV (mV)	13.8 ± 6.1	10.8 ± 5.3	6.1 ± 2.6	<0.0001
BP (mV)	3.88 ± 2.4	3.03 ± 2.15	1.7 ± 1.36	0.0001
FI	1.41 ± 0.5	1.64 ± 0.5	1.83 ± 0.7	0.1054

*Linear model with Huber-White robust standard error.

LLS : local linear shortening. UV : unipolar voltage. BP : bipolar voltage. FI : fragmentation index.

Unipolar Voltage Map

Overall UV correlated significantly with ^{201}Tl activity and particularly the electromechanical maps could distinguish segments with normal (>75%) and impaired (50-75%) ^{201}Tl uptake (UV: 13.8 ± 6.1 versus 10.8 ± 5.3; p < 0.001), and viable impaired regions and non-viable (UV: 10.8 ± 5.3 versus 6.1 ± 2.6; p< 0.001). In addition among the segments classified as non-viable with a ^{201}thallium uptake < 50% a trend toward lower UV values was observed in the segments with a fixation < 20% compared to segments with ^{201}thallium uptake between 20% and 50% (UV : 4.64 ± 1.29 versus 6.91 ± 2.88; p = 0.084).

Based on these data the lower limit for UV to discriminate normal myocardium was 10.3 mV, with a sensitivity of 67.9 (95% CI: 60.8 – 74.4) and a specificity of 62.1 (95% CI: 51.0 – 72.3). The UV threshold to distinguish non-viable myocardium was 6.5 mV, with a sensitivity of 68.2 (95% CI: 45.1 – 86.1) and a specificity of 84.9 (95% CI: 79.9 – 89.9).

Linear Local Shortening Map

Overall LLS correlated significantly with ^{201}Tl activity and particularly the maps could distinguish segments with normal (>75%) and impaired (50-75%) ^{201}Tl uptake (LLS: 8.9 ± 7.6 versus 6.5 ± 5.8; p=0.0032), and viable impaired regions and non-viable (LLS: 6.5 ± 5.8 versus 2.9 ± 6.4; p< 0.015).

Bipolar Voltages map

Overall BP correlated significantly with ^{201}Tl activity (p=0.0001) and particularly the could distinguish segments with normal (>75%) and impaired (50-75%) ^{201}Tl uptake (BP: 3.88 ± 2.36 versus 3.03 ± 2.15; p < 0.01), and between viable impaired regions and non-viable (BP: 3.03 ± 2.15 versus 1.70 ± 1.36; p< 0.0001).

Fragmentation index

Overall the fragmentation index was not significantly correlated to redistribution ^{201}Tl activity (Table 3: p = 0.10), but the small number of data and the scattered distribution, results in insufficient statistical power to find a correlation between FI values and SPECT data.

Electromechanical maps values according to myocardial regions

Overall a significant difference was observed between the UV, LLS, and BP values in the basilar in comparisons to the mid-ventricular regions (UV: 9.65 ± 4.85 mV versus 14.49 ± 5.82 mV; p < 0.0001. LLS: 5.97 ± 7.15% versus 9.17 ± 6.03%; p < 0.0002. BP: 3.07 ± 2.31 mV versus 3.88 ± 2.79; p = 0.039). Nevertheless the ability of these parameters to distinguish between infarcted, ischemic and normal myocardium according to the perfusion status in radionuclide SPECT imaging is not different among the basilar and the mid-ventricular segments (Interaction mid-ventricle versus basilar for LLS, UV and BP p = NS). The average LLS values, UV and BP potentials were higher in regions with normal ^{201}thallium uptake and lower in regions with ^{201}thallium activity < 50%. The segments with ^{201}thallium uptake between 50% and 75% showed intermediate values (Figure 1).

Figure 1

Local linear shortening, Unipolar voltages and Bipolar voltages according to thallium activity in basal and mid-ventricular regions

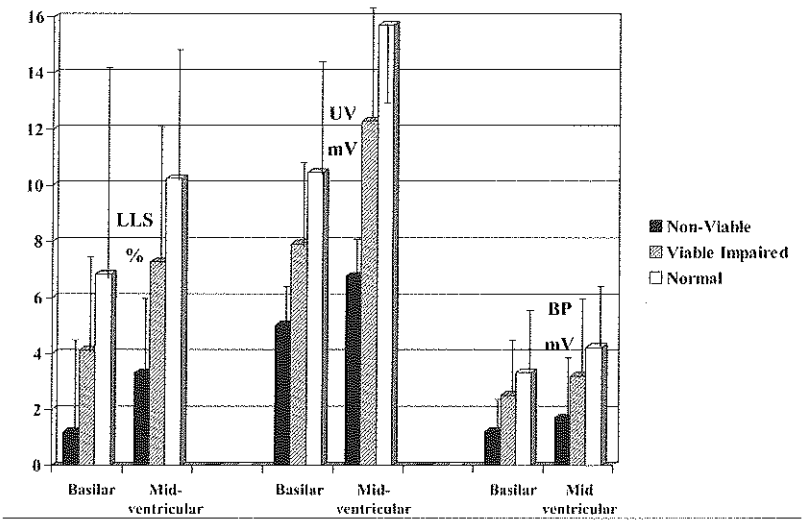

LLS- local linear shortening, UV- unipolar voltage, BP- bipolar voltage.
Overall a significant difference was observed between the UV, LLS and PB values in the basal as compared to the mid-ventricular regions (UV: p<0.0001, LLS : p<0.0002, BP : p<0.039).
The ability of these parameters to distinguish between infarcted, ischemic and normal myocardium according to Thallium perfusion studies is preserved (interaction mid-ventricle versus basal for LLS, UV, BP = NS).

Electromechanical coupling assessment

Overall the distribution of the electromechanical coupling index values correlates with redistribution thallium activity (p <0.0001). Significantly lower values of EMC index were found in non viable segments compared with viable impaired (25.18 ± 60.5 versus 86.8 ± 95.6; p = 0.003) and normal regions (25.18 ± 60.5 versus 138.4 ± 137.7 p < 0.0001). LLS and UV were combined to provide an estimate of electromechanical coupling (EMC) which significantly correlates with redistribution thallium uptake as shown in Table 3.

Table 3

Distribution of estimate of EMC according to redistribution of ^{201}Tl activity.

EMC	Normal N=192	Viable impaired N=68	Non-viable N=20	P value
LLS < 6.5%, UV < 6.5 mV	14	14	11	
LLS < 6.5%, UV ≥ 6.5 mV	45	21	3	
LLS ≥ 6.5%, UV ≥ 6.5 mV	124	31	3	
LLS ≥ 6.5%, UV ≤ 6.5 mV	9	2	3	< 0.001

LLS : local linear shortening. UV : unipolar voltage. EMC : electromechanical coupling.

Automatic and manual editing

The Lin's concordance correlation coefficient for agreement between the automated edited maps and the manual edited maps was 0.72 (p<0.001) for the LLS and 0.95 (p<0.001) for UV respectively. Overall both LLS and UV maps automatically and manually edited could discriminate between normal, viable impaired and non-viable myocardium as assessed by perfusion studies (LLS automated edited: 10.7 ± 7.1 versus 9.4 ± 6.8 versus 7.3 ± 6.8; p= 0.044. UV automated edited: 13.8 ± 6.1 versus 10.7 ± 5.3 versus 7.8 ± 4.1; p = 0.0001).

Intra-patients reproducibility

The intra-patient reproducibility of the NOGA map's data has been evaluated in five patients in whom the NOGA study was performed in two times (as a clinical assessment and as part of a DMR protocol) few weeks apart without any revascularization procedure between. The LIN's concordance correlation coefficient rho of 0.61 (p<0.001) was observed for the UV data. The relatively small number of segments results in insufficient statistical power to raise any definitive conclusion for the intra-patient reproducibility of NOGA myocardial assessment.

Discussion

The Biosense electromechanical mapping system has been proved in animal studies and in preliminary clinical experience to distinguish infarcted from healthy myocardium by a reduction in both electrical voltage and mechanical activity. In these preliminary studies local endocardial shortening was significantly impaired in MI zones compared with controls and significant electrical impairment was observed in the infarct zones.

Kornowski, observed that segments with reversible perfusion defects at the 99m Tc-sestamibi after adenosine stress scintigraphy, have a moderate reduction (15%) in endocardial potentials and mechanical function, while segments with fixed perfusion defects showed a profound electromechanical impairement. In our study comparing redistribution thallium images with Noga parameters, we could discriminate between ischemic but viable and non viable myocardium. Interestingly among the segments with a thallium uptake < 50% of maximal, unipolar voltages show a trend toward higher values in the regions with a thallium uptake between 20% and 50% compared to regions with

thallium activity < 20% (p=0.08). This observation raises the question of whether a regions of patchy ischemia within fibrotic areas still retain some electrical activity and possibly myocardial viability which should be accurately detect with endocardial mapping.
Mechanical dysfuction could indicate irreversible myocardial necrosis as well as restorable ischemic or hibernating myocardium, and Kornowski suggested that the existance of electromechanical uncoupling (impaired mechanical activity with preserved electrical activity) migth signify retained myocardial viability. This issue has been addressed by Koch who evaluates myocardial viability in hypocontractile and underperfused myocardium, comparing the endocardial electrical signals with F-18 FDG uptake at PET and Tc-99m sestamibi at SPECT studies respectively. In this study electrical unipolar signals using 6 mV as threshold amplitude correctly identifies scar areas from areas with preserved viability and may predict improvement in wall motion abnormalities six months after successful revascularization.
Concordantly with the series of van Dahl we found an overall threshold for the UV of 6.5 mV defining viable tissue, while a threshold of 10.3 mV characterizes the normal viable tissue. This is consistent with the average unipolar voltages observed by Van Langenhove in segments with or without improvement at low dose dobutamine stress echocardiography (10.2 ± 5.7 mV and 6.9 ± 3.1 mV respectively).
In our series significant lower values of LLS and of UV were observed in the basal myocardial regions versus the mid ventricle. At the regional level, there appears to be remarkably spatial heterogeneity of myocardial deformation. Midwall segment shortening is higher at the apex than at the base of the LV, and circumferential shortening is higher in the anterior than in the posterior left ventricular wall. The presence of the valve apparatus (electrically inactive) should possibly explain the lower average voltages values recorded basilar regions. Nevertheless despite different absolute values, within the midventricular and the basilar regions the UV accurately detect viable from non viable myocardium, with possibly a somewhat more overlapping in the mitral anulius area as already observed by Kornowski. These observations raises the issue of possibly different threshold according to LV regions for a better definition of the myocardial viability status.
In our study an estimate of the electromechanical coupling and the electromechanical index appear to significantly correlate with redistribution thallium perfusion, but with a not negligeable overlapping between non-viable, viable impaired and normal myocardium. This is possibly due to the limit of using a standard segmentation of endocardial surface and average values of data points.
Overall higher fragmentation index values compared to those reported by Keck, were observed in our series (1.41 ± 0.5 versus 1.15 ± 0.18 and 1.83 ± 0.7 versus 1.28 ± 0.23 in normal and non viable segment respectively), but the difference between normal, viable imapired and scar areas was not statistically significative probably due to an excessive scattering of the signal in our maps. More sophisticated signal analysis and algorithms could better define the fragmentation phenomena in the aim of a precise detection of viable myocardium.
The correct interpretation and clinical significance of the obtained data are totally dependent by the quality of the acquired points. The system provides an automatic editing of the undesired points. From our data the automated postprocessing appears to be as accurate as the manual editing for the UV maps and slightly less precise for the LLS interpretation based on the version 2. of the sofware, possibly due to the weight of the

unedited inner points and the clustered points on mathematical function which calculated the LLS. The clinical relevance of these observation implies a reliability of the interpretation of the voltages data even in presence of "bad" points, for the detection of normal, ischemic and non viable myocardium.
Moreover it appears that the electrical information is reproducible over the time in the same patients not treated by any revascularization procedure. This implies a reliability of the UV maps interpretation and permits to utilize the NOGA myocardial assesment to define changes in viability status after different revascularization procedures.

Study Limitations

As all comparative studies, there is the potential for anatomic misalignment, because the orientation of the heart is inherently different between the techniques. Particularly with NOGA the reconstruction of the chamber is sequential and irregular and the 3-D geometry of the chamber depends on the number of point sampled. Hence the temporal resolution of the method is limited and failure to collect data points homogeneously from the entire ventricle results in underestimation of the true LV chamber.
The mechanical function derived from the by use of local endocardial shortening for each endocardial site is the average from all the neighboring points and this may result in reduction of the reduced LLS area.
Unipolar voltage measurements may potentially be affected by far-field potentials which could decrease the amplitude of the unipolar electrograms at infarcted region.
Bipolar electrograms with the actual mapping catheter have certain limitations because of changes in the electrode orientation relative to the activation wave front. These limits should be overwhelmed with the splitted tip mapping catheter.
A mathematical algorithm provides a reliable estimation of the QRS complex fragmentation, but the real intracardiac signals are contaminated with noise and other small disturbances which could affect the level of fragmentation and may result in reduction of the ability to detect viable tissue within a scar.

Clinical implication

Electromechanical mapping could provide new intriguing insight in the comprehension of myocardial ischemia and of myocardial viability. The possibility of discriminate viable myocardium should have an importance in the revascularization decision-making directly in the cath-lab. The ability of navigating into the left ventricle permits the guidance of catheters for direct myocardial revascularization both by laser energy and gene transfer. The on-line assessment of myocardial viability should be advantageous both for targeting the treatment zone and avoiding the laser energy delivery within then scar.

Conclusions

Electromechanical maps distinguish normal, non viable and ischemic myocardium as assessed thallium perfusion imaging studies.
The electromechanical assessment could enable the discrimination of hypocontractile, but still viable myocardium. The myocardial viability status as assessed by the unipolar voltage appears to be reproducible over the time.

References

1. Smeets J, Ben-Haim S, Rodriguez LM et al. New method for nonfluoroscopic endocardial mapping in humans. Accuracy assessment and first clinical results. Circulation 1998; 97:2426-2432.
2. Gepstein L, Goldin A, Lessick J et al. Electromechanoical characterization of chronic myocardial infarction in the canine coronary occlusion model. Circulation 1998;98:2055-2064.
3. Kornowski R, Hong MK, Gepstein L et al. Preliminary animal and clinical experiences using an electro-mechanical endocardial mapping procedure to distinguish infarcted from healthy myocardium. Circulation 1998; 98: 1116-1124.
4. Kornowski R, Hong MK and Leon MB. Comparison between left ventricular electro-mechanical mapping and radionuclide perfusion imaging for detection of myocardial viability. Circulation. 1998; 98: 1837-1841, 1998.
5. Corvaya N, Kornowski R, Wang XD et al. Correlation between myocardial Biosense NOGA electromechanical map and radionuclide perfusion imaging. Eur Heart J 1998; Suppl A: P 1600 (abstr).
6. Keck A, Schwartz Y, Weber T et al. On-line assessment of myocardial viability using electromechanical mapping. Eur Heart J 1999; Suppl A: P 1692 (abstr).
7. vom Dahl J, Koch K-C, Schultz G et al. Myocardial viability assessment by endocardial electroanatomical mapping: validation by comparison with F-18 FGD positron emission tomography. J Am Coll Cardiol 1999; Suppl A:1035-141 (abstr).
8. Koch K-C, Keck A, Kitzing R et al. Nonfluoroscopic 3-dimensional catheter based electroanatomical mapping: follow-up study after successful myocardial revascularisation. J Am Coll Cardiol 1999; Suppl A:1035-140 (abstr)..
9. Koch K-C, Schultz G, Oswald E et al. Myocardial viability assessment by catheter based electroanatomical mapping. Validation of a new method by radionuclide imaging. J Am Coll Cardiol 1999; Suppl A:1186-138 (abstr).
10. Vale P, Losordo D, Tkebuchava T et al. Catheter-based myocardial gene transferutilizing nonfluoroscopic electromechanical left ventricular mapping. J Am Coll Cardiol. 1999;34:246-54.
11. Kornowski R, Fuchs S, Vodovotz Y et al. Successful gene transfer in a porcine ischemia model using the Biosense guided transendocardial injection catheter. J Am Coll Cardiol 1999; Suppl A:826-4 (abstr).
12. Fuchs S, Kornowski R, Shiran A et al. Electromechanical characterization of chronic experimental myocardial ischemia in a pig model. J Am Coll Cardiol 1999; Suppl A:849-5 (abstr).
13. Heush G. The relationship between regionalblood flow and contractile function in normal, ischemic and reperfused myocardium. Basic Res Cardiol 1991;86:197-218
14. Bonow R. Identification of viable myocardium. Circulation 1996;94:2674-2680.
15. Vanoverschelde J-L, Wijns W, Borgers M et al. Chronic myocardial hibernation in humans. From bedside to bench. Circulation 1997; 95:1961-1971.
16. Kornowski R, Hong M, Leon M. Current prospectives on direct myocardial revascularization. Am J Cardiol 1998;81 (7A):44E-48E.
17. Laham R, Simons M, Pearlman J et al. Biosense catheter direct myocardial revascularization (DMR) improves 30-day angina class, regional wall motion perfusion of the treated zone(s) using MRI. J Am Coll Cardiol 1999; Suppl A:1035-138 (abstr).
18. Kornowski R, Moses JW, Baim DS et al. Percutaneous direct myocardial revascularization guided by Biosense left ventricular mapping in patients with refractory coronary ischaemic syndromes. Eur Heart J 1999; Suppl A: P 2823 (abstr).
19. Koch K C, Stellbrink C, Sasse A et al. Electromechanical 3D endocardial mapping: follow-up study after successful myocardial revascularization. Eur Heart J 1999; Suppl A: P 2780 (abstr).
20. I Bossi, AJ Black, R Choussat, et al. Biosense noga electromechanical mapping accurately predicts left ventricular wall motion at cineventriculography. Am J Cardiol, 1999 Supplement. TCT- 255 (abstr).

Chapter 8

Nonfluoroscopic electromechanical mapping for detection of viable myocardium: a comparison with dobutamine stress echocardiography.

Authors:
Glenn Van Langenhove[1], MD; Jaap N. Hamburger[1], MD; Irenee Bossi[3], MD; Paul Van den Heuvel[4], MD; Dirk Stockman[4], MD; Mariano Albertal[1], MD; Peter C. Smits[1], MD; Emile Onderwater[1], BSc; Don Poldermans[2], MD; Marc Vaerenberg[4], MD; Jean Fajadet[3], MD; Jean Marco[3], MD; Patrick W. Serruys[1], MD.

From the Departments of [1]Interventional Cardiology and [2]Echocardiography, Thoraxcenter Rotterdam, Dijkzigt Hospital, Erasmus University, Rotterdam, The Netherlands, [3] the Department of Interventional Cardiology, Clinique Pasteur, Toulouse, France and the Department of Cardiology, Middelheim Hospital Antwerp, Belgium.

Short title: NOGA™ mapping for detection of myocardial viability

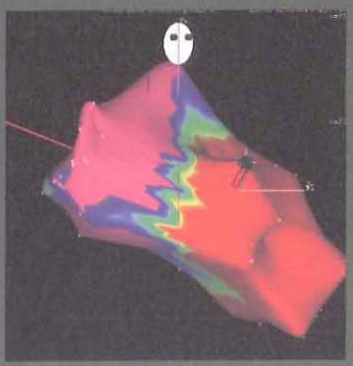

Abstract

Background

Nonfluoroscopic electromechanical mapping (NEM) has recently emerged as a novel in-cathlab method to assess electromechanical functioning of the myocardium and to detect myocardial viability. Up to now, no comparison with dobutamine stress echocardiography has been reported. We therefore compared the results of NEM to those of DSE for the detection of myocardial viability in a subset of patients with severe coronary artery disease.

Methods and Results

Myocardial viability was assessed through both DSE and NEM in 30 patients, a majority of whom suffered a previous myocardial infarction (83%). A segment-to-segment comparison was made in 324/360 segments (90%). Logistic regression and receiver operator characteristics (ROC) curve analysis revealed highly significant predictive values for both linear local shortening (LLS) and unipolar voltages (UPV) : area under the curve was 68% and 74% respectively ($p<0.0005$ for both). ROC curve analysis revealed LLS= 7.2% and UPV=8.2 mV as optimal cut-off values to define viability. The combination of both parameters proved to be the strongest predictor for viability (RR=6.5 , CI 3.0-13.9, $p<0.0005$).

Conclusion

NEM can predict recovery in previously injured myocardium when compared to DSE. Both LLS and UPV have added value in the assessment of viability. Strongly significant cut-off values for both LLS (7.2%) and UPV (8.2 mV) were found.

Condensed abstract

Nonfluoroscopic electromechanical mapping (NEM) has recently emerged as a novel technique for in-cathlab assessment of myocardial viability. We compared the findings of NEM in 30 patients with the results of dobutamine stress echocardiography. We found highly significant cut-off values for both linear local shortening and unipolar voltages for the detection of viable myocardium. Moreover, the combination of both parameters has the highest value in predicting recovery of previously injured myocardium.

List of Key Words

Coronary disease
Myocardium
Hibernation
Ventricles
Stress Echocardiography

Introduction

Assessment of viability in patients that previously suffered myocardial injury remains a challenge in clinical cardiology, as revascularization of viable myocardial segments may improve prognosis.[1,2] DSE is a widely accepted method to define the presence of myocardial viability,[3,4] and has been found superior to information obtained solely from coronary anatomy at cardiac catheterization.[5] DSE however is not easy to apply inside the cathlab, and is usually performed with a certain time delay from the index diagnostic catheterization.

Nonfluoroscopic mapping has recently emerged as a novel in-cathlab method to assess electromechanical functioning of the myocardium. This system allows measurement of local electrical (unipolar voltage, UPV) and mechanical (local linear shortening, LLS) properties of the left ventricle.[6] These properties have been implied in the assessment of potentially recoverable myocardium post-infarction.[7,8] Kornowski et al. recently described the value of nonfluoroscopic electromechanical mapping (NEM) in the detection of reversible perfusion defects as compared to radionuclide perfusion imaging.[9] Up to now, no comparison with DSE has been reported.

We therefore, for the first time, compared the results of NEM to those of DSE for the detection of myocardial viability in a subset of patients with severe coronary artery disease and defined cut-off values for electrical (UPV) and mechanical (LLS) parameters for viable myocardial tissue.

Methods

Study population

We studied 30 patients with severe chronic coronary artery disease. Mean age was 61 ± 8 years. Twenty-seven (90%) were male. Twenty-five patients (83%) previously suffered a myocardial infarction, 16 (53%) had a Q-wave on the ECG. Twenty-seven patients (90%) underwent one or multiple revascularization procedures. All patients had stable anginal complaints (7 patients in CCS class 1, 11 in CCS class 2, 6 in CCS class 3, and 6 in CCS class 4). The study was approved by the respective medical ethical committees, and all subjects gave informed consent.

Nonfluoroscopic electromechanical mapping

The components of the system and the technique have been described extensively.[6-11] In short, the NEM system (NOGA™, Biosense-Webster, Cordis, Johnson & Johnson) is able to acquire electromechanical data from the endoluminal surface of the left ventricle through the use of a 7 French catheter with a locatable tip placed in the left ventricle. A low magnetic field surrounding the patient enables the system to threedimensionally locate the catheter tip at all times. The tip of the catheter also contains electrodes to acquire local electrophysiological voltage data. Thus uni- (UPV) and bipolar voltages and linear local shortening (LLS) data of the left ventricle endoluminal surface can be assessed.[6-11] Presuming that in healthy myocardium any two points move closer to each other during contraction, the LLS assessment as measurement of distances between neighboring points is therefore the basis for calculation of myocardial shortening. The computer algorithm takes into account the density of points around a point p, and gives a

negligible weight to points too close (sampling noise) and points too far (of no influence as they provide non-local information). The algorithm for LLS is calculated as follows [12]: for any two points on the map, i and j, LLS is calculated as the change in distance between these two points from end-diastole to end-systole, normalized for the length at end diastole:

$$LLS_{ij} = (L(ED)_{ij} - L(ES)_{ij})/ L(ED)_{ij}$$

For any point p LLS is calculated as a function of the LLSpj, for all points j=1 to n on the map, so that

$$LLS_p = (Sj=1..n\ W_{pj}\ (L(ED)_{pj})x\ LLS_{pj}\ ) / Sj=1..n\ W_{pj},$$

where W is the weight of a certain point as a function of the distance Lij between two points i and j, the average distance D around point p (D is defined in the computer algorithm as the average distance of the ten closest points to p) and the volume V at end-diastole. The weight is therefore function of the point density in a defined region, the volume of the heart and the distances between points at end-diastole.[12]

To ensure maximum validity of the data obtained, we applied an intense filtering mechanism. First, an inner points filtering was applied. This computer algorithm removes points that are located deep within the reconstructed left ventricle. Therefore, the cone angle (the angle of the cone formed around a line connecting the investigated point and the center, defining the closest vicinity of a neighboring point) was set at 20%, whereas the relative depth percentage was set at 20%, meaning elimination of points located 20% deeper than neighboring points. Maximum location displacement of the catheter tip was set at 4 mm, trajectory instability was maximum 4 mm, and median cycle length was set at 10%, thus deleting all points which cycle length differed more than 10% from the preset values. After this thorough editing, local trajectories were examined for points with questionable behavior (which could imply loss of contact with the ventricular wall), endocardial ST segment elevation was evaluated for marked elevations (caused by intense impression by the mapping catheter), and ECG tracings were evaluated to ensure that data were not obtained during or immediately after an extrasystole.
We considered a map successful when more than 40 points throughout the ventricle were acquired, and when no procedural complications occurred. Segments were evaluated only if at least three points per segment were acquired.

Dobutamine stress echocardiography

Dobutamine stress echocardiography (DSE) using a standard protocol was performed prior to the mapping procedure.[13,14] For wall motion analysis, we used a 16-segment subdivision as described previously[15]. These 16 different segments were analyzed by an operator blinded for the mapping results. Segments were evaluated using the 5-point scoring system according to the American Society for Echocardiography (1=normal, 2=hypokinetic, 3=akinetic, 4=dyskinetic, and 5=aneurysmal) at rest, during low dose (10 mg/kg/min) and high dose dobutamine (up to 40 mg/kg/min, and additional atropine until maximum heart rates were obtained).

Segments were than qualified as worsened, unchanged or improved, depending on their change in score on the 5 point ranking. These results were than compared to the average local linear shortening (LLS, mm) and the unipolar voltages (UP, mV) of the same segments obtained during the NOGA™ procedure.
As standard echocardiography techniques divide the left ventricle into 16 segments, we had to imply a reduction to 12 segments to produce a comparable data set with the 12 segments provided by the NEM bull's eye view. The validity of this comparison has been shown previously.[16] The basal, mid and apical anterior segment were taken from the apical two-chamber view; the basal, mid and apical lateral segment from the apical four-chamber view, and the basal, mid and apical posterior segment from the apical long-axis view (figure 1).

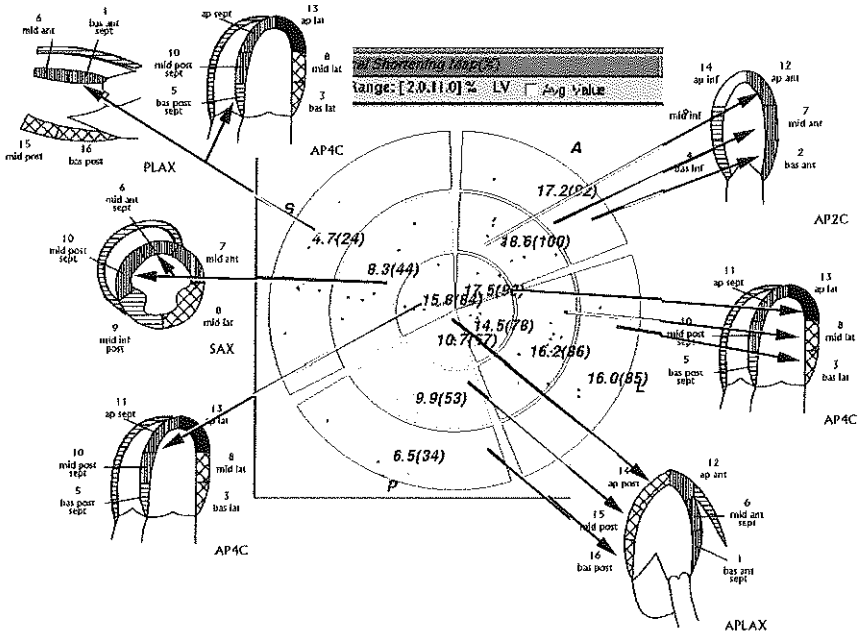

Figure 1

Comparison of NOGA™ segments and echocardiographic segments. The central square illustrates the bull's eye view of the left ventricle map as provided by the NOGA™ system. Clockwise from upper right A (anterior), L (lateral), P (posterior) and S (septal) divisions are shown. From the center to the outer part they are divided into apical, mid and basal segments. The arrows show the comparable segments on echocardiography. AP2C = apical 2-chamber view; AP4C= apical 4-chamber view; APLAX= apical long axis view; SAX= parasternal short axis view; PLAX= parasternal long axis view.

The apical septal segment was taken from the apical four-chamber view, whereas the mid septal segment was derived from the mid posterior and mid anterior septal segments on the parasternal short axis view, and the basal septal segment from the basal posterior (apical four-chamber view) and basal anterior septal segments (parasternal long axis view) (figure 1). When there was disagreement on the scoring of one of these combined DSE segments, the worst score was chosen.

Statistics: Correlation was measured using Pearson's test. Means of values were compared using the unpaired Student's t-test. Multivariate logistic regression (forward stepwise) analysis was used to determine independent predictors of viability. Receiver operator characteristic (ROC) analyses were applied to determine the optimal cut-off values for LLS and UPV to predict viability, so that any value above that point would be considered as positive (ie predictive for viability), and any value below as negative. Sensitivity, specificity, and positive and negative predictive values were calculated at each threshold. We defined the best threshold of a significant predictive variable to de the cut-off point where sensitivity equals specificity, defining the point with the highest diagnostic accuracy. Using this threshold, the population was divided in two times two categories. The frequency of viability in all categories was determined, and differences were evaluated by chi-square analysis. Relative risks were calculated. A p-value <0.05 was considered significant.

Results

All mapping procedures and dobutamine stress echocardiograms were successful. No complications were seen. An example is shown in figure 2.

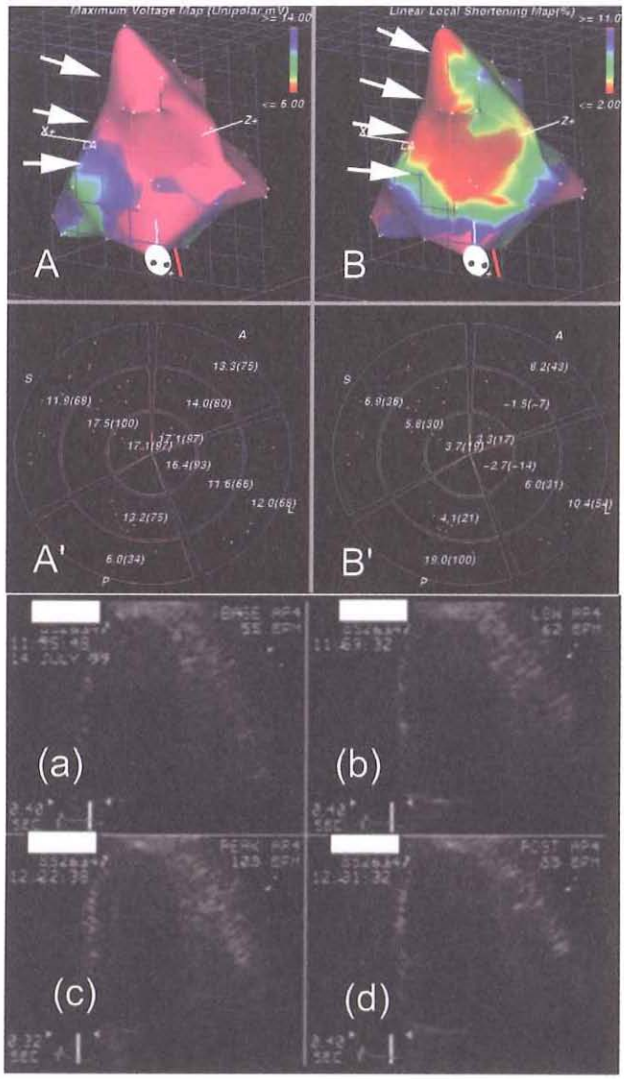

Figure 2

NOGA™ map and dobutamine stress echocardiogram sequence of the same patient. The upper panel demonstrates the NOGA™ map from a superior view (apex of the left ventricle is shown at the top of the picture, basis at the bottom) to facilitate comparisons with the dobutamine stress echo images. A shows the unipolar voltage (UPV, mV) maps in the same view, and its respective bull's eye view(A'). B shows the linear local shortening (LLS, %) map, with its respective bull's eye view. Color codes are shown to the right of the maps (UPV from red (<6mV) to purple (>14mV), and LLS from red (<2%) to purple (>11%)). The arrows in A and B show a region with high UPV and low LLS, suggesting myocardial viability in the affected basal, mid, and apicolateral segments and in the mid anterior segment. The absolute values can be appreciated in the bull's eye maps. Dobutamine stress echocardiographic apical 4 chamber images are shown at the bottom of the figure. (a) shows akinesia of the basal, mid and apical lateral segments at rest, (b) and (c) reveal viability with low and high dose dobutamine respectively , (d) shows the image during recovery.

In 30 patients, 324 (of 360, 90%) segments were compared. Twenty-four segments (7%) could not be compared due to insufficient amount of points acquired during NEM, 12 segments (3%) could not be analyzed due to insufficient echocardiographic image quality. Of these 324 segments, DSE showed that 100 (31%) were "truly" normal (normal at rest and normal during dobutamine infusion), 75 segments (23%) showed no viability, and 149 (46%) segments were viable. UPV for normal versus all other segments was 14.9 mV ± 5.7 versus 9.0 mV ± 4.3, respectively. LLS was 12.8% ± 6.1 versus 6.9% ± 6.6, respectively ($p<0.005$ for both comparisons).

Of the 100 normal segments, 15 showed ischemia and 85 did not. UPV did not differ significantly amongst the two groups (14.2 mV ± 5.7 versus 14.9 mV ± 8.1 , respectively, $p=0.70$). The difference in LLS for the ischemic segments (8.7% ± 8.2) versus the non-ischemic segments (12.8% ± 6.1) was borderline significant ($p=0.047$). Hypokinetic segments (n=79) showed ischemia in 21 segments (27%) and no ischemia in 58 segments (73%). UPV was higher in the ischemic segments (11.5 mV ± 5.3) than in the non-ischemic segments (8.7 mV ± 3.1) ($p=0.004$). LLS however, did not differ significantly between both groups (8.2% ± 6.5 vs. 8.5% ± 5.1, respectively, $p=0.87$).
The correlation between UPV and LLS for all segments is shown in figure 3.

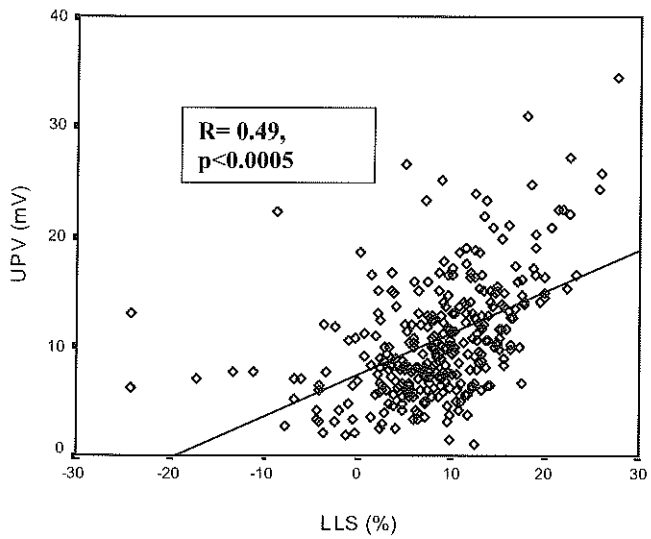

Figure 3

Correlation between unipolar voltages (UPV, mV) and linear local shortening (LLS,%) for the same segments.

Although only moderate (r=0.49), the correlation proved highly significant ($p<0.0005$). For the further analysis on viability, only the segments that were not normal were used.

Table 1

Logistic regression and receiver operator characteristics (ROC) curve analysis of LLS and UPV for detecting viable myocardium.

Variable	Cut-off	ROC area (95% CI)	P (multivariable)	Sens, %	Spec, %	PPV, %	NPV, %
LLS -%	7.2	68 (61-75)	<0.0005	64	68	80	48
UPV-mV	8.2	74 (67-80)	<0.0005	70	77	85	61

Sens= sensitivity, spec= specificity, PPV= positive predictive value, NPV= negative predictive value, LLS= local linear shortening, ROC= receiver operator characteristics, CI= confidence interval.

Table 1 shows the results of the logistic regression and the ROC analyses.

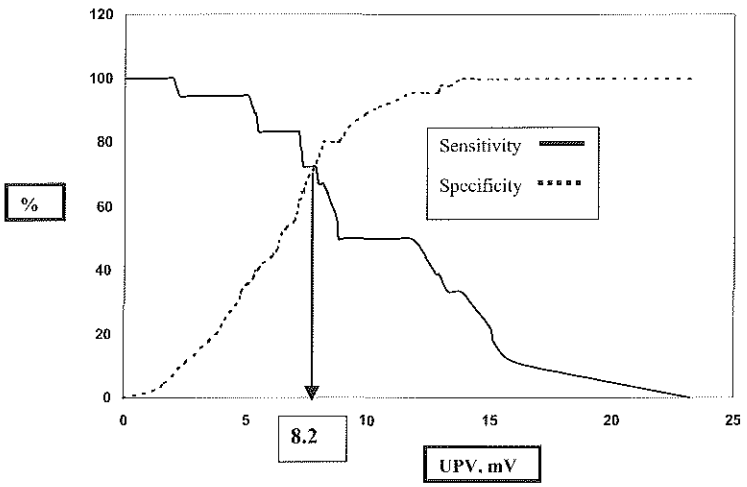

Figure 4

Receiver operator characteristics (ROC) curve for UPV. The graph demonstrates the optimal cut-off value for UPV as the optimal sensitivity and specificity for detecting myocardial viability.

Figure 4 shows the ROC curve for UPV. LLS has a moderate prognostic value in the prediction of viability (ROC area 68%, p<0.0005); the optimal cut-off value for LLS was 7.2%. UPV had a stronger prognostic value in predicting viability (ROC area 74%, p<0.0005); the optimal cut-off value for UPV was 8.2 mV. The multivariate logistic regression analysis showed that both LLS and UPV were highly significant independent parameters to predict viability.
According to these cut-off values, we then stratified segments into four subsets according

to low (<7.2%) versus high (>7.2%) LLS and low (<8.2mV) versus high (>8.2mV) UPV. The segments that were most likely to be viable had LLS>7.2% and UPV>8.2mV (group 1). Conversely, the segments that were least likely to be viable had LLS<7.2% and UPV<8.2mV (group 4). The segments with either LLS>7.2% or UPV>8.2mV had intermediate likelihood of viability (group 2 and 3, see figure 5).

Figure 5

Division of segments into four categories according to the optimal cut-off values of UPV= 8.2 mV and LLS= 7.2%. Group 1 represents segments that have both optimal UPV as well as LLS. Group 4 represents segments that have both decreased UPV and LLS. Groups 2 and 3 represent groups with high LLS and low UPV, and vice versa. The closed squares represent non-viable segments; the open squares represent viable segments.

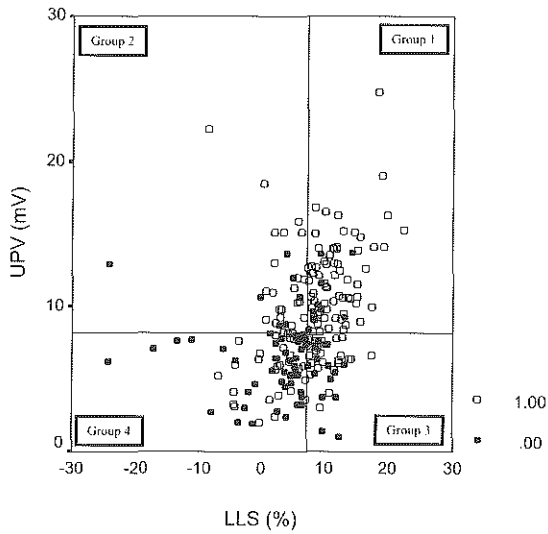

The result of this division into 4 subgroups according to the presence of viability is also shown in figure 6.

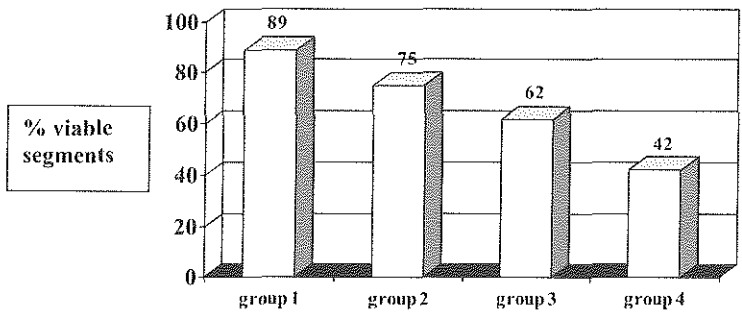

Figure 6

Percentage of viable segments in each group (as defined in figure 5)

In this figure, the segments viable on DSE are depicted as open circles, whereas solid points represent those that were not viable. The right upper quadrant contains most of the segments that were viable on DSE, whereas segments that did not show viability are abundant in the left lower quadrant.

The optimal cut-off criteria of the combined categorical variables were subsequently used to establish the relative "risk" (RR) of the presence of viability (see table 2).
Segments in group 1 (LLS ≥ 7.2% and UPV ≥ 8.2 mV) had a 6.5 times higher probability of being viable than segments in group 4 (LLS < 7.2% and UPV < 8.2 mV).

Discussion

The most important finding of this study is the high predictive value of nonfluoroscopic mapping as a tool for in-cathlab assessment of viability. We have – for the first time- identified strong threshold values of LLS (7.2%) and UPV (8.2 mV) that characterize a subgroup of hibernating myocardial segments that are likely to be viable. Although the risk analysis showed that both LLS (RR 2.4) and UPV (RR 4.5) were independently predictive of viability, a combination of both parameters showed an even stronger predictive value (RR 6.5).
This is the first study that demonstrates the possibilities of electromechanical mapping as compared to dobutamine stress echocardiography to predict recovery of injured myocardial segments. The correlation of NEM with radionuclide testing in the detection of reversible perfusion defects is well established.[8,9] Recent studies however have suggested a preference for dobutamine stress echocardiography for viability assessment when compared to radionuclide techniques.[17-19] Indeed, Arnese et al. comprehensively demonstrated that a specificity of 48% with poststress reinjection ^{201}Tl single-photon emission computed tomography (SPECT) before surgery induced a significant amount of unnecessary grafting procedures to segments that were deemed viable, but proved not to be when reassessed after bypass surgery.[18] A comparison with DSE may therefore be of added value to the ongoing search for cut-off values in the electromechanical assessment of myocardial viability.
The results of our study are somewhat discordant with previously published reports.[9] Kornowski et al. comprehensively demonstrated that in their population of 18 patients with symptomatic chronic angina, reversible perfusion defects showed LLS and UPV values of 10.3% ± 3.7 and 12.0 mV ± 2.8, respectively.[9] This discordance may be induced by the difference in study population, the small amount of patients in both studies or the differences in sensitivity and specificity between DSE and radionuclide scanning.[20-22]
Although the electromechanical mapping technique is not readily available in every cathlab and is not easy to master, some advantages can be put forward. 1) The interobserver disagreement in stress echocardiography and radionuclide scintigraphic techniques may reach up to 20%[23]; the NEM technique is not based on interpretation, but puts forward clear values of electromechanical properties and may therefore have better reproducibility and may provide a more straightforward interpretation. Others have suggested that radionuclide techniques may over- as well as underestimate the amount of possibly recoverable myocardial tissue.[21,23]
In this study, we found significant differences in electromechanical parameters in ischemic versus non-ischemic segments that showed a normal baseline contraction pattern on echocardiography. The fact that LLS showed a borderline significant lower value in segments that proved to be ischemic during dobutamine infusion, could reflect the minimal changes in regional contraction of the jeopardized myocardium that cannot be seen using echocardiography but become apparent with NEM. In segments that show

hypokinesia on baseline echocardiography, UPV was higher in segments that were ischemic during DSE. This may reflect the viability that is still present in these segments.

Limitations

The small number of patients limits us in drawing final conclusions about true cut-off values for viable and non-viable segments. Also, it may be of importance that in the group with both low LLS as and low UPV, DSE suggested still 40% of the segments to be viable. This issue is addressed in the forthcoming DINO study, which will evaluate the assessment of NEM for predicting recovery of injured myocardial segments as compared to true recovery after bypass surgery. Last, 40 points may not be enough to adequately map all myocardial regions.

Conclusion

NEM can predict recovery in injured myocardium when compared to DSE. Both LLS and UPV have added value in the assessment of viability. Strongly significant cut-off values for both UPV (8.2 mV) and LLS (7.2%) are set forward.

References

1. Pfeffer MA, Braunwald E, Moye LA, et al. Effect of captopril on mortality and morbidity in patients with left ventricular dysfunction after myocardial infarction. Results of the survival and ventricular enlargement trial. The SAVE Investigators [see comments]. N Engl J Med 1992;327(10):669-77.
2. St. John Sutton M, Pfeffer MA, Plappert T, et al. Quantitative two-dimensional echocardiographic measurements are major predictors of adverse cardiovascular events after acute myocardial infarction. The protective effects of captopril. Circulation 1994;89(1):68-75.
3. Naguch SF, Zoghbi WA. Stress echocardiography for the assessment of myocardial ischemia and viability. Curr Probl Cardiol 1996;21(7):445-520.
4. Lualdi JC, Douglas PS. Echocardiography for the assessment of myocardial viability. J Am Soc Echocardiogr 1997;10(7):772-80.
5. Carlos ME, Smart SC, Wynsen JC, Sagar KB. Dobutamine stress echocardiography for risk stratification after myocardial infarction [see comments]. Circulation 1997;95(6):1402-10.
6. Ben-Haim SA, Osadchy D, Schuster I, Gepstein L, Hayam G, Josephson ME. Nonfluoroscopic, in vivo navigation and mapping technology. Nat Med 1996;2(12):1393-5.
7. Gepstein L, Goldin A, Lessick J, et al. Electromechanical characterization of chronic myocardial infarction in the canine coronary occlusion model. Circulation 1998;98(19):2055-64.
8. Kornowski R, Hong MK, Gepstein L, et al. Preliminary animal and clinical experiences using an electromechanical endocardial mapping procedure to distinguish infarcted from healthy myocardium. Circulation 1998;98(11):1116-24.
9. Kornowski R, Hong MK, Leon MB. Comparison between left ventricular electromechanical mapping and radionuclide perfusion imaging for detection of myocardial viability. Circulation 1998;98(18):1837-41.
10. Gepstein L, Hayam G, Shpun S, Ben-Haim SA. Hemodynamic evaluation of the heart with a nonfluoroscopic electromechanical mapping technique. Circulation 1997;96(10):3672-80.
11. Gepstein L, Hayam G, Ben-Haim SA. A novel method for nonfluoroscopic catheter-based electroanatomical mapping of the heart. In vitro and in vivo accuracy results. Circulation 1997;95(6):1611-22.
12. Biosense-Webster. NOGA Cardia Electromechanical Mapping System. User's Manual. Software Revision 2 ed, June 1998.
13. Marcovitz PA, Armstrong WF. Accuracy of dobutamine stress echocardiography in detecting coronary artery disease. Am J Cardiol 1992;69(16):1269-73.
14. Sawada SG, Segar DS, Ryan T, et al. Echocardiographic detection of coronary artery disease during dobutamine infusion. Circulation 1991;83(5):1605-14.
15. Bourdillon PD, Broderick TM, Sawada SG, et al. Regional wall motion index for infarct and noninfarct regions after reperfusion in acute myocardial infarction: comparison with global wall motion index. J Am Soc Echocardiogr 1989;2(6):398-407.
16. Van Langenhove G, Hamburger J, Albertal M, Smits P, Onderwater E, Serruys P. Comparison of mechanical properties of the left ventricle in patients with severe coronary artery disease by nonfluoroscopic mapping versus two dimensional echocardiograms. Am J Cardiol 2000:In Press.
17. Cornel JH, Bax JJ, Fioretti PM. Assessment of myocardial viability by dobutamine stress echocardiography [see comments]. Curr Opin Cardiol 1996;11(6):621-6.
18. Arnese M, Cornel JH, Salustri A, et al. Prediction of improvement of regional left ventricular function after surgical revascularization. A comparison of low-dose dobutamine echocardiography with ^{201}Tl single-photon emission computed tomography [see comments]. Circulation 1995;91(11):2748-52.
19. Elhendy A, Trocino G, Salustri A, et al. Low-dose dobutamine echocardiography and rest-redistribution thallium- 201 tomography in the assessment of spontaneous recovery of left ventricular function after recent myocardial infarction. Am Heart J 1996;131(6):1088-96.

20. Amanullah AM, Chaudhry FA, Heo J, et al. Comparison of dobutamine echocardiography, dobutamine sestamibi, and rest-redistribution thallium-201 single-photon emission computed tomography for determining contractile reserve and myocardial ischemia in ischemic cardiomyopathy. Am J Cardiol 1999;84(6):626-31.

21. Claeys MJ, Rademakers FE, Vrints CJ, et al. Comparative study of rest technetium-99m sestamibi SPET and low-dose dobutamine stress echocardiography for the early assessment of myocardial viability after acute myocardial infarction: importance of the severity of the infarct-related stenosis. Eur J Nucl Med 1996;23(7):748-55.

22. Cornel JH, Bax JJ, Elhendy A, Reijs AE, Fioretti PM. Dobutamine stress-redistribution-reinjection versus rest-redistribution thallium-201 SPECT in the assessment of myocardial viability. Int J Card Imaging 1997;13(1):59-64.

23. Bjornstad K, al Amri M, Lingamanaicker J, Ogaili I, Hatle L. Interobserver and intraobserver variation for analysis of left ventricular wall motion at baseline and during low- and high-dose dobutamine stress echocardiography in patients with high prevalence of wall motion abnormalities at rest. J Am Soc Echocardiogr 1996;9(3):320-8.

Chapter 9

Acute changes of global and regional left ventricular function immediately after direct myocardial revascularization.

Glenn Van Langenhove, MD; Evelyn Regar, MD; David P. Foley, MD, PhD; Jaap N. Hamburger, MD, PhD; Peter C. Smits, MD, PhD; Mariano Albertal, MD; Patrick W. Serruys, MD, PhD. Thoraxcenter Rotterdam, Dijkzigt Hospital, Erasmus University, The Netherlands

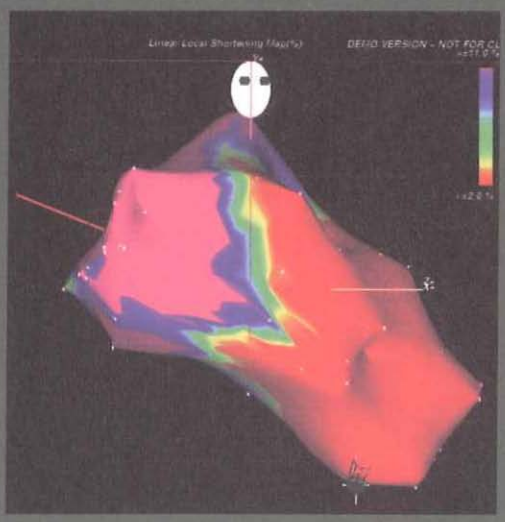

Summary

Direct myocardial revascularization (DMR) has been proposed to treat patients with severe coronary artery disease who are not amenable for classical revascularization techniques such as percutaneous coronary intervention (PCI) or bypass surgery (CABG). Although recent reports suggest its benefit in alleviating the patients' complaints in the long term, there is still a paucity of data on the immediate impact on regional and global myocardial functioning following this treatment. In this overview we discuss our own experience and provide a summary of other data currently available.

Text

Introduction

Direct myocardial revascularization (DMR) has been proposed to treat patients with severe coronary artery disease who are ineligible for classical revascularization techniques due to inappropriate coronary anatomy or due to highly increased risk for re-operation.[1-4] The principle of DMR is based on the direct treatment of the myocardial muscle by creating channels within the myocardium by mechanic or by thermic injury. Since the very first experimental application, the technology has been continuously improved. Modern systems for clinical application create channels by use of laser energy. Currently, two methods are available: the surgical transmyocardial approach[5,6], and the percutaneous catheter-based technique[7,8]. Although recent data suggest the benefit of both techniques in alleviating the patients' complaints,[9, 10] information on the immediate impact on myocardial functioning is still lacking. Indeed, most studies provide data on the effect on left ventricular (LV) function 3 [11-13] or 6 months after the index procedure.[9, 13] The acute effects on LV function however remain unclear. Perioperative morbidity and mortality after surgical transmyocardial revascularization range up to 50 and 20% respectively, including a high incidence of congestive heart failure[14]. Also, there is no conformity on the inclusion of severely diseased left ventricles: where in some studies patients were included with LV ejection fraction (LVEF) as low as 20% [9] or 25%[10, 14], others used 30%[15] as cut-off to include patients. In most trials, average LVEF on inclusion was quite high, ranging between 50 and 60%[14, 16, 17], suggesting the inclusion of patients with relatively good LV function in these trials. For the above-mentioned reasons we felt it important to unravel some of the mechanisms that lead to these early failures. This overview will therefore mainly focus on acute effects of DMR on the LV function. In addition, we provide the Thoraxcenter data on the acute effects on the left ventricular function before and immediately after percutaneous DMR in 15 patients treated in our institution.

Thoraxcenter experience

Patients with medically refractory angina and coronary artery disease that could not be treated with percutaneous or surgical revascularization were assigned to undergo percutaneous DMR. They all suffered severe and diffuse coronary artery disease or did not have a target vessel or conduit suitable for bypass grafting. All had reversible ischemia as demonstrated by dobutamine stress testing or radionuclide perfusion imaging. The only exclusion criterion was a left ventricular ejection fraction lower than 30%. The study was approved by the Erasmus University Hospital medical ethics committee, and all patients signed an informed consent.

Following a diagnostic angiogram, a DMR procedure was performed. According to the preference of the investigator, one of two available systems was used. The Cardiogenesis system (CardioGenesis, CA, USA) uses biplane fluoroscopy for navigation. The system is made up by an Axcis aligning 9 F catheter and a Holmium (HO): yttrium-aluminum-garnet (YAG) single fiber 330? laser catheter incorporating a tip lens for controlled laser energy delivery.[4,7] The catheter has nitinol pedals near its tip to prevent deep penetration into the myocardium. The energy delivered is 2 Joules (J) per pulse for 4 pulses. The Biosense system (Biosense-Webster, Cordis, a Johnson & Johnson Company) uses a recently developed nonfluoroscopic 3-dimensional electromechanical mapping technique

that has been described previously.[18-21] In short, the system is composed of a miniature passive magnetic field sensor incorporated in a catheter, an external magnetic field emitter (location pad), and a processing unit. The deflectable-tip catheter contains both a location sensor proximal to its tip, and standard electrodes that allow recording of unipolar (UPV) and bipolar (BPV) electrical signals. The locator pad placed beneath the operating table consists of three radiators that generate magnetic fields ($5x10^{-6}$ to $5x10^{-5}$ Tesla) that contain the information necessary to resolve the location and orientation of the sensor in 6 degrees of freedom. As the catheter tip is dragged over the LV endocardial surface, the system continuously analyzes its location in 3-dimensional space without the use of fluoroscopy. Chamber geometry is then reconstructed, in real time, using the set of sampled location points. The system thus allows for 3-dimensional guiding of the laser catheter to the region of interest. The laser system is a Ho:YAG single-fibre 300? laser catheter that delivers energy at 2 J per pulse.[22]

LVA's in RAO 30° and LAO 60° were performed using standard techniques[23], before and immediately after the DMR procedure. We assessed regional myocardial function using the area-length method and the Slager method[23] and compared treated and non-treated segments.

Between October 1998 and September 1999, 15 patients were included. Seven patients were treated with the Cardiogenesis system, and 8 with the Biosense system. Eighty-seven percent (13/15) of patients were male. Average age was 60 ± 9 years. Twelve patients (80%) were in stable angina class CCS 3 or 4 while 3 patients were unstable. On average, 20 ± 5 channels were created, in an average procedure time of 96 minutes ± 31. All procedures were successful, and no complications occurred. The relative decrease in LVEF was 18% ± 10 after DMR, the relative decrease in regional wall motion was 9% ± 18 for the non-treated and 26% ± 17 for the treated regions. Further results are shown in the table.

Table

	Number of Channels (n ± SD)	LVEF before (%)	LVEF after (%)	RMW treated area before DMR (%)	RMW treated area before DMR (%)	RMW non-treated area before DMR (%)	RMW non-treated area after DMR (%)
Average	**20 ± 5**	**65 ± 11**	**53 ± 10**	**19.80 ± 6.40**	**14.60 ± 5.40**	**16.90 ± 6.60**	**15.60 ± 6.10**
Wilcoxon signed ranks test		**P= 0.001**		**P=0.001**		**P=0.031**	

The table shows the average number of channels created per patient, the overall left ventricular function (LVEF) and the regional (RWM) myocardial function of treated and non-treated areas. SD: standard deviation; LVEF: left ventricular ejection fraction; RWM: regional wall motion; DMR: direct myocardial revascularization.

Effects of Catheter-Based Direct Laser Myocardial Revascularization on Regional and Global LV Function: The U.S Experience

Transthoracic echocardiography was performed within 24 hours before left ventricular (LV) mapping guided DMR, within 24 hours after the procedure and again at one month in 77 patients enrolled into the BiosenseTM DMR phase I safety and feasibility study conducted in the U.S. There was no change in average measured LV ejection fraction after DMR or during follow up (48±12% post procedure, 46±11% at one month vs. 48±11% at baseline, P=NS for both comparisons).[24] Regional wall motion was assessed by transesophageal echocardiography (TEE) in a sub-study that included 10 patients undergoing catheter-based DMR using a Ho:YAG laser before and immediately after the procedure.[25] Mild deterioration in wall motion score occurred in only 3/160 (1.9%) segments carefully assessed by TEE and did not induce clinical heart failure. Overall, there was no change in wall motion score index after laser myocardial revascularization (0.74±0.98 before versus 0.76±0.98 after DMR, p=0.3).[25]

Discussion

Our experience suggests that myocardial function immediately following DMR is impaired, causing a decrease in LVEF. These data are consistent with findings of animal studies that clearly show an acutely reduced global LV function after DMR.[26, 27] Gassler et al. showed that transmyocardial laser revascularization causes acute irreversible damage of tissue surrounding the laser channels, creating necrosis up to 2 mm from the laser application site[28]. Even beyond this zone, irreversible damage may occur.[28] The damage thus incurred may in part explain for the decrease in local myocardial function.

Data on the immediate impact of surgical and percutaneous DMR are scarce. Recently, Hughes et al. reported the incidence and spectrum of perioperative morbidity and mortality in 34 patients treated with surgical DMR.[29] In their study, baseline LVEF was 50 ± 9% (assessed with radionuclide techniques). Perioperative morbidity was 47%, perioperative mortality 6%. No immediate post-intervention assessment of LVEF was performed, but the authors carefully examined all adverse events in the postoperative period. Two patients died as a result of perioperative myocardial infarction. It is however of interest that 29% of the patient population suffered an episode of congestive heart failure (CHF) in the immediate postoperative period. Preoperative presence of unstable angina was the only predictor for perioperative death, while lack of experience and the absence of furosemide infusion were the sole predictors of morbidity. The authors suggest that the use of IV furosemide in the immediate postoperative period might reduce the incidence of myocardial edema caused by laser injury of the myocardium, thus reducing the incidence of diastolic failure and CHF.[29] The same group very recently reported on the acute effects of surgical DMR using holmium:YAG and carbon dioxide laser in the swine. They comprehensively demonstrated the increase in myocardial water content and thus impaired diastolic relaxation possibilities of lased myocardial regions, suggesting a possible mechanism of increased incidence of perioperative morbidity following DMR.[30] Aaberge et al. recently reported an incidence of CHF of 35% after surgical DMR. At 3 and 12 months however, no significant change in LVEF was reported. Lutter et al. reported on 7 patients with LVEF <35% treated with surgical DMR. Swan Ganz catheter examinations showed deterioration of LV-function after laser revascularisation

intraoperatively and improvement after 2 h and further after 6 h. (31) In this study, final outcome was favorable possibly due to the use of intraaortic balloon pumping, as suggested by the authors.[31]

Although our preliminary findings suggest no acute beneficial effect on LV function, myocardial laser revascularization has shown to improve anginal status in a subgroup of patients that were not amenable for classical revascularization procedures.[9, 10, 14, 16, 32, 33] Recently, three randomized trials showed improvement in clinical status in DMR-treated patients six to twelve months after the index procedure[9, 10]. Whether this treatment also improves myocardial perfusion, or global LV function, however remains to be proven. Current literature shows conflicting reports; while some authors suggest increase in LV function[34], others have found no change[17] or even decrease[35, 36] in the long run. These discrepancies may be explained by differences in duration of follow-up, in LV assessment methods,[37] differences in LV function assessment or differences in baseline LVEF. Nagele et al. recently showed that patients with lower LVEF at baseline had worse long-term outcome after laser revascularization[36]. Our results may – for the first time – elucidate the basis for these findings. The decrease of LV function immediately following DMR may well be the pathophysiological basis for the high incidence of CHF in the periprocedural era. Indeed, if an acute decrease in left ventricular performance immediately following DMR is to be expected, one can appreciate the reluctance one has to generate in treating patients with low baseline LVEF. On the other hand, recent data on percutaneous catheter-based DMR suggest no detrimental immediate effect on the left ventricle.[24, 25]

Conclusion

Although DMR can causes acute decrease of the LV function, most studies suggest that there is no detrimental effect in the long term. Also, recent data from other centers suggest that percutaneous DMR may not be so detrimental in the acute phase as the findings in our patient group suggest. It however remains troublesome that up to 45% of patients may experience an adverse event in the immediate post-intervention era. Therefore, one must be careful when performing myocardial laser revascularization in patients with a low (<30%) baseline LVEF. Prolonged observation in a coronary or intensive care unit, the use of intraaortic balloon pumping and the use of high dose IV furosemide may be warranted. Whether percutaneous DMR will prove to be safer than surgical DMR, remains to be shown.

References

1. Mirhoseini M, Cayton MM. Revascularization of the heart by laser. J Microsurg 1981;2(4):253-60.
2. Okada M, Ikuta H, Shimizu K, Horii H, Nakamura K. Alternatives method of myocardial revascularization by laser: experimental and clinical study. Kobe J Med Sci 1986;32(5):151-61.
3. Mirhoseini M, Shelgikar S, Cayton MM. New concepts in revascularization of the myocardium. Ann Thorac Surg 1988;45(4):415-20.
4. Kornowski R, Hong MK, Leon MB. Current perspectives on direct myocardial revascularization. Am J Cardiol 1998;81(7A):44E-48E.
5. Mirhoseini M, Fisher JC, Cayton M. Myocardial revascularization by laser: a clinical report. Lasers Surg Med 1983;3(3):241-5.
6. Mirhoseini M, Cayton MM, Shelgikar S, Fisher JC. Laser myocardial revascularization. Lasers Surg Med 1986;6(5):459-61.
7. Oesterle SN, Reifart NJ, Meier B, Lauer B, Schuler GC. Initial results of laser-based percutaneous myocardial revascularization for angina pectoris. Am J Cardiol 1998;82(5):659-62, A6.
8. Kim CB, Oesterle SN. Percutaneous transmyocardial revascularization. J Clin Laser Med Surg 1997;15(6):293-8.
9. Frazier OH, March RJ, Horvath KA. Transmyocardial revascularization with a carbon dioxide laser in patients with end-stage coronary artery disease [see comments]. N Engl J Med 1999;341(14):1021-8.
10. Allen KB, Dowling RD, Fudge TL, Schoettle GP, Selinger SL, Gangahar DM, et al. Comparison of transmyocardial revascularization with medical therapy in patients with refractory angina [see comments]. N Engl J Med 1999;341(14):1029-36.
11. Donovan CL, Landolfo KP, Lowe JE, Clements F, Coleman RB, Ryan T. Improvement in inducible ischemia during dobutamine stress echocardiography after transmyocardial laser revascularization in patients with refractory angina pectoris. J Am Coll Cardiol 1997;30(3):607-12.
12. Kantor B, McKenna CJ, Caccitolo JA, Miyauchi K, Reeder GS, Mullany CJ, et al. Transmyocardial and percutaneous myocardial revascularization: current and future role in the treatment of coronary artery disease. Mayo Clin Proc 1999;74(6):585-92.
13. Trehan N, Mishra Y, Mehta Y, Jangid DR. Transmyocardial laser as an adjunct to minimally invasive CABG for complete myocardial revascularization. Ann Thorac Surg 1998;66(3):1113-8.
14. Horvath KA, Cohn LH, Cooley DA, Crew JR, Frazier OH, Griffith BP, et al. Transmyocardial laser revascularization: results of a multicenter trial with transmyocardial laser revascularization used as sole therapy for end-stage coronary artery disease. J Thorac Cardiovasc Surg 1997;113(4):645-53; discussion 653-4.
15. Aaberge L, Nordstrand K, Dragsund M, Saatvedt K, Endresen K, Golf S, et al. Transmyocardial revascularization with CO2 laser in patients with refractory angina pectoris. Clinical results from the Norwegian randomized trial [In Process Citation]. J Am Coll Cardiol 2000;35(5):1170-7.
16. Dowling RD, Petracek MR, Selinger SL, Allen KB. Transmyocardial revascularization in patients with refractory, unstable angina. Circulation 1998;98(19 Suppl):II73-5; discussion II75-6.
17. Cooley DA, Frazier OH, Kadipasaoglu KA, Lindenmeir MH, Pehlivanoglu S, Kolff JW, et al. Transmyocardial laser revascularization: clinical experience with twelve-month follow-up. J Thorac Cardiovasc Surg 1996;111(4):791-7; discussion 797-9.
18. Ben-Haim SA, Osadchy D, Schuster I, Gepstein L, Hayam G, Josephson ME. Nonfluoroscopic, in vivo navigation and mapping technology. Nat Med 1996;2(12):1393-5.
19. Gepstein L, Hayam G, Shpun S, Ben-Haim SA. Hemodynamic evaluation of the heart with a nonfluoroscopic electromechanical mapping technique. Circulation 1997;96(10):3672-80.
20. Gepstein L, Hayam G, Ben-Haim SA. A novel method for nonfluoroscopic catheter-based electroanatomical mapping of the heart. In vitro and in vivo accuracy results. Circulation 1997;95(6):1611-22.
21. Kornowski R, Hong MK, Leon MB. Comparison between left ventricular electromechanical mapping and radionuclide perfusion imaging for detection of myocardial viability. Circulation 1998;98(18):1837-41.

22. Kornowski R, Hong MK, Haudenschild CC, Leon MB. Feasibility and safety of percutaneous laser revascularization using the Biosense system in porcine hearts. Coron Artery Dis 1998;9(8):535-40.
23. Slager CJ, Hooghoudt TE, Serruys PW, Schuurbiers JC, Reiber JH, Meester GT, et al. Quantitative assessment of regional left ventricular motion using endocardial landmarks. J Am Coll Cardiol 1986;7(2):317-26.
24. Kornowski R, Baim D, Moses J, Hong M, Laham R, Fuchs S, et al. Acute and Intermediate-Term Clinical Outcomes from Direct Myocardial Laser Revascularization Guided by Biosense Left Ventricular Electro-Mechanical Mapping. Circulation (in press) 2000.
25. Shiran A, Goldstein S, Ellahham S, Leon M, Kornowski R. Immediate Effect of Biosense Guided Percutaneous Direct Myocardial Revascularization with Holmium:YAG Laser on Myocardial Contractility Assessed by Transesophageal Echocardiography in Patients. Coronary Artery Dis (in press) 2000.
26. Lutter G, Yoshitake M, Takahashi N, Nitzsche E, Martin J, Sarai K, et al. Transmyocardial laser-revascularization: experimental studies on prolonged acute regional ischemia. Eur J Cardiothorac Surg 1998;13(6):694-701.
27. Lutter G, Martin J, Takahashi N, Yoshitake M, Schwarzkopf J, Nitzsche E, et al. Transmyocardial laser revascularization: experimental studies in healthy porcine myocardium. Ann Thorac Surg 1999;67(6):1708-13.
28. Gassler N, Wintzer HO, Stubbe HM, Wullbrand A, Helmchen U. Transmyocardial laser revascularization. Histological features in human nonresponder myocardium. Circulation 1997;95(2):371-5.
29. Hughes GC, Landolfo KP, Lowe JE, Coleman RB, Donovan CL. Perioperative morbidity and mortality after transmyocardial laser revascularization: incidence and risk factors for adverse events. J Am Coll Cardiol 1999;33(4):1021-6.
30. Hughes GC, Shah AS, Yin B, Shu M, Donovan CL, Glower DD, et al. Early postoperative changes in regional systolic and diastolic left ventricular function after transmyocardial laser revascularization: a comparison of holmium:YAG and CO2 lasers. J Am Coll Cardiol 2000;35(4):1022-30.
31. Lutter G, Saurbier B, Nitzsche E, Kletzin F, Martin J, Schlensak C, et al. Transmyocardial laser revascularization (TMLR) in patients with unstable angina and low ejection fraction. Eur J Cardiothorac Surg 1998;13(1):21-6.
32. Aranki SF, Nathan M, Cohn LH. Has laser revascularization found its place yet? Curr Opin Cardiol 1999;14(6):510-4.
33. Hattler BG, Griffith BP, Zenati MA, Crew JR, Mirhoseini M, Cohn LH, et al. Transmyocardial laser revascularization in the patient with unmanageable unstable angina. Ann Thorac Surg 1999;68(4):1203-9.
34. Shawl FA, Domanski MJ, Kaul U, Dougherty KG, Hoff S, Rigali GE, et al. Procedural results and early clinical outcome of percutaneous transluminal myocardial revascularization [published erratum appears in Am J Cardiol 1999 Jun 1;83(11):1594]. Am J Cardiol 1999;83(4):498-501.
35. Burns SM, Sharples LD, Tait S, Caine N, Wallwork J, Schofield PM. The transmyocardial laser revascularization international registry report. Eur Heart J 1999;20(1):31-7.
36. Nagele H, Stubbe HM, Nienaber C, Rodiger W. Results of transmyocardial laser revascularization in non-revascularizable coronary artery disease after 3 years follow-up [ssee comments]. Eur Heart J 1998;19(10):1525-30.
37. Pasquet A, Williams MJ, Secknus MA, Zuchowski C, Lytle BW, Marwick TH. Correlation of preoperative myocardial function, perfusion, and metabolism with postoperative function at rest and stress after bypass surgery in severe left ventricular dysfunction. Am J Cardiol 1999;84(1):58-64.

Chapter 10

Improved Regional Wall Motion 6 Months After DirectMyocardial Revascularization (DMR) With the NOGA DMR System

Glenn Van Langenhove, MD; Jaap N. Hamburger, MD; Peter C. Smits, MD; David P. Foley, MD; Mariano Albertal, MD; Patrick W. Serruys, MD

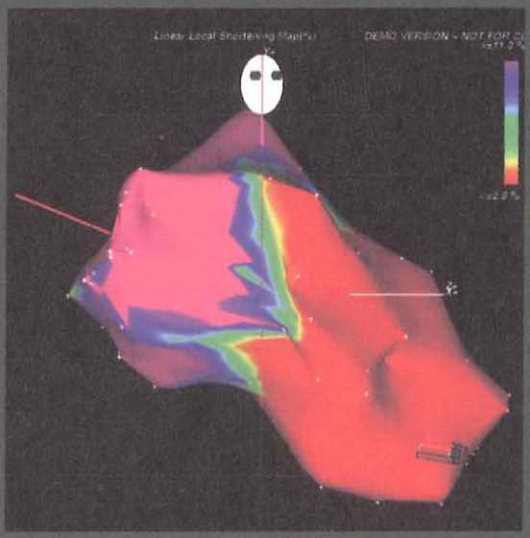

A 60-year-old man was referred to our intervention laboratory for direct myocardial revascularization (DMR). He had received maximal medical therapy and had undergone coronary bypass surgery 10 years earlier, and his peripheral coronary anatomy was now found to be unsuited for surgical revascularization. In addition, the lesions on coronary angiography proved to be unfit for percutaneous revascularization. Consequently, a DMR procedure was performed. We used the NOGA nonfluoroscopic electromechanical mapping system (Biosense-Webster) as a guidance tool to deliver laser energy at the exact target locations. The system has been described previously.[1,2]

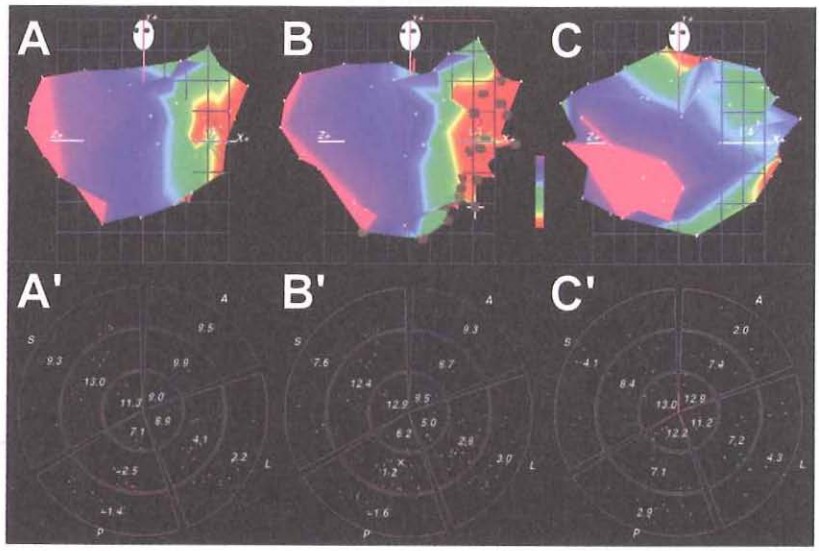

In the Figure, A shows the local linear shortening (LLS) map in the left anterior oblique view and its corresponding bull's eye view (A9) at baseline. The map is color-coded (see color bar in B), ranging from red (LLS, 2%) to purple (LLS. 11%), with red zones thought to delineate akinetic zones and purple normokinetic zones.[2] The bull's eye view shows basal (outer circle), mid, and apical (inner circle) regions of (clockwise from top) the anterior (small A), lateral (L), posterior (P), and septal (S) segments. In the picture, the low LLS values in the basal and mid portions of the posterior and lateral segments can be seen (21.4%, 22.5%, 2.2%, and 4.1%, respectively). Because the unipolar voltage map suggested viability, these regions were thought to be eligible for DMR. B and B9 show the LLS map after the DMR procedures, with the brown tags showing the precise locations of the laser energy applications. Similar LLS values in this region support the belief that regional wall motion improvement can be expected only after a certain time delay and not immediately after DMR. The control map taken at 6 months is shown in C and C9. The improvement of regional wall motion can easily be appreciated in C. Indeed, the posterolateral zone, formerly colored red, is now green-blue, suggesting increased LLS and thus improved wall motion. The bull's eye shows increases in LLS of 2.9%, 7.1%, 4.3%, and 7.2% for basal and mid portions of the posterior and lateral segments, respectively (average increase, 4.8±3.3%). This case suggests, for the first time, a local shortening increase as a function of left ventricular wall motion improvement 6 months after a DMR procedure.

References

1. Ben-Haim SA, Osadchy D, Schuster I, et al. Nonfluoroscopic, in vivonavigation and mapping technology. Nat Med. 1996;2:1393–1395.
2. Kornowski R, Hong MK, Gepstein L, et al. Preliminary animal andclinical experiences using an electromechanical endocardial mappingprocedure to distinguish infarcted from healthy myocardium. Circulation.1998;98:1116 –1124.

From the Thoraxcenter, Heart Center, Dijkzigt Hospital, Erasmus University Rotterdam, Netherlands.Reprint requests to Professor Patrick W. Serruys, Head of the Department of Interventional Cardiology, Thoraxcenter Bd 418, University Hospital Dijkzigt, Dr Molewaterplein 40, 3015 GD Rotterdam, Netherlands. E-mail serruys@card.azr.nl The editor of Images in Cardiovascular Medicine is Hugh A. McAllister, Jr, MD, Chief, Department of Pathology, St Luke's Episcopal Hospital and Texas Heart Institute, and Clinical Professor of Pathology, University of Texas Medical School and Baylor College of Medicine. Circulation encourages readers to submit cardiovascular images to the Circulation Editorial Office, St Luke's Episcopal Hospital/Texas Heart Institute, 6720 Bertner Ave, MC1-267, Houston, TX 77030. (Circulation. 2000;102:e44-e45.) Circulation is available at http://www.circulationaha.org 1 Images in Cardiovascular Medicine

Chapter 11

Efficacy of percutaneous intramyocardinal injections using a nonfluoroscopic 3-D mapping based catheter system

Pieter C. Smits[a], MD, PhD; Glenn van Langenhove[a], MD; Michael Schaar[b]; Ambrose Reijs[b], PhD; Willem H. Bakker[b], PhD; Wim J. van der Giessen[a,c], MD, PhD; Pieter D. Verdouw[c], PhD; Eric P. Krenning[b], MD, PhD and Patrick W. Serruys[a], MD, PhD

a.Department of Interventional Cardiology, Heartcenter Rotterdam
b.Department of Nuclear Medicine of the University Hospital Rotterdam
c.Experimental Cardiology, Thoraxcenter, Erasmus University Rotterdam, The Netherlands

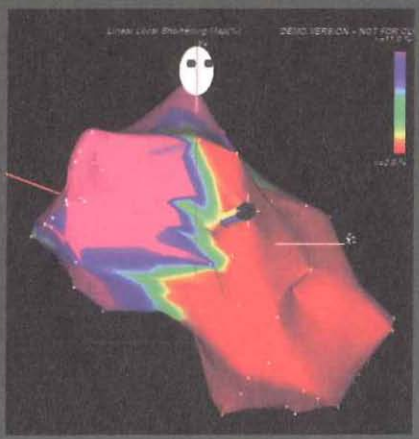

ABSTRACT

Background. Percutaneous transendomyocardial injection with an injection catheter is a new drug delivery method for e.g. therapeutic angiogenesis. Little is known about the efficacy of this drug delivery technique. We studied efficiency and retention of transendomyocardial injections with a NOGA guided injection catheter system by using scintigraphy with radio-labeled model drugs.

Methods. Ten non-ischemic landrace pigs were used. In each animal 2-3 transendomyocardial injections were performed using a 3-D mapping based catheter system called NOGA. As a model for proteins like angiogenic growth factors or particles like microspheres or adenovirus we used 99mTc labeled albumin and 99mTc labeled colloid albumin, respectively. Efficiency of the injections and retention of the transendomyocardial deposited substance was evaluated by a gamma camera during and after injection of 0.1 or 0.2 ml.

Results. All 29 injections showed scintigraphic proof of intramyocardial deposition. The average injection efficiency of all 29 injection was 26 ± 23%. The average injection efficiency of 0.1 and 0.2 ml injections were 33 ± 30% (n=8) and 24 ± 20% (n=21), respectively (p=0.33). Intramyocardial retention curve of albumin showed a rapid wash-out within the first 2 hours of the injection, whereas the retention of colloid albumin showed no decrease.

In conclusion, transendomyocardial delivery of proteins and particles with an injection catheter show favourable efficiency rates, however the retention time of intramyocardial deposited small proteins like albumin is short. This may indicate the need for sustained release systems of angiogenic growth factors for intramyocardal injection in therapeutic angiogenesis.

Keywords

Experimental, heart, growth factors, gene therapy, pharmacokinetics, angiogenesis

INTRODUCTION

Chronic myocardial ischemia caused by coronary artery stenosis or occlusion has been shown to increase growth of the coronary collateral circulation. Vascular growth factors, like some isoforms of Vascular Endothelial Growth Factor (VEGF), Fibroblast Growth Factor (FGF) or Platelet-derived Growth Factor (PDGF) are important modulators in the complex process of collateral artery formation.[1-3] Animal studies have proven the feasibility of enhancing collateral function by delivery of these angiogenic factors (cytokines) to the myocardium.[4,5]. Currently, therapy by applying vascular growth factors or genetic material that encodes for these angiogenic factors (therapeutic angiogenesis) is under clinical evaluation. Besides the method of delivery i.e.: growth factors, naked DNA (plasmids) or viral transfection of genetic material, also duration and route of administration of the angiogenic factors are important variables for the efficiency, efficacy and safety of the therapy.[6]

Intramyocardial delivery of angiogenic drugs by transendomyocardial injection with an injection catheter is a novel administration route. Little is known about the efficiency of this percutaneous transendomyocardial injection technique as well as the retention time of the injected substance in the myocardium. Therefore, we investigated the efficiency and the retention time of percutaneous intramyocardial injected radio-labeled proteins with a new injection catheter system.

METHODS

Animals. Ten landrace pigs (weight 36-62 kg) were pre-medicated with Ketamine (25 mg/kg i.m.), anesthetized with pentobarbital (10 mg/kg per hour i.v.) and ventilated with a nitrous oxide/ oxygen mixture (2:1). Catheterization was performed through a 8 F sheath in the right femoral artery. During the procedure arterial blood pressure and ECG were monitored. All experiments were performed in accordance with the "Guiding Principles in the Care and Use of Laboratory Animals, as approved by the American Physiological Society and with prior approval of the Animal Care Committee of the Erasmus University Rotterdam.

Material. Analog to the local drug delivery studies in the coronary artery by our group[7,8] we investigated the efficiency and retention time of intramyocardial injected drugs with scintigraphy. As a model for vascular growth factors we used human serum albumin (HSA) coupled to Technetium (99mTc), using the TechneScanR HSA kit (Mallinckrodt Medical BV, Petten, The Netherlands). Albumin is like the vascular growth factors a protein with a comparable molecular size (Albumin 69 kilodalton (kDa), VEGF165 49 kDa, FGF-2 between 18-24 kDa and PDGF between 28-34 kDa). Furthermore, as a model for much larger molecules (macroaggregates of growth factors) or particles (microspheres or adenovirus) we used human albumin microcolloidal particles (ALBU-RESR, Amersham Sorin S.r.l. Saluggia, Italy) coupled to Technetium (99mTc). The size of the microcolloidal particles range between of 0.1 - 3.0 micrometer, whereas the size of an adenovirus is 0.13 micrometer and microspheres can range between 1.0-10 micrometer.

Labeling procedure. 99mTc-HSA and 99mTc-colloid albumin were prepared by adding 2 ml 0.9% NaCl with 99mTc of 92.5 MBq/ml (Mallinckrodt Medical, Petten, The Netherlands) to the TechneScanR HSA-kit or the ALBU-RESR kit, respectively. After the substance was homogenized, labeling efficiency of 99mTc-HSA or 99mTc-colloid

albumin complex was measured using the Instant Thin Layer Chromatography (ITLC) method (Gelman Sciences, Ann Arbor, Michigan, USA). Activity was measured by a Veenstra CRC-100 dosiscalibrator (Veenstra Instruments BV, Leeuwarden, The Netherlands). The average labeling efficiency of all labeling procedures was 98.3 ± 2.3%.
Injection procedure. After a left ventricle angiogram, a NOGA map of the left ventricle was obtained with an electromechanical mapping system (Biosense-Webster, Waterloo, Belgium). As described previously[9-11], the electromechanical mapping system uses (1) a triangular location pad with 3 coils generating ultralow magnetic field energy, (2) a stationary reference catheter with a miniature magnetic field sensor located on the back of the animal, (3) a navigation sensor mapping catheter (7F) with a deflectable tip and electrodes providing endocardial signals and (4) a workstation (Silicon Graphics, California, USA) for information processing and 3-dimensional LV reconstruction. After the NOGA map, the 7 F mapping catheter was changed for an 8 F injection catheter (Biosense-Webster, Waterloo, Belgium). The injection catheter consisted of a combination of an electro-mechanical mapping catheter and needle injection catheter (figure 1).

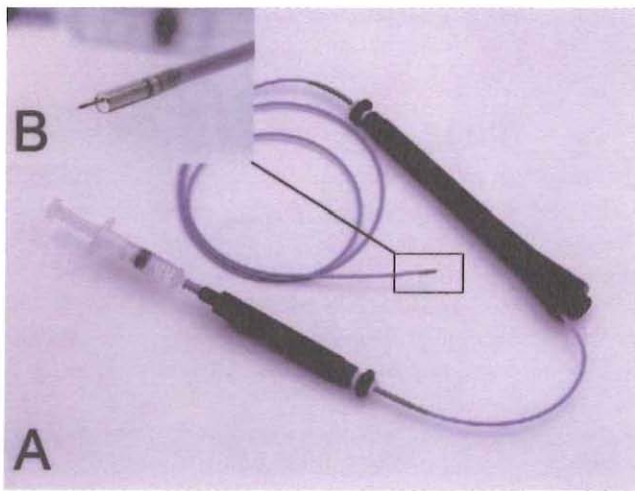

Figure 1A & B

This figure represents the Biosense injection catheter (A) and catheter tip (B). The catheter has a 7 F shaft with a distal active deflectable tip of 8 F. The tip consists of an electromagnetic sensor, a ring and tip electrode and the housing of a 0.014 x 0.009 inch extendable nitinol needle. At the proximal end of the catheter the nitinol shaft is connected with a luer lock fitting for a syringe.

Through a nitinol tubing, that was connected with an extendable and retractable needle at the distal end of the catheter, drugs could be administered. The injection catheters used had a fixed needle length of 4.5 mm.
The NOGA map served as a guide for positioning the injection catheter perpendicular against the endomyocardium at different locations in the left ventricle (figure 2).

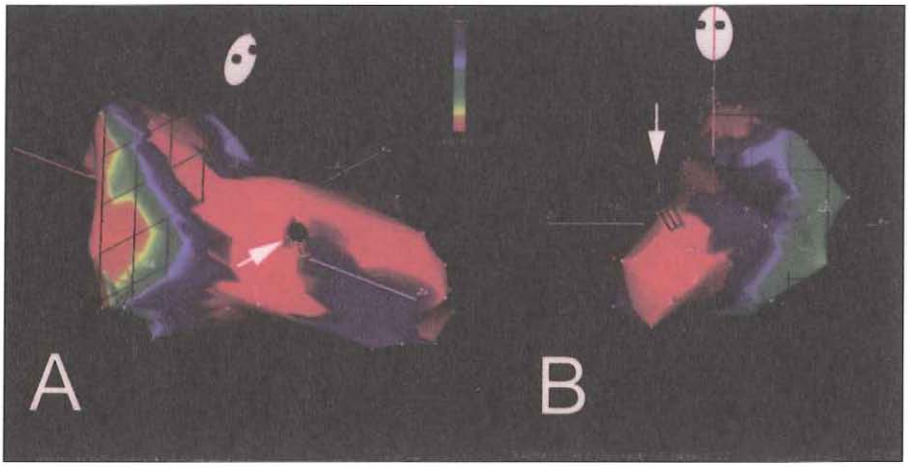

Figure 2

Example of NOGA™ catheter position perpendicular to the basal anterior of the left ventricle wall (white arrowhead). The figure shows the right superior oblique (A) and the left anterior oblique (B) view of the left ventricle in a unipolar voltage map. The color coding to the right shows the voltage range: blue-purple indicates normal myocardium (high voltage, > 14 mV); red indicates infarcted tissue (low voltage, <6 mV).

The endomyocardial voltage signal indicated endomyocardial contact and location stability and loop stability of the NOGA system 11 indicated a stable position of the cathetertip against the endomyocardium during the cardiac cycles. In order to ensure that all individual injections were done at a single site, a four step injection protocol was used.

1. After a stable catheter position against the target zone was obtained a NOGA point was taken and tagged.
2. After extension of the needle a second NOGA point was taken and tagged.
3. After injection, a third NOGA point was taken and tagged.
4. Finally, after retraction of the needle location of the cathetertip was identified by a tagged NOGA point.

During all injection procedures, the endomyocardial position of the cathetertip remained unchanged. Figure 3 illustrates the injection sites and tagged NOGA points during the injection procedure.

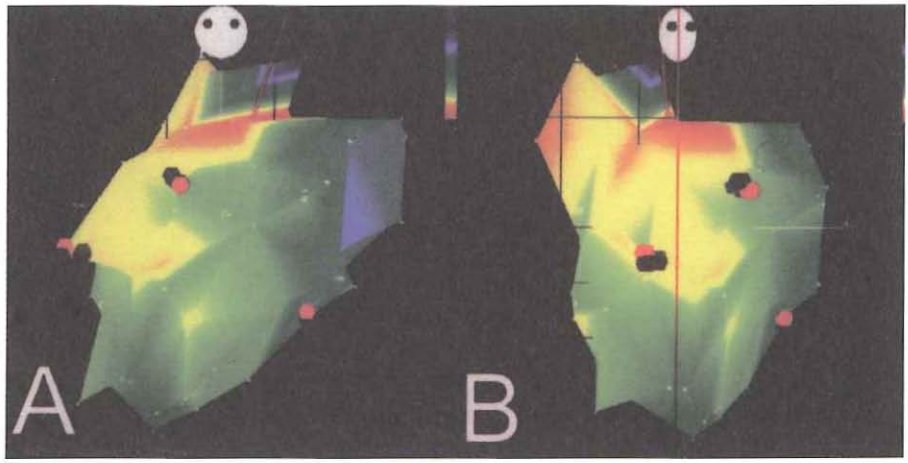

Figure 3

Figures A and B represent the NOGA local activation map of the left ventricle of one of the pigs in frontal and right oblique view, respectively. The three areas with the colored dots indicate the three injection sites. Each injection site has four colored dots according to the used injection procedure. No shift in endomyocardial position of the injection cathetertip was noted during the injection procedure.

All injection catheters were pre-loaded with the 99mTc-HSA or 99mTc-colloid albumin with a 1 ml syringe with a luer lock fitting attached to the injection port of the injection catheter. After the pre-loading procedure, the distal end of the catheter was cleaned in order to prevent contamination of 99mTc outside the injection compartment. After positioning of the catheter at the injection site, 0.1 or 0.2 ml 99mTc-HSA or 99mTc-colloid albumin was manually injected in 20 seconds. After each injection procedure the catheter was retracted and the needle injection system cleaned and checked. Thereafter, the catheter was advanced and positioned in the left ventricle again for another injection at a different site.

Scanning procedure. Before injection the radioactive activity of the syringe with the injected substance was measured on the gamma camera (t=0) in order to recalculate the activity in time during the experiments. During and 2-4 hours after the injection counts per region were acquired by the mobile gamma camera (Cardiac, Siemens, Erlangen, Germany) close above the chest in an anterior-posterior projection. Scintigraphic data was stored on a PDP 11/34 computer system (Digital). During the injections, dynamic scans of 60 frames per 2 seconds were obtained in order to visualize direct systemic loss of the injected substance. After the injection at regular intervals 1 minute scans were acquired. At the end of the experiment a scan after thoracotomy was performed in order to calculate the attenuation by the anterior chest wall (see appendix). The average attenuation correction factor was 1.36 ± 0.18.

After the animals were sacrificed, the hearts were excised and inspected macroscopically. The injection regions were easily identified as "hot spots" on the gamma camera.

Definition. Efficiency of the injection was defined as the percentage of the amount injected that showed an intramyocardial deposition at 1 minute after the injection. The efficiency

was calculated by measuring the counts of the "hot spot" on the gamma camera during the first minute after the injection and dividing this by the expected counts of the total injected substance (0.1 or 0.2 ml) for that time period. Retention was defined as the percentage of the intramyocardial deposition in time. The retention was calculated as the counts of the "hot spot" on the gamma camera in time and compared to the counts of the "hot spot" at one minute after the injection. Efficiency and retention of all injections were corrected for the decay of the 99mTc in time and the attenuation of the anterior chest wall (see appendix).

Statistics. All values are presented as mean ± standard deviation. Comparison of efficiency between the 0.2 and 0.1 ml injections was done with a double-sided student-t test. A p value less than 0.05 was considered statistically significant.

Results

A total of 29 injections were done in 10 animals. All 29 injections showed scintigraphic proof of intramyocardial deposition. The average injection efficiency of all 29 injection was 26 ± 23%. The average injection efficiency of 0.1 and 0.2 ml injections were 33 ± 30% (n=8) and 24 ± 20% (n=21), respectively (p=0.33)(figure 4).

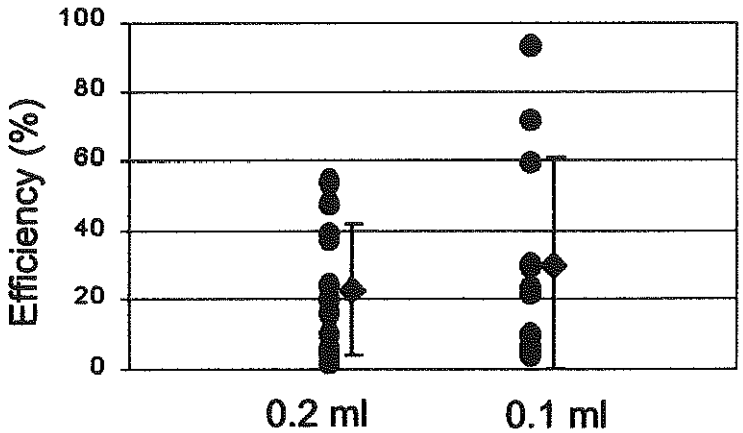

Figure 4

This figure represents the percentage efficiency of the 0.2 and 0.1 ml injections. The 0.2 and 0.1 ml injections had an average injection efficiency of 24 ± 20% and 33 ± 30%, respectively.

The injection efficiencies between albumin and colloid albumin injections were 23 ± 19% and 30 ± 30% (p=0.46).

Intramyocardial retention of albumin showed a rapid wash-out within the first 2 hours of the injection, whereas the retention of albumin-colloid showed no decrease after a small initial drop-off (figure 5).

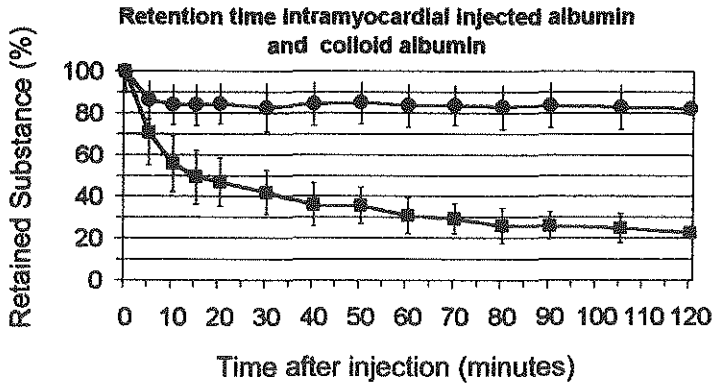

Figure 5

This figure represents the retention time of the intramyocardial deposited 99mTc-albumin (v) and 99mTc-colloid albumin (r). After 2 hours 23 ± 9% and 82 ± 10% of the initial deposited amount of 99mTc-albumin and 99mTc-colloid albumin, respectively, was still present at the injection site.

During 8 injection procedures, a backflow of injected substance could be identified on the dynamic acquisition scan (figure 6).

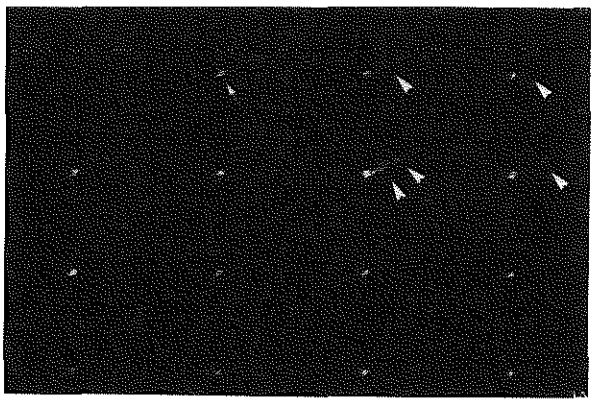

Figure 6

This figure represents 16 frames of 2 seconds each during the dynamic scan acquisition at the time of one of the injections. At frame number 9 a "hot spot" emerged, indicating an intramyocardial deposition (small arrow). From frame 9 to frame 14 backflow of the injected substance during the injection procedure is noted into the left ventricle cavity (arrow heads). Simultaneously, background activity increased during and after this injection.

In all these 8 cases the injection efficiency rates were less than 30% and were mainly observed in the 0.2 ml injections (n=7).

No sustained ventricular rhythm disturbances or other hemodynamic changes occurred during or after the injections. Furthermore, myocardial perforation was not noted either scintigraphically or macroscopically.

Discussion

This study reports on the efficacy of a novel intramyocardial drug delivery method, using a non-fluoroscopic guided transendomyocardial injection catheter system. Analog to a previously described scintigraphic method[7,8], our study shows that the average efficiency of an transendomyocardial injection with this catheter system is 26 ± 23%. Furthermore, we show that intramyocardial retention after transendomyocardial injection of small proteins like albumin is short compared to the stable retention rates of small particles like colloid-albumin.

The obtained efficiency rates in this study seem to be better compared to the low myocardial recovery rates of 0.5 and 3-5% that were obtained after intravenous or intracoronary administration of 125I labeled basic FGF as shown by Lazarous et al.[12] using an autoradiography method.

In our study, we noted a wide range in efficiency of the injections. Although our injection protocol showed that during the injection procedure the cathetertip did not change its endomyocardial position, still a large variation in injection efficiency existed between 2 and 93%. This was probably caused by insufficient penetration of the needle into the myocardium or by rapid loss of injected substance out of the injection site. As shown in figure 6, in 28% of the injections we observed a backflow of the injected substance during the injection. This backflow was probably along the needle shaft into the left ventricle cavity, as only low injection efficiency rates and increase of background activity were noted together with this observation. This phenomenon is likely to occur whenever the pressure at the deposition region is high for instance after a high volume dose injection and perhaps at regions with non-compliant tissue characteristics like a scar. Furthermore, rapid loss from the injection site may also be augmented by the myocardial contractions.

Another observation in our study was the difference in retention between albumin as model for small proteins like growth factors and colloid-albumin as model for small particles, like adenovirus or microspheres. The consistent intramyocardial retention of colloid albumin, in contrast to the rapid wash out of albumin, is probably explained by the physical properties of the colloidal particles. Due to their sizes, the colloidal particles are likely to be lodged between the myocardial muscle cells, whereas small proteins like albumin are likely to dissolve quickly into the extracellulair fluid compartment. Another possible explanation for the difference in the retention time is the gradual loss of substance through the neck of the injection channel, which is likely to be faster with small proteins.

We noted some helpful properties of the NOGA system during the injection experiments.

1. The 3-D NOGA map functioned as a cast of the left ventricle and gave an indication whether the cathetertip was in endomyocardial contact.
2. Firm endomyocardial contact was confirmed by the endomyocardial ECG signal from the cathetertip electrode.
3. Perpendicular positioning of the cathetertip against the endomyocardium was assessed by looking at the NOGA map from different angles.

4. The system allowed accurate spatial positioning and tagging of the injection sites with no or little use of fluoroscopy. Apart from the above mentioned procedural advantages, the electro-mechanical assessment of the left ventricle by the NOGA system has also the potential to direct the injection therapy towards on-line identified viable myocardial regions[10].

All the injections showed scintigraphic proof of intramyocardial deposition without any adversary event. This is consistent with the observations of Kornowski[13] and also of Vale et al.[14] that this percutaneous transendomyocardial injection technique is a safe and a reliable drug delivery method.

Limitations: First, a major llimitation of the study is the use of a model drug for evaluation of the intramyocardial retention. The model drugs used in our study disregard the cell receptor binding capacity of angiogenic growth factors. Therefore, it is likely that the use of receptor binding cytokines will show a longer retention time. Second, the needle length of the injection catheters in our study was fixed at 4.5 mm. We noted a gradual decrease (0.5-1.0 mm) in needle length after one or more injections. Although, little is known about the influence of the needle length for intramyocardial drug delivery, we believe that a needle length of less than 4.5 mm results in less efficient injections. Therefore, new injection catheters were used for each animal and when the needle length was less than 3.5 mm. Probably, the small variation in needle length can also explain in part the variation in efficiency of the different injections. Third, scanning with the gamma camera was done in one plane (anterior-posterior), therefor scintigraphic evidence of backflow of the injected substance during the injection could have been missed when the catheter tip was coaxial towards the scanning plane.

In conclusion, transendomyocardial delivery of proteins and particles with an injection catheter show favourable efficiency rates, however the retention time of intramyocardial deposited small proteins like albumin is short. This may indicate the need for sustained release systems of angiogenic growth factors for intramyocardal injection in therapeutic angiogenesis.

Acknowledgments

Technical support by Geert Gijsbers (Biosense-Webster Benelux) and delivery of the mapping and injection catheters by Biosense-Webster was greatly appreciated.

Appendix

Activity at time (x) was calculated according to the following formula:

$$A(x)=A(0).e^{-[0{,}693\ .\ t(x)\ /\ t(1/2)^{99m}Tc]}$$

A(x) = Activity at time x minutes after calibration
A(0) = Activity at time of calibration
t(x) = time in minutes after calibration
$t(1/2)^{99m}Tc$ = half life time of ^{99m}Technetium (360 minutes)

Attenuation of the anterior chest wall was calculated according to the following formula:

A(x) corrected = A(x) . [$A(x_2)$ open chest / $A(x_1)$ closed chest]

References

1. Schaper W. Collateral vessel growth in the human heart. Role of fibroblast growth factor-2. Circulation. 1996; 94:600-601.
2. Schaper W, Ito WD. Molecular mechanisms of coronary collateral vessel growth. Circ Res.1996; 79:911-919.
3. Risau W. Mechanisms of angiogenesis. Nature. 1997; 386:671-674.
4. Folkman J. Angiogenic therapy of the human heart. Circulation.1998; 97:628-9.
5. Unger EF, Banai S, Shou M, Lazarous DF, Jaklitsch MT, Scheinowitz M, Correa R, Klingbeil C, Epstein SE. Basic fibroblast growth factor enhances myocardial collateral flow in a canine model. Am J Physiol.1994; 266:H1588-1595.
6. Kornowski R, Fuchs S, Leon MB, Epstein SE. Delivery strategies to achieve therapeutic myocardial angiogenesis. Circulation.2000; 101:454-458.
7. Camenzind E, Bakker WH, Reijs A, van Geijlswijk IM, Foley D, Krenning EP, Roelandt JRTC, Serruys PW. Site-specific intravascular administration of drugs: history of a method applicable in humans. Cathet Cardiovasc Diagn.1997; 41:342-347.
8. Camenzind E, Bakker WH, Reijs A, van Geijlswijk IM, Boersma E, Kutrijk MJB, Krenning EP, Roelandt JRTC, Serruys PW. Site-specific intracoronary heparin delivery in humans after balloon angioplasty. A radioisotopic assessment of regional pharmacokinetics. Circulation. 1997; 96:154-165.
9. Ben-Haim SA, Osadchy D, Schuster I, Gepstein L, Hayam G, Josephson ME. Nonfluoroscopic, in vivo navigation and mapping technology. Nat Med. 1996; 2:1393-1395.
10. Kornowski R, Hong MK, Leon MB. Comparison between left ventricular electromechanical mapping and radionuclide perfusion imaging for detection of myocardial viability. Circulation.1998; 98:1837-1841.
11. Gepstein L, Hayam G, Ben-Haim SA. A novel method for nonfluoroscopic catheter-based electroanatomical mapping of the heart. In vitro and in vivo accuracy results. Circulation.1997; 95:1611-1622.
12. Lazarous DF, Shou M, Stiber JA, Dadhania DM, Thirumurti V, Hodge E, Unger EF. Pharmacodynamics of basic fibroblast growth factor: route of administration determines myocardial and systemic distribution. Cardiovasc Res.1997; 36:78-85.
13. Kornowski R, Leon MB, Fuchs S, Vodovitz Y, Epstein SE. Electromagnetic guidance for catheter-based transendocardial injection: a platform for intramyocardial angiogenesis therapy. Results in normal and ischemic porcine models. J Am Coll Cardiol. 2000; 35:1031-1039.
14. Vale PR, Losordo DW, Tkebuchava T, Chen D, Milliken CE, Isner JM. Catheter-based myocardial gene transfer utilizing nonfluoroscopic electromechanical left ventricular mapping. J Am Coll Cardiol. 1999; 34:246-254.

Chapter 12

Nonfluoroscopic Endoventricular Electromechanical Three-dimensional Mapping. Current Status and Future Perspectives.

Glenn Van Langenhove, MD, Ken Kozuma, MD, Patrick W. Serruys, MD, PhD. Department of Interventional Cardiology, Thoraxcenter Rotterdam, Academic Hospital Dijkzigt, Erasmus University, The Netherlands

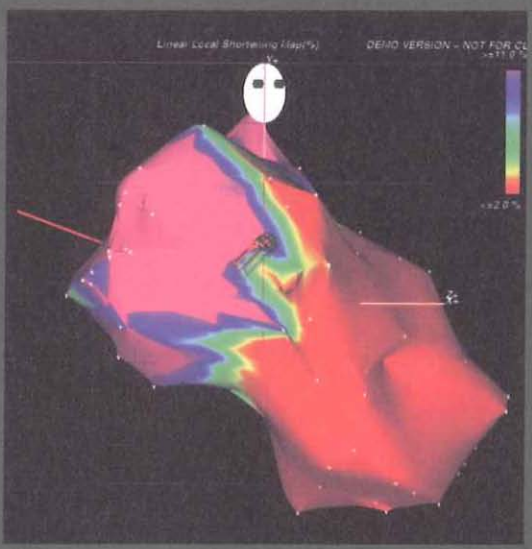

INTRODUCTION

Nonfluoroscopic electromechanical mapping (NOGA™, Biosense-Webster, a Johnson & Johnson Company) is a recently developed technique that enables the acquisition of on-line information on electrical and mechanical endoventricular functioning of myocardial tissue1. The rationale of this new technique is of two kinds. First, no currently available in-cathlab method can distinguish viable from non-viable myocardium. Accepted techniques as radionuclide scintigraphy and dobutamine stress echocardiography may not be readily available, and can only be performed out of the cathlab. Second, applications such as myocardial laser revascularization or intramyocardial gene-injection may prove cumbersome when performed using echocardiography or fluoroscopy with only two-dimensional projections available on-line1. A major pitfall in these is indeed the inability to accurately associate the two-dimensional positioning with a specific endocardial site. It has been shown previously that localization of the recording sites with fluoroscopy is inaccurate, cumbersome, and associated with high x-ray exposure for both the patient and the physician[2]. Although clinical application of on-line 3D echocardiography and magnetic resonance imaging are underway, until recently no technique for real-time three-dimensional guiding of intervention tools and assessment of myocardial electromechanical functioning was available. Indeed, nonfluoroscopic electromechanical mapping has become the first navigation technique to accurately determine the trajectory of a tool inside the human heart, to guide the interventional device to a specific site, and to meticulously couple functional and anatomical properties[1].

In this overview, we shall describe the NOGA™ system components, the left ventricular mapping technique, the current experimental and clinical data available, the ongoing trials and the possible future applications of this technique.

The system

The system exists of a mapping catheter, a magnetic field emitter, a data acquisition unit and a workstation. The deflectable-tip catheter (NOGA-STAR™, Biosense-Webster, A Johnson & Johnson company) contains both a location sensor just proximal to its tip, and standard electrodes that allow recording of unipolar (unipolar voltages, UPV) and bipolar (BPV) electrical signals.

The locator pad placed beneath the operating table consists of three radiators that generate low magnetic field energy ($5x10^{-5}$ to $5x10^{-6}$ Tesla). This way, the system is provided with the information necessary to resolve the location and orientation of the catheter-sensor in 6 degrees of freedom (figure 1).

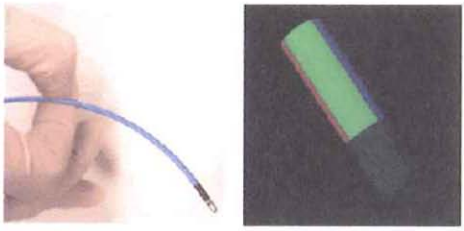

Figure 1
Close-up of the catheter tip (left). The exact location in three different degrees of freedom pitch, roll and yaw) can be appreciated throughout the procedure; at the start of the procedure, a "calibration" has to be performed in order to know the color coding of the different orientations of the catheter. In the figure (right), for instance, the green color could be the upper side of the catheter.

The amplitude, phase and frequency of the emitted magnetic signals recorded by the location sensor allow the computer algorithm to solve a number of complicated algebraic equations yielding the location (x, y and z) and orientation (roll, pitch and yaw) of the sensor. The NOGA™ processing unit consists of a computer that updates the acquired information in real-time, and a Silicon Graphics work station that displays the 3D left ventricular endocardial reconstruction (figure 2).

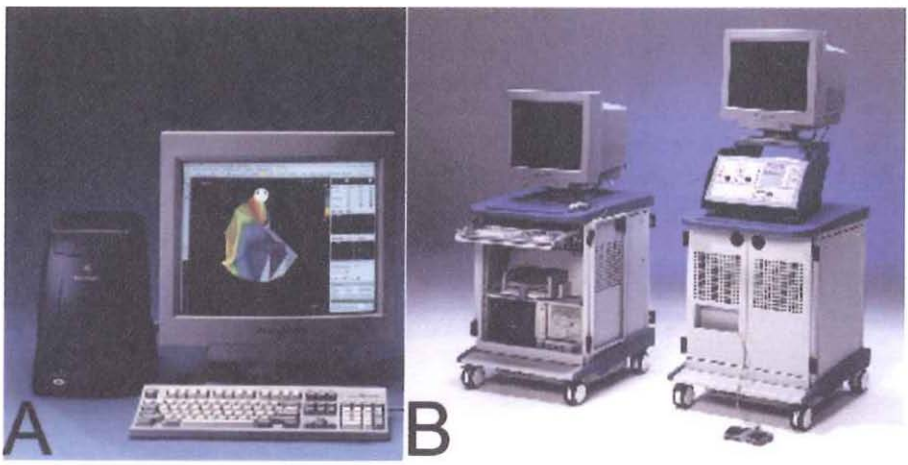

Figure 2
The system's components. (A) shows the different components of the work station, with the Silicon graphics computer and the monitor displaying a NOGA™ map. (B) shows the system incorporated in a moveable cart, with on the right a cart with the cable connecting board visible underneath the monitor.

The operator chooses whatever view he wishes to work with during point acquisition, can add a second view in a separate window, and can change views whenever he wishes to do so, during the mapping procedure. Besides electrical activation maps, minimum voltage maps (showing uni- or bipolar voltages), local shortening maps, and bull's eyes views, a variety of other features are provided by the system. A full length description however would lead us to far.

Definitions and acronyms

Point loop stability: measures the maximum of distances between the locations of the selected point in two consecutive heart cycles. Low point loop stability indicate a reproducible catheter movement trajectory.

Cycle length (CL) stability: the difference between the length of the current cycle and the average of the last 100 cycles recorded.

Local activation time (LAT) stability: measure of how stable the LAT is between cycles. Reliable points show a LAT variation of <3ms.

Location stability: a measure of the variability in position of the catheter tip on the endoventricular wall during two consecutive cardiac cycles.

Triangle fill threshold: by setting a "triangle fill threshold" value, the operator chooses the minimum triangle size for which the program will close a face on the reconstructed chamber. This feature allows the operator to determine the degree to which the system will interpolate between actual data points and will ensure that a minimal level of point density will be met at each mapped region. Usually an interpolation threshold of 30 mm between adjacent points is taken[3].

Inner points filtering: computer algorithm that removes points thought to be located inside the ventricular lumen (and not on the ventricular wall) or on a papillary muscle. The algorithm calculates relative position of points as compared to at least three neighboring ones and is therefore able to remove these contending points.

Local linear shortening (LLS): The local linear shortening assessment is based on the assumption that in healthy myocardium any two points move closer to each other during contraction. Measurement of distances between neighboring points is therefore the basis for calculation of myocardial shortening. The computer algorithm takes into account the density of points around a point p, and gives a negligible weight to points too close (sampling noise) and points too far (of no influence as they provide non-local information). The algorithm for regional linear shortening is calculated as follows: for any two points on the map, i and j, LLS is calculated as the change in distance between these two points from end-diastole to end-systole, normalized for the length at end diastole:

$$LLS_{ij} = (L(ED)_{ij} - L(ES)_{ij}) / L(ED)_{ij}$$

For any point p LLS is calculated as a function of the LLSpj, for all points j=1 to n on the map, so that

$$LLS_p = (S_{j=1..n} W_{pj} (L(ED)_{pj} \times LLS_{pj}) / S_{j=1..n} W_{pj},$$

where W is the weight of a certain point as a function of the distance Lij between two points i and j, the average distance D around point p (D is defined in the computer algorithm as the average distance of the ten closest points to p) (figure 4) and the volume V at end-diastole. The weight is therefore function of the point density in a defined region, the volume of the heart and the distances between points at end-diastole.

Unipolar Voltages (UPV): The maximum peak-to-peak voltage (expressed in mV) of the intracardiac signal measured at the tip of the mapping catheter. This unipolar recording may identify subtle changes in the local myocardial voltages.

Bipolar Voltages (BPV): Maximum peak-to-peak voltage of the cardiac signal measured

at the catheter tip and the catheter ring (located more proximally). Although it has been hypothesized that BPV, as it is less likely to be influenced by contact stability and "far-field" potentials, may be more accurate than UPV, only UPV is currently being used in the electromechanical assessment of the left ventricle. Possibly, future studies can elucidate the importance of BPV measurements.

The 3D mapping procedure

The mapping catheter is introduced through a 7F or 8F femoral sheath. Prior to the actual mapping procedure, heparin is given intravenously (5 to 10,000 IU); additional heparin is given to maintain an activated clotting time (ACT) above 200s. A reference catheter is applied to the back of the patient. A mapping catheter is then inserted into the left ventricle. The location of the tip of the mapping catheter while inside the heart is gated to end diastole and is recorded relative to the fixed reference catheter, thus compensating for subject motion[3].

As the catheter tip is dragged over the LV endocardial surface, the system continuously analyzes its location in 3-dimensional space without the use of fluoroscopy. The set of points thus collected comprises an irregularly sampled data set of location points that are members of the endocardial surface. Chamber geometry is then reconstructed, in real time, using the set of sampled location points (figure 3).

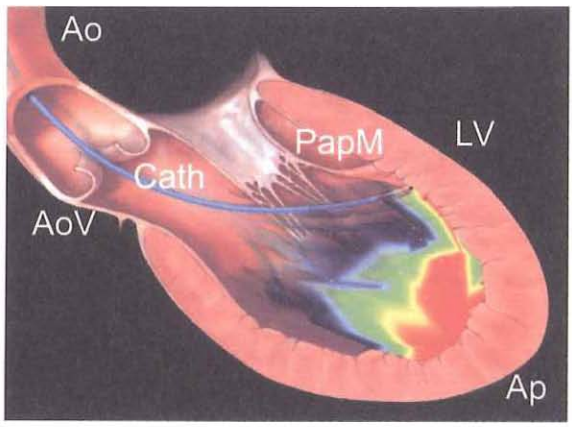

Figure 3

Dragging of the catheter (Cath) throughout the ventricle with acquisition of electromechanical information. The mapping information is superimposed on anatomical information in this figure. Ao denotes the ascending aorta, AoV is the aortic valve, LV is the left ventricle, PapM is a papillary muscle, and Ap is the apex of the left ventricle.

The endocardial surface is presented as a set of polygons (triangles) whose vertices are the sampled points. The local activation time (LAT) at each site is determined as the time difference between a selected fiducial point on the body-surface ECG and the steepest negative intrinsic deflection in the unipolar intracardiac electrogram (filtered at 0.5 to 400 Hz) recorded from the tip of the mapping catheter. The activation map is color coded and superimposed on the 3D chamber geometry. The center of mass of the reconstructed chamber is automatically calculated from the set of the surface points. The volume of the chamber can be calculated from the sum of the volumes of all tetrahedrons constructed when connecting the center of mass to all triangles forming the reconstructed surface[2]. Thus, left ventricular end-diastolic (LVEDV) and end-systolic (LVESV) volumes, stroke volume (LVEDV-LVESV) and ejection fraction (LVEF, SV/LVEDV) can be calculated and displayed (figure 4).

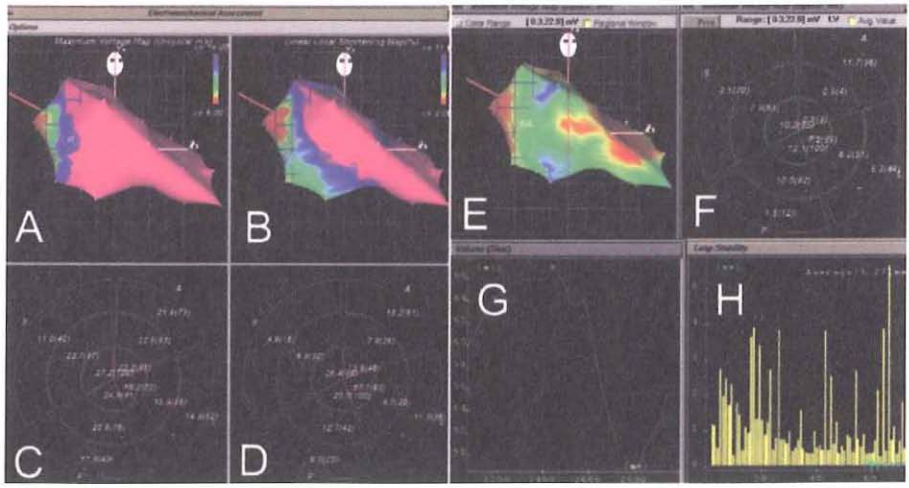

Figure 4

Example of a normal map. (A) demonstrates the maximum voltage map (UPV) in the right anterior oblique (RAO) position. The color bar on the right shows the color coding ranging from red (≤ 6.0 mV) to blue-purple (≥ 14.0 mV). (B) shows the local linear shortening (LLS) map in the same RAO view. The color bar ranges from red (LLS ≤ 2.0%) to blue-purple (≥ 11.0%). (C) shows the bull's eye view of the unipolar voltage map as displayed by the system. The numbers displayed are the absolute UPV values, with the percentages of the maximum values in brackets. Four regions (clockwise from top: anterior (A), lateral (L), posterior (P) and septal (S)) are each subdivided in 3 segments (apical, mid and basal), dividing the whole map in twelve segments. (D) shows the bull's eye view of the LLS map. (E) and (F) show the bipolar map and its bull's eye view, respectively. (G) shows the volume-time curve, with the blue markers denoting minimum and maximum volumes. (H) shows the loop stability histograms; the average value of 1.27 mm indicates a reproducible catheter movement trajectory.

The stability of the catheter-to-wall contact is evaluated at every site in real time, and points can be manually deleted from the map if 1 of the following criteria is met:

(1) a premature beat or a beat after a premature beat;
(2) location stability, defined as a difference of >4 mm in end-diastolic location of the catheter at 2 sequential heartbeats;
(3) loop stability, defined as an average distance of >4 mm between the location of the catheter at 2 consecutive beats at corresponding time intervals in the cardiac cycle (figure 4);
(4) cycle length that deviated >10% from the median cycle length;
(5) different morphologies of the local ECG at 2 consecutive beats, or severe ST-elevation of the intracardiac electrogram depicting excessive myocardial impression by the mapping catheter;
(6) local activation time differences of >3 ms between 2 consecutive beats;
(7) different QRS morphologies of the body surface ECG;
(8) inner point location;
(9) adjacent points closer than 5 mm;

(10) points not related to the left ventricle (such as atrial location)[3].
The moderate filtering algorithm incorporated in the system covers most of these issues. A normal map is shown in figure 4.

Experimental and clinical studies

The initial validation studies of the mapping system were reported by Gepstein et al.[4] These authors first tested the in vitro accuracy of the locatable-catheter capabilities. By using a test jig with several holes at precise known distances from each other, they showed that repeated measurements of the location of one specific site differed 0.16 mm maximally, and that distances between specific points were equally highly reproducible (mean error 0.42 mm). Also, the intracardiac electrical signal from the locatable catheter was found to correlate highly with the signal acquired using a standard nonlocatable electrophysiological catheter placed in the immediate vicinity of the mapping catheter (cross-correlation = 0.96 ± 0.01). In the same study, they tested the reproducibility of measurements performed on the beating pig's heart. Again, standard deviation (SD) for measurements at the same site were low (0.74 ± 0.13 mm), and the overall mean error of distances measured inside the body (through the use of a long sheath with markers every 10 mm) proved to be low (0.73 ± 0.03 mm)[4]. Furthermore, Gepstein and colleagues found a consistent activation pattern of the left ventricle in pigs. During ventricular pacing, the earliest site of activation was at the site of pacing. During sinus rhythm, the earliest site of activation was on the superior part of the septum. Invariably, the latest site of activation in both rhythms was on the left lateral wall close to the mitral valve annulus. The total activation time of the left ventricle varied between 40 and 80 ms during sinus rhythm and between 57 and 87 ms during paced rhythm[4].
In a second series of validation studies by the same group, volumetric measurements of test jigs and pig ventricles were analyzed[2]. Phantom objects with known volumes showed that the measured volumes were very close to the actual volumes, with an average deviation of about 2.7%. Measurements of LV casts (with a more difficult anatomy) showed an average deviation of 9.6%. , with a correlation r=0.94 with the actual volumes. Measurements of volumes in a dynamic test jig showed high accuracy with known volumes, deviating only 1.4, 0.7, 6.0 and 5.2% for maximal volume, minimal volume, SV and EF respectively[2]. In 12 pigs tested in this study, the intra- and interobserver variability proved to be very low. Also, SV measurements acquired with the mapping system proved to be highly correlated with thermodilution cardiac output measurements (see also figure 7, chapter 1)[2].
As further validation of the system as a tool for the assessment of local left ventricular function, Gepstein et al. acquired the left ventricular electromechanical regional properties in 11 dogs with chronic infarction (4 weeks after ligation of the proximal LAD) and 6 controls and compared them to the pathology results. Average endocardial local shortening (LS, measured at end systole and normalized to end diastole) and intracardiac bipolar electrogram amplitude were quantified at 13 LV regions. Endocardial LS was significantly lower at the infarcted area (1.2+/-0.9%, P<0.01) compared with the noninfarcted regions (7.2+/-1.1% to 13. 5+/-1.5%) and with the same area in controls (15.5+/-1.2%, P<0.01). Average bipolar amplitude was also significantly lower at the infarcted zone (2.3+/-0.2 mV, P<0.01) compared with the same region in controls (10.3+/-1.3 mV) and with the noninfarcted regions (4. 0+/-0.7 to 10.2+/-1.5 mV, P<0.01) in the infarcted group. Also, the electrical maps could accurately delineate both the

location and extent of the infarct, as demonstrated by the high correlation with pathology (Pearson's correlation coefficient=0.90) and by the precise identification of the infarct border. The authors concluded that chronic myocardial infarcted tissue could be accurately characterized and quantified by abnormal regional mechanical and electrical functions[5]. The first human studies with the NOGA™ system were reported by Kornowski et al.[3] In 24 patients (12 patients with prior myocardial infarction (MI) and 12 control patients) LV endocardial mapping was performed to assess electromechanical function in infarcted versus healthy myocardial tissue. In patients with prior MI, the average voltage was 7.2+/-2.7 mV (UPV)/1.4+/-0.7 mV (BPV) in MI regions, 17.8+/-4.6 mV (UPV)/4.5+/-1.1 mV (BPV) in healthy zones remote from MI, and 19.7+/-4.4 mV (UPV)/5.8+/-1.0 mV (BPV) in control patients without prior MI (P<0.001 for MI values versus remote zones or control patients). They clearly showed that both UPV and local endocardial shortening were significantly impaired in MI zones compared with controls. Also, concordance with echocardiographic wall motion analysis was good[3]. An example is given in figure 5.

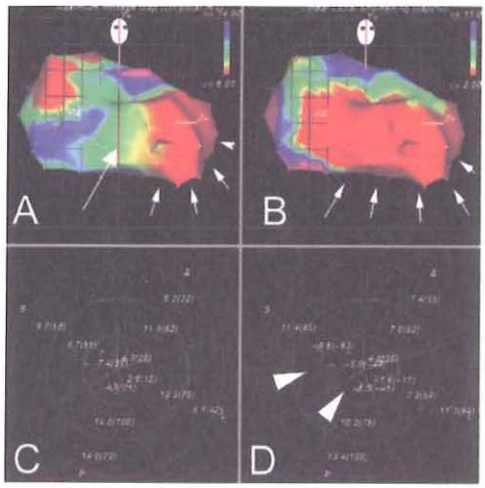

Figure 5
Example of an electromechanical assessment map in a patient with a mid anterior descending artery occlusion and a subsequent apicoposteroseptal infarction. (A) shows the unipolar voltage (UPV) map and (B) the linear local shortening (LLS) map in the right anterior oblique view. (C) and (D) show the respective bull's eye views. The small arrows in (A) and (B) delineate the infarction zone, which can be clearly appreciated from the red areas. The arrowheads in (D) show the negative LLS values, suggestive for dyskinesia in the apical, septal and posterior regions. The larger arrow in (A) suggests a region of moderate UPV (corresponding with a zone of low LLS), suggestive for viability ("electromechanical mismatch").

Kornowski et al. later reported on a comparison between NOGA™ mapping and radionuclide perfusion imaging[6]. They showed that UPV (14.0+/-2.0 mV) and LLS values (12.5+/-2.8%) were highest when measured in myocardial segments (n=56) with normal perfusion and lowest (7.5+/-3.4 mV and 3.4+/-3.4%) when measured in myocardial segments with fixed perfusion defects (n=20) (P0.0001) on single photon emission computed tomography imaging studies using ^{201}Tl at rest and 99mTc-sestamibi after adenosine stress. A significant difference in UPV and LLS values was found between groups (P<0.001 for each comparison by ANOVA). Myocardial segments with reversible perfusion defects (n=66) had intermediate UPV (12.0+/-2.8 mV, P=0.048 versus normal and P=0.005 versus fixed segments) and LLS values (10.3+/-3.7%, P=0.067 versus normal and P=0.001 versus fixed segments). From these results it was concluded that NOGA™ mapping might allow the detection of myocardial viability.

Van Langenhove et al. compared enddiastolic (EDV) and endsystolic volumes (ESV), stroke volume (SV) and ejection fraction in 44 patients with both LV angiogram and NOGA™ mapping. Although a strong correlation (r=0.78, p<0.001) for EF measurement between the two techniques was found, the Bland-Altman analysis (figure 11) demonstrates the disagreement and the absence of interchangeability between both methods. Indeed, on average, a difference of about 30% in LVEF was found[7]. We also compared local linear shortening assessed with nonfluoroscopic electromechanical mapping (NEM) as a function of regional wall motion with echocardiographic data in a subset of 40 patients with severe coronary artery disease and subsequently decreased left ventricular function. Our study showed that NEM mapping can accurately assess regional wall motion. In addition, this study showed a significant decrease in unipolar voltages amongst segments with declining regional function.[8]
The same authors described significant correlations between regional wall motion assessment using LV angiography as compared to LLS data acquired in the same segments(p<0.001)[9], see figure 6.

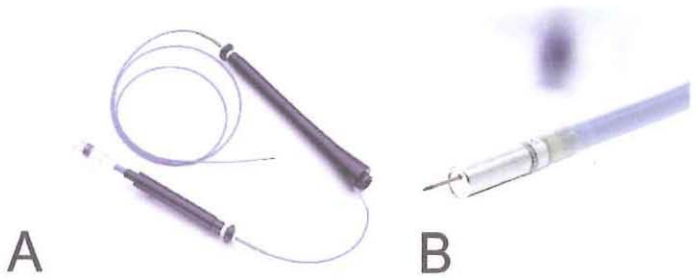

Figure 6

Left ventricular angiogram in RAO (A-B) and LAO (C-D) views in respectively end-diastole (A-C) and end-systole (B-D). Corresponding linear local shortening (LLS) map in the same views (A'-D'). The arrows in (A-B) are suggestive of apical akinesia, the arrowheads in (C-D) show akinesia in the septal region. The arrows in (A'-B') show the red zone in the apical region; low LLS values are also suggested in the septal region (red zone in septal area in (A'-B') and red-yellow-green zone in (C'-D', arrowheads).

Finally, dobutamine stress echo was compared to LLS and UPV data for comparable segments in patients with a previous myocardial infarction. ROC curves showed significant cut-off values for myocardial viability of UPV=9.0 mV (sens 56%, spec 81%, p<0.0001) and LLS=6.8% (sens 56%, spec 92%, p<0.0001)[10, 11] (see also figure 5).
Fuchs et al. assessed in-vivo electromechanical changes following gradual coronary artery occlusion in a pig ameroid constrictor model using NOGA™[12]. UPV and LLS were measured in the ischemic lateral and non-ischemic anterior zones in animals at rest (n = 9) and 5 weeks after the implantation of ameroid constrictors around the left circumflex artery. Echocardiography was used to assess regional contractility (% myocardial thickening), and an echo-contrast perfusion study was performed using acoustic densitometry methods. The ischemic lateral zone showed reduced myocardial perfusion at

rest (peak intensity; 3.4 +/- 1.7 versus 20.7 +/- 14.8, P = 0.005), impaired mechanical function (percentage wall thickening 22 +/- 19% versus 40 +/- 11%, P = 0.03; local endocardial shortening 2.9 +/- 5.5% versus 11.7 +/- 2.1%, P = 0.002), and preserved electrical activity (unipolar voltage 12.4 +/- 4.7 versus 14.4 +/- 1.9 mV, P = 0.25; bipolar voltage 4.1 +/- 1.1 versus 3.8 +/- 1.5 mV, P = 0.62), compared with the anterior region. The authors concluded that gradual coronary artery occlusion resulting in regional reduced perfusion and function at rest (i.e. hibernating myocardium) is characterized by preserved electrical activity. Electromechanical left ventricular mapping may be of diagnostic value for identifying the hibernating myocardium[12]. Botker et al. compared the findings of FDG-positron emission tomography (PET) with data derived from NOGA™ mapping and found that segments with reversible perfusion defects had UPV/LLS of 7.3 ± 3.1 mV and 4.0 ± 2.4% respectively. Normal segments showed UPV 11.5 ± 3.7 mV, LLS 7.7 ± 3.3%. Infarcted areas with irreversible perfusion defects showed UPV 4.8 ± 2.2 mV, LLS 2.9 ± 2.8%.[13]

Kornowski et al. recently presented preliminary results on the first NOGA™-guided direct myocardial revascularization (DMR) study.[14] They showed that DMR using this technique was safe and feasible, that in 77 patients no deaths occurred, and that early efficacy endpoints showed an improvement in anginal status, and a prolonged exercise capacity 6 months after the index procedure. Laham et al. reported on improvement in regional wall motion score and collateralization in a subgroup of 15 patients also treated with laser-DMR.[15] Some caution however may be appropriate. As previous studies had shown a substantial amount of patients suffering an episode of heart failure following transmyocardial laser revascularization[16, 17] we sought to determine the acute effects on the left ventricular function. We found that in 15 patients, where we performed a left ventricular angiogram before and immediately after the DMR procedure, that the relative decrease in LVEF was 18% ± 10 after DMR, and that the relative decrease in regional wall motion was 9% ± 18 for the non-treated and 26% ± 17 for the treated regions. From this study, we concluded that the physician should be cautious when performing myocardial laser revascularization in patients with a low (<30%) baseline LVEF.[18]

Recently, Vale et al. showed feasibility and safety of percutaneous, catheter-based, nonfluoroscopic mapping guided myocardial gene transfer[19]. In six pigs in which the injection catheter was used to deliver plasmid using cytomegalovirus promoter/enhancer, encoding nuclear-specific LacZ gene (pCMV-nlsLacZ) (50 microg/ml) to a single LV myocardial region, peak beta-galactosidase activity after five days was documented in the target area of myocardial injection in each pig. As all pigs survived until sacrifice, and no complications were observed with either the mapping or the injection procedures, the authors concluded that percutaneous myocardial gene transfer can be successfully achieved in normal and ischemic myocardium without significant morbidity or mortality[19]. It is furthermore important to underline the importance of the 3D mapping technique for gene application procedures, as exact delineation of the area to be treated seems mandatory. To test the feasibility of myocardial angiogenic gene expression, through endocardial transfection of adenovirus vascular endothelial growth factor-121 using the NOGA™ system as a guidance, Kornowski et al. transfected transgenes into designated myocardial sites of the pig model. They demonstrated that this less invasive catheter-based system offers a similar gene delivery efficiency and, thus, may have clear advantages compared with the surgically-based transepicardial injection approach.[20] In a recent study,

our group demonstrated in a pig model that the average efficiency of an endomyocardial catheter injection using the NOGA™ system as a guidance is 26 ± 23%. Also, we showed that intramyocardial retention after endomyocardial injection of small proteins like albumin is short compared to the stable retention rates of small particles like colloid-albumin.[21] An injection catheter is shown in figure 7.

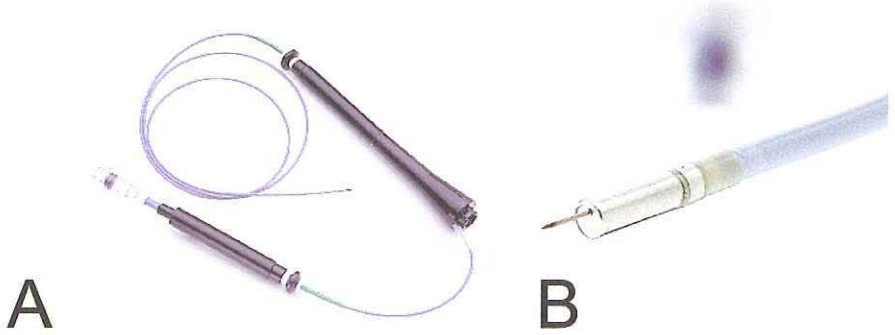

Figure 7

This figure represents the Biosense injection catheter (A) and catheter tip (B). The catheter has a 7 F shaft with a distal active deflectable tip of 8 F. The tip consists of an electromagnetic sensor, a ring and tip electrode and the housing of a 0.014 x 0.009 inch extendable nitinol needle (B). At the proximal end of the catheter the nitinol shaft is connected with a luer lock fitting for a syringe, that may contain injectable substances.

Ongoing and clinical investigations

Some burning questions related to the clinical usability of the NOGA™ mapping system in clinical practice still need to be addressed. Up to now, no clear evidence has shown that the local shortening function really is a reflection of the local wall motion. We do not know if assessment of bipolar voltages could further improve the performance of the system. Also, we do not know if the system is able to detect true viability. It also needs further investigation whether there need for this expensive technique for in-cathlab detection of viability/ischemia – when other techniques have already proven their value. It also needs further investigation whether direct myocardial revascularization, for which this system seems to be an ideal guiding tool, really improves the clinical status of the patient. It is also unclear if local gene application, again for which this system seems an optimal platform, is going to be applied clinically.

Some of these questions will be answered by ongoing investigations. The DIRECT and EURO-DIRECT trials are currently enrolling patients in the USA and Europe respectively; these trials (single blinded, randomized NOGA™ mapping without versus with DMR in patients not suitable for classical revascularization) are aiming to answer the question if the presumed benefit with DMR is simply a placebo effect, or does really improve the patient's clinical and functional status. The DIRECT trial has included 300 patients and the first results will be available by the end of september 2000. The EURO-DIRECT is aiming at 200 patients. Studies assessing "true viability" in patients scheduled for bypass surgery will answer the question if NOGA™ can predict recuperation of

myocardial segments with wall motion abnormalities after revascularization. The DINO study is currently enrolling patients; goal of this trial is to assess the possibilities of the NOGA™ system to accurately determine viability in hibernating myocardial segments, as compared to stress echocardiography, radionuclide perfusion scintigraphy and angiography performed before and 6 months after coronary bypass surgery. A study assessing the possible additional benefit of low-dose dobutamine during NOGA™ mapping is currently performed at the Thoraxcenter. Future investigations will evaluate the possible value of adenosine in the detection of ischemic segments, the diagnostic value of NOGA™ mapping as compared to magnetic resonance imaging (MRI) in myocardial viability, the efficacy of growth factors to induce myocardial angiogenesis and additional comparisons with radionuclide perfusion imaging studies[13-15, 22, 23]. Also, the possibility of the pericardial approach to acquire electromechanical mapping information and the intrapericardial delivery of angiogenic factors may offer a theoretical advantage of prolonged exposure of either coronary or myocardial tissue to the administered drug as result of a reservoir function of the pericardium, and is currently under investigation.[24] Investigations to shorten the mapping time, to acquire multiple point information through a multi-sensor catheter, and to incorporate fluoroscopic information into the NOGA™ system, are underway.

Conclusions

Left endoventricular 3D real-time electromechanical mapping is a new, intriguing technique for in-cathlab assessment of mechanical and electrical functioning of the left ventricle. Although initial studies have shown safety, feasibility and reproducibility of this technique, and have provided similar results as compared to established techniques in the quest for viability, data on the additional clinical value of the system are still scarce. Ongoing trials on the prediction of viability, the benefit of DMR and intramyocardial gene injection, may definitely establish its place among currently used techniques in interventional cardiology.

References

1. Ben-Haim SA, Osadchy D, Schuster I, Gepstein L, Hayam G, Josephson ME. Nonfluoroscopic, in vivo navigation and mapping technology. Nat Med 1996; 2:1393-5.
2. Gepstein L, Hayam G, Shpun S, Ben-Haim SA. Hemodynamic evaluation of the heart with a nonfluoroscopic electromechanical mapping technique. Circulation 1997; 96:3672-80.
3. Kornowski R, Hong MK, Gepstein L, et al. Preliminary animal and clinical experiences using an electromechanical endocardial mapping procedure to distinguish infarcted from healthy myocardium. Circulation 1998; 98:1116-24.
4. Gepstein L, Hayam G, Ben-Haim SA. A novel method for nonfluoroscopic catheter-based electroanatomical mapping of the heart. In vitro and in vivo accuracy results. Circulation 1997; 95:1611-22.
5. Gepstein L, Goldin A, Lessick J, et al. Electromechanical characterization of chronic myocardial infarction in the canine coronary occlusion model. Circulation 1998; 98:2055-64.
6. Kornowski R, Hong MK, Leon MB. Comparison between left ventricular electromechanical mapping and radionuclide perfusion imaging for detection of myocardial viability. Circulation 1998; 98:1837-41.
7. Van Langenhove G, Hamburger J, Smits P, et al. Nonfluoroscopic Electromechanical Mapping for Evaluation of Left Ventricular Hemodynamics. A Comparison with Contrast Ventriculography. Am Heart J 2000;(In Press).
8. Van Langenhove G, Hamburger J, Albertal M, Smits P, Onderwater E, Serruys P. Comparison of mechanical properties of the left ventricle in patients with severe coronary artery disease by nonfluoroscopic mapping versus two dimensional echocardiograms. Am J Cardiol 2000:In Press.
9. Van Langenhove G, Smits P, Serrano P, et al. Assessment of regional wall motion: a comparison between computerized LV angiography and nonfluoroscopic electromechanical mapping (Abstract). Circulation 1999; 100:I-725.
10. Van Langenhove G, Smits P, Albertal M, et al. NOGA mapping for the detection of viable and ischemic myocardium: a comparison with dobutamine stress echocardiography (Abstract). Circulation 1999; 100:I-23.
11. Van Langenhove G, Smits P, Hamburger J, Serrano P, Serruys P. Hibernating myocardium diagnosed with nonfluoroscopic electromechanical (NOGA) mapping: a comparison with dobutamine stress echocardiography. J Am Coll Cardiol 2000; 35:81A.
12. Fuchs S, Kornowski R, Shiran A, Pierre A, Ellahham S, Leon MB. Electromechanical characterization of myocardial hibernation in a pig model. Coron Artery Dis 1999; 10:195-8.
13. Botker H, Lassen J, Bottcher M, et al. Left ventricular electromechanical mapping for detection of myocardial viabilityin patients with impaired left ventricular function due to chronic ischemic heart disease (Abstract). Circulation 1999; 100:I-22.
14. Kornowski R, Baim D, Moses J, et al. Six month results following percutaneous direct myocardial revascularization guided by Biosense left ventricular mapping in patients with refractory coronary ischemic syndromes. (Abstract). Circulation 1999; 100:I-22.
15. Laham R, Pearlman J, Datta R, Gao L, Baim D. Biosense-guided laser myocardial revascularization improves 30-day and 6-month regional wall motion, perfusion and collateralization of the treated zone(s) (Abstract). Circulation 1999; 100:I-22.
16. Frazier OH, March RJ, Horvath KA. Transmyocardial revascularization with a carbon dioxide laser in patients with end-stage coronary artery disease [see comments]. N Engl J Med 1999; 341:1021-8.
17. Allen KB, Dowling RD, Fudge TL, et al. Comparison of transmyocardial revascularization with medical therapy in patients with refractory angina [see comments]. N Engl J Med 1999; 341:1029-36.
18. Van Langenhove G, Regar E, Foley D, et al. Acute changes of global and regional left ventricular function immediately after direct myocardial revascularization. Semin Intervent Cardiol 2000; 5:In Press.
19. Vale PR, Losordo DW, Tkebuchava T, Chen D, Milliken CE, Isner JM. Catheter-based myocardial gene transfer utilizing nonfluoroscopic electromechanical left ventricular mapping. J Am Coll Cardiol 1999; 34:246-54.

20. Kornowski R, Leon MB, Fuchs S, et al. Electromagnetic guidance for catheter-based transendocardial injection: a platform for intramyocardial angiogenesis therapy. Results in normal and ischemic porcine models. J Am Coll Cardiol 2000; 35:1031-9.
21. Smits P, Van Langenhove G, Schaar M, et al. Efficiency of percutaneous intramyocardial injections using a nonfluoroscopic 3-D mapping based catheter system. Cardiovasc Res 2000:In Press.
22. Vale P, Tkebuchava T, Milliken C, Chen D, Symes J, Isner J. Percutaneous electromechanical mapping demonstrates efficacy of pVGL1(VEGF2) in an animal model of chronic myocardial ischemia (Abstract). Circulation 1999; 100:I-22.
23. Fuchs S, Hendel R, Kuntz R, et al. Left ventricular electromechanical mapping reflects resting myocardial perfusion and viability: comparative analysis with SPECT radionuclide myocardial imaging (Abstract). Circulation 1999; 100:I-22.
24. Kornowski R, Fuchs S, Leon MB, Epstein SE. Delivery strategies to achieve therapeutic myocardial angiogenesis. Circulation 2000; 101:454-8.

Summary and Conclusions

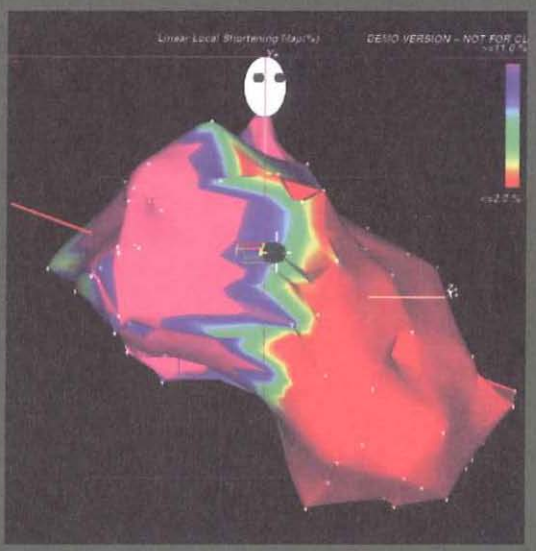

Nonfluoroscopic electromechanical real-time on-line 3-dimensional mapping using the NOGA™ device broadens our insights into left ventricular functioning.

The thesis exists of three parts. In the first part of this thesis (chapters 1-5) we compare the NOGA™ technique to established methods for evaluating left ventricular function and wall motion. In Chapter 1 we explain the technique and its physical basis. In chapter 2 we evaluate NOGA™ maps in patients without previous myocardial infarction and with normal ventricles on contrast angiogram. In this study, we show that although unipolar and bipolar voltages and linear local shortening tend to be consistently high throughout the left ventricle in subjects with normal left ventricular functioning on angiography, basal septal and posterior areas of the left ventricle do have lower values, probably due to the presence of the mitral annulus. Also, large variations in absolute values of unipolar voltages and linear local shortening can be appreciated amongst patients and amongst segments in the same patients. In chapter 3 we compare volumetric measurements and left ventricular ejection fraction assessment as provided by the NOGA™ system to the standard in-cathlab technique to produce these measurements, i.e. contrast ventriculography. We show that – although the data provided by the NOGA™ system are strongly correlated to those given by computerized ventriculography- the absolute values of both volumetric measurements and ejection fraction calculation are clinically not interchangeable. Differences up to 30-40% in left ventricular ejection fraction are shown. Although the new software version (NOGA™ 4.0) reduces these differences (chapter 2), they still mount up to ± 20%. In chapter 4 we compare the linear local shortening function as assessed with NOGA™ as a function of regional wall motion with echocardiographic data in a subset of patients with severe coronary artery disease and subsequently decreased left ventricular function. We show that NOGA™ accurately assesses regional wall motion and that myocardial segments with declining regional function also show decrease in unipolar voltages. In chapter 5 we compare linear local shortening data to dedicated area analyses using computerized left ventricular angiography. The per-segment analysis shows that linear local shortening data are significantly correlated with area data derived from the ventriculogram. Moreover, it becomes clear that linear local shortening is a reliable parameter for the evaluation of regional left ventricular wall motion.

In the second part of the thesis (chapters 6-8), we evaluate the ability of the NOGA™ system to detect viable myocardium. In chapter 6 we analyze electromechanical properties of target myocardial regions of occluded coronary arteries. We show that the electromechanical properties of previously injured myocardial segments are significantly correlated with the quality of collateral coronary artery supply to the target region of occluded coronary arteries. This further underscores the potential of nonfluoroscopic mapping in assessing myocardial viability. In chapter 7 we demonstrate that – as compared to radionuclide scanning techniques- NOGA™ is able to differentiate myocardial scar tissue from regions that are still viable. A value of unipolar voltage of 6.5 mV is set forward as the optimal cut-off to suggest viability in a defined region. In chapter 8 we compare data on myocardial viability assessment derived from dobutamine stress echocardiography with NOGA™ mapping data of the same patient cohort. We conclude that NOGA™ can predict recovery in injured myocardium when compared to dobutamine stress echocardiography. In this study we demonstrate that both linear local shortening as well as unipolar voltages have added value in the assessment of viability. Receiver operator characteristics analyses revealed 8.2 mV for unipolar voltage and 7.2% for linear local

shortening as the optimal cut-off values to distinguish non-viable from potentially recoverable myocardium.

In the third part of the thesis (chapters 9-12), we evaluate novel techniques that use nonfluoroscopic 3-dimensional electromechanical mapping as a vehicle to deliver respective therapies. In chapter 9 we provide an overview of currently available information on the evolution of left ventricular function after direct myocardial revascularization. We show that –although in the acute phase following therapy, a decrease in LV function can be seen - in the long-term, recovery is to be expected. We also provide data from our center showing that direct myocardial revascularization may cause acute deterioration of the left ventricular function and that hence one has to refrain from performing myocardial laser revascularization in patients with a low baseline left ventricular ejection fraction. In chapter 10 we provide the first follow-up NOGA™ images 6 months after direct myocardial revascularization. Improvement in regional functioning of the treated areas is clearly shown. In chapter 11 we describe the efficiency of percutaneous intramyocardial injections of albumin and albumin microcolloidal particles in animals as possible future carriers of drugs for direct myocardial injection therapy. We show that the technique of intramyocardial injection is feasible, that the efficiency is around 25%, and that small proteins as albumin have a shorter retention time than small particles such as the microcolloids we used. In chapter 12 we reflect on the possible future diagnostic and therapeutic applications of the NOGA™ system.

In conclusion, the NOGA™ system is a safe and feasible technique that, when in experienced hands, provides reliable data on the electromechanical functioning of the myocardium. The system is able to detect viability and may therefore be of added value in the assessment of revascularization strategies. Also, the technique is a strong vehicle to deliver specific intramyocardial therapeutic measures, through its ability to accurately define regions of interest in 3-dimensional space.

Some questions however remain unanswered: What is the cause of discordance in volumetric measurements when compared to other techniques? Is linear local shortening- a parameter that describes tangential movement of myocardial points during contraction- really comparable to the well-accepted myocardial thickening or perpendicular wall motion? Is the accuracy of viability detection high enough to warrant the adaptation of this system as the golden standard? Is there need for an expensive, not easy-to-master, technique for in-cathlab detection of viability and/or ischemia, when other validated, accepted, less expensive, easily applicable techniques already have proven their value? Does direct myocardial revascularization, for which the system seems to be an ideal guiding tool, really improve the clinical status of the patient? Is local gene application, again, for which this system seems an optimal platform, going to be applied clinically? Forthcoming multicenter randomized trials will answer some of these issues.

Samenvatting en Conclusies

Zonder röntgendoorlichting in real-time 3-dimensioneel evalueren van de electromechanische eigenschappen van het hart verbreedt onze kijk op het functioneren van de linker kamer.

Deze thesis is opgebouwd uit drie delen. In het eerste deel van de thesis (hoofdstukken 1-5) vergelijken we gegevens gegenereerd door het NOGA™ systeem met technieken erkend voor de evaluatie van de linker kamerfunktie en de lokale beweging van de hartspier. In hoofdstuk 1 beschrijven we de techniek en zijn fysische basis. In hoofdstuk 2 evalueren we de NOGA™ techniek bij patienten zonder voorgeschiedenis van myocardschade en bij wie gedurende contrast ventriculografie een normale linker ventrikel contractiliteit is gezien. In deze studie tonen we dat, hoewel uni-(UPV) en bipolaire voltages (BPV) en local linear shortening (LLS) meestal hoge waarden tonen in deze normale linker ventrikels, er duidelijk lagere waarden worden gezien in het posteroseptale gebied, waarschijnlijk ten gevolge van de aanwezigheid van de mitralisklepring aldaar. Ook zien we grote variaties in absolute waarden voor zowel UPV als LLS. In hoofdstuk 3 vergelijken we volume-metingen en ejectiefraktiebepalingen gemeten met de NOGA™ techniek met de meest gebruikte standaardtechniek, namelijk contrast ventriculografie. We tonen aan dat, hoewel beide meettechnieken sterk gerelateerde resultaten geven, de technieken klinisch niet uitwisselbaar zijn, m.a.w. dat men niet de ene keer de ejectiefraktie kan meten met de ene techniek, en de volgende keer met de andere. Verschillen tot 30-40% worden gezien. Ondanks dat de nieuw ontwikkelde software deze verschillen kleiner maakt, bedragen ze toch nog om en bij de 20% (Hoofdstuk 2) In hoofdstuk 4 vergelijken we de LLS als een graadmeter voor lokale wandbeweging van het myocard met echocardiografie gegevens in een subgroep van patiënten met ernstig coronairlijden en –als gevolg daarvan- verminderde linker ventrikel funktie. We tonen aan dat NOGA™ op betrouwbare wijze de regionale wandbeweging van het hart visualiseert, en dat naargelang de regionale funktie vermindert, ook de absolute waarden van de unipolaire voltages afnemen. In hoofdstuk 5 vergelijken we LLS gegevens met precieze bepalingen van de regionale funktie van het myocard d.m.v. gecomputerizeerde linker ventrikel angiografie. De segment-per-segment analyse toont dat LLS data significant gecorreleerd zijn aan de gegevens betreffende de lokale wandbeweging afgeleid uit het contrast ventriculogram.Hieruit wordt duidelijk dat LLS een goede parameter is om de locoregionale myocardfunktie te bestuderen.

In het tweede deel van de thesis (hoofdstukken 6-8), evalueren we de mogelijkheid om aan de hand van de NOGA™ techniek viabel myocard te onderscheiden. In hoofdstuk 6 analyzeren we de electromechanische eigenschappen van hartspierweefsel dat voorheen door een nu geoccludeerde coronaire arterie werd bevloeid. We tonen aan dat de electromechanische eigenschappen, en –hieruit afgeleid- mogelijks de hoeveelheid leefbaar hartspierweefsel bepaald worden door de kwaliteit van de collateraalcirculatie die deze regio's van bloed voorzien. Dit onderlijnt de mogelijkheid om viabiliteit te detecteren aan de hand van de NOGA™ techniek. In hoofdstuk 7 tonen we dat – in vergelijking met nucleaire viabiliteitsdetectie- NOGA™ de mogelijkheid biedt een onderscheid te maken tussen littekenweefsel in de hartspier en weefsel dat reversibele schade heeft opgelopen. Een absolute waarde van het unipolaire voltage van 6.5 mV wordt vooropgesteld als de optimale cut-off waarde om viabel van niet-viabel weefsel te onderscheiden. In hoofdstuk 8 vergelijken we data afkomstig van dobutamine stress echocardiografie met gegevens afkomstig van NOGA™ om hartspierviabiliteit te

definiëren. We tonen dat NOGA™ accuraat reversibiliteit van hartspierbeschadiging kan voorspellen, wanneer vergeleken met dobutamine stress echo. In deze studie zien we dat zowel LLS als UPV additieve waarde hebben in het vaststellen van reversibiliteit van de hartspierbeschadiging. Receiver operator characteristics (ROC) analyses tonen 8.2 mV voor UPV en 7.2% voor LLS als de optimale cut-off waarden om non-viabel (of littekcn) weefsel te onderscheiden van potentieel recupereerbaar myocard.
In het derde deel van de thesis (hoofdstukken 9-12), bekijken we innoverende therapieën die NOGA™ gebruiken als vehikel om respectievelijke therapeutische akties te ondernemen. Zo is er in hoofdstuk 9 een overzicht van de informatie beschikbaar over de effekten van percutane direct revascularisatie van het myocard (DMR) d.m.v. laser. Wij beschrijven dat –ondanks dat een acute deterioratie van de myocardfunktie kan optreden onmiddellijk na de laserbehandeling- er een trend tot volledig herstel lijkt te zijn . Onze data leren dat gezien de mogelijkheid van acute deterioratie van de linker ventrikel funktie, DMR bij patiënten met een zeer slechte linker kamerfunktie weloverwogen dient te gebeuren. In hoofdstuk 10 zien we het verbeteren van de regionale myocardfunktie 6 maand na een DMR procedure. In hoofdstuk 11 beschrijven we de efficiëntie van percutane intramyocardiale injecties van albumine en albumine microcolloidale deeltjes in proefdieren; deze substanties fungeren als mogelijke toekomstige vehikels voor het transporteren van geneesmiddelen of andere faktoren voor directe intramyocardiale injectie. We tonen aan dat de techniek haalbaar is, dat de efficiëntie om en bij de 25% bedraagt en dat kleinere molecules zoals albumine een kortere retentietijd hebben dan grotere, zoals de microcolloidale partikels. In hoofdstuk 12 reflecteren we over de mogelijke toekomstige diagnostische en therapeutische implicaties van het NOGA™ systeem.
Samengevat, is NOGA™ een veilige techniek die, in geoefende handen, betrouwbare gegevens verschaft over het electromechanisch funktioneren van de linker hartkamer. Aan de hand van deze techniek is het mogelijk viabiliteit te detecteren, hetgeen van belang kan zijn bij het bepalen van de revascularisatiestrategie bij de individuele patiënt. Ook is de techniek een belangrijk vehikel om specifieke intramyocardiale therapieën ter plaatse te brengen, door de mogelijkheid van het systeem interessegebieden in een 3-dimensionele ruimte te definiëren en weer te geven.
Een aantal vragen blijft echter onbeantwoord: wat is de reden van de discordantie in de volume-bepalingen wanneer deze techniek met andere wordt vergeleken? Is LLS – een parameter die een tangentiële beweging van de cathetertip tijdens hartspiercontractie beschrijft- wel te vergelijken met geaccepteerde evaluaties van locoregionale wandbeweging zoals hartspierverdikking of perpendiculaire beweging van de cathetertip t.o.v. de wand? Is de accuraatheid van de viabiliteitsdetectie groot genoeg om dit systeem als de nieuwe gouden standaard aan te nemen? Wat is de noodzaak voor een dure, niet makkelijk te beheersen in-cathlab techniek voor de detectie van viabiliteit wanneer andere, geaccepteerde, eenvoudige, goedkope technieken reeds hun waarde bewezen hebben? Verbetert DMR, waarvoor dit systeem de ideale methode lijkt, daadwerkelijk de klinische status van de patiënt? Zal lokale gentherapie, waarvoor deze techniek –opnieuw- een ideaal platform is, gebruikt worden in de klinische praktijk? Een aantal geplande studies zal proberen op minstens een deel van deze vragen een antwoord te geven.

Acknowledgements

First of all, I want to thank the Rotterdam Police force, for having made my stay in Rotterdam as an unforgettable joy. For instance the time when my car was stolen, and I went to the Rotterdam Police Department to report the theft. The officer on call said « there's really no use, your car is probably crossing the East German border as we speak ». After insisting, he- very against his will- finally wrote a report. My repeated calls one, two, three and four days following the event were consistently answered with : « do you think we have nothing better to do than to search for your car ? » Later I learned that indeed they had something better to do: writing tickets. Big was my surprise when 14 days later I got a letter from –yes- the Rotterdam Police Department, stating that my car had been towed away as a preventive measure to keep it from being stolen, as somebody had crashed the window to steal the car stereo. The letter said that I could pick up the car at the Rotterdam Police Parking Lot. Even bigger was my amazement when I arrived there, and they told me I had to pay 800 Dutch guilders for « parking costs ». I thought that they had checked the oil and cleaned it for that price, but nothing was less true. I then learned that shouting and being impolite does actually help: I didn't pay for the parking costs. One week later, I was driving back to my apartment around 12 p.m., when I noticed a Police car following me. I checked my lights, slowed down to 40 km/h, locked my seat belt and drove on. Suddenly, after turning a few corners, I was blocked by two Police cars in front, and two in the back. The Policemen howled through a megaphone « LEAVE THE CAR AND PUT YOUR HANDS WHERE WE CAN SEE THEM ». I sat in amazement for a few seconds, when they repeated their demands, angrier than the first time. I did what I was ordered, and immediately two cops jumped upon me, and handcuffed me firmly. When I urged them to be careful, because I suffered from recurrent shoulder luxations, they looked at me as if I was coming from another planet, not understanding one word of what I said. When I told them that I was willing to write it down, but that it was useless because they probably didn't learn how to read anyway, they got really angry. By the time I asked them what would be the fine to call them a..holes (censored), they fulminated, pulled me by the hair, and threw me into the police car. When I said they were making a big mistake, they laughed, saying everybody they arrested said the same thing. When I asked them what I was arrested for, they shouted "YOU STOLE THIS CAR". They didn't understand my outburst of laughter. The two hours I spend at the office downtown were unforgettable. I knew I could curse them as much as I wanted, because they were bound to discover their mistake sooner or later. And –I must admit- it's great to be able to say to policemen things like "where did they find such a bunch of dumb people?","do you guys actually get paid for this?" or "why do they forbid IQ's above 100 in the Rotterdam Police Department?", when you know you're not going to be punished for it. Anyway, after two hours they realized their huge mistake, blamed it all on the computer system, and overloaded me with excuses. Thanks again guys for letting me have so much fun.

Also, many thanks to the several Parking supervisors to provide me with lots of parking tickets, and helping me in trying to abide by the Parking Rules. You've really been a great help. Forgive me for not paying you, but it's difficult to find a medical company to fund this.

Many thanks also to the people of "Stadswonen", one of the housing companies in Rotterdam. I really appreciated your help when I came into your office naked, only covered with a far too small towel, asking for a spare key as I locked myself out of my room when going to the shower, and you people told me to wait in line as everybody else. It is true

that being naked does not free you from having to wait for your turn. I also understand your refusal to give me the spare key because I couldn't pay the 25 guilders bail.
Unfortunately I do not know the people who helped me in getting rid of four car stereos. Therefore, I cannot thank them personally. I really apologize for always locking the doors, so that each time you had to crush the windows. To the guy who stole my laptop in the Hospital while I was on the toilet: thank you very much, you really helped me in rewriting part of this thesis (former versions are on your hard disk, call me if you want the latest version).
I sincerely apologize for being such a bad customer to all the nice people who –almost on a daily basis- offered me a variety of goods to buy, like cocaine, heroin, crack, marihuana, and so on.
My infinite thanks also goes to Mrs. E.S., former manager at the Thoraxcenter for saying no to every request I made (I'm not mentioning difficult things like a parking card or so). You've initiated my self-sustaining policy.

The first time I met Patrick W Serruys in the Thoraxcenter, I caught him on a bad day. Something went wrong somewhere, and the first person he caught sight of, was me. "YOU'RE NOT GOING TO GET ANYWHERE SIPPING COFFEE" he shouted. It was the last coffee I drank in the hall next to his office. Later, I came to realize the importance of the man for the Thoraxcenter and for Interventional Cardiology in general. His tremendous working force, his immense and seemingly unlimited knowledge, his insights into the world of interventional cardiology but also into the people surrounding him, his ubiquitous availability, his willingness to take risks, his dedication and professionalism, are a true example to whomever wants to succeed in the international academic medical field, or a warning to whomever wants a life. Which brings us to his wife, Danielle. It really needs a great woman to build the foundation under a big man. As most of the time he forgets to tell her this himself, he pays the fellows to write it in their theses. Additional funding by PW Serruys is herewith gratefully acknowledged. I would however like to thank Danielle personally for the food, the wine, the coffee, and for telling me the score in Turkey-Belgium during EURO 2000, when Patrick confiscated me while I actually wanted to see the game.
I would like to express my thanks to the members of the promotion committee for their time and support: Prof. Victor Legrand, Prof. Shlomo Ben-Haim, Prof. Ad Bogers, Dr. Geert Gijsbers, Dr. Pieter Smits, Prof. Ivan de Scheerder and Prof. Luc Jordaens.
Thanks also to Pim de Feyter, another stronghold of the Thoraxcenter, for telling me that having a life outside of the cathlab is also nice. Sorry Pim for not listening enough to you. Thanks to David Foley for cleaning up my mess and for the beers, to Benno Rensing and Jeroen Vos for always being in a good mood (don't ever loose that!), to Marcel van den Brand, Wim van der Giessen and Stephane Carlier, to Jaap Hamburger and Pieter Smits for helping me in writing parts of this thesis. My infinite gratitude also goes to Anja, for not being on my back all of the time; thanks for helping me with a lot of stuff, sometimes until late at night! Thanks to Claudia, for always offering me tea ("Would you like something? Coffee? Tea? Me?"), to Titia for always being ready to arrange things, to Arita and Willeke for taking care of some financial and secretarial concerns, and to Helen for keeping the place together.
The Thoraxcenter would not be what it is today without the outstanding group of

technicians and nurses that it's lucky to have. It's mostly through their friendliness and support that one forgets the hardships and suffers from a long stay abroad. I had a closer relationship with Jurgen Ligthart, who taught me the basis of IVUS, and Emile Onderwater, who initiated me in NOGA.
I want to express my thanks to the people of the Hemodynamics Department on the 23th floor of the Erasmus University. Especially Rob Krams, Yolanda Wentzell and Cees Slager initiated me into the interesting world of coronary blood velocity patterns, wall thickness and shear stress in the coronary artery, and were always willing to lend me their ears. Thanks also to Serge Trines, for helping me in all the pig stuff. I hope you have a great career.
In every situation in life, one tends to seek comfort in the group of people that suffers the same fate. In my case, this was the group of the fellows. The first one I met was Michael Kutryk (Winnipeg, Canada). I really hope that his stay was rewarding and that he finally got out of the dark and found a life in Canada. Manel Sabate (Barcelona, Spain) was an example to all of us: hard working, friendly, integer, honest and always ready to help. Mariano Albertal (Buenos Aires, Argentina) was my roommate in room H556. He initiated me in some of the most forcefull Hispanic statements as "no me inches las pelotas", "la concha de tu madre" and "la puta que te parillo". I do not want to translate these. Thanks my friend, for being there, and for making me laugh (although you didn't have to eat that 1 kg steak to show me that you're a real man). Pedro Serrano (Zaragoza, Spain) revealed me the possibilities of imaging and taught me all about statistics. Thanks Pedro, have a good life and congratulations for both the wedding and your appointment. Pavel Cervinca (Prague, Tsjechia) convinced me that a lot of beautiful women reside in his country. Invite me again next year, Pavel! Marco "Circulation 99" Costa (Sao Paulo, Brazil) showed me that pushability is not a property solely of metallic stents. I really enjoyed our Belgian team beating the "world selection" in soccer on the beach in California. Congratulations also to you, to Erica and to the real father of the kid that's going to join your little family soon (I don't know where you would have found the time to do it). Ken Kozuma (Tokyo, Japan) is a wonderful guy never to tired to help you with anything. Evelyn Regar (Munchen, Germany)(I knów a woman has to be twice as good as a man to accomplish the same), Attila Thury (Budapest, Hungary)(Don't get to shear stressed with all the situations) and Nestor (Medellin, Columbia)(I don't know who you'll have to talk to at 2 a.m. when I'm gone) are the latest acquisitions into this strong team.
One day last February I met Leonidas Diamantopoulos. Until this time, I though that scientists that cover the whole spectrum, no longer existed. But when he showed me his skills in interventional cardiology, revealed me his correspondence with the space engineers from NASA, when he made the people at the electronics shop blush because he knew more about the equipment in their store than they did, when he made the software specialists ashamed because he showed them their mistakes, when he bought brake pads to fix his car or a radar to build his own sailing boat, when he constructed – out of the blue, without any help- a very high-tech machine that is able to show intracoronary wall temperature in 3-D mode (I can continue for a few pages), I knew this man was either insane, or a genius. Later I learned he was both (Leo, this is a joke). Together with him, Jean-Sébastien Vincent, another very dear friend of mine, and John Yianni, my best friend on the web, we founded a company. Leo was delighted when I bought him a sign for his door, saying "Thermocore Diagnostics NV. Dedicated to reduce the impact of coronary heart disease". With the blessing of Patrick Serruys we're going to try to prove our point,

namely that by discovering and treating hot unstable plaques, we might save lives.
I'm deeply indebted to the people of the Middelheim Hospital, Antwerp, Belgium, where I took my first steps in interventional cardiology. They also funded my stay in Rotterdam. A very big thanks to Frank ("Money is a technical detail. Of course I will fund your stay in Rotterdam" – thanks Frank for being a friend next to a boss) Van den Branden, Paul ("Maybe we should send another abstract, Glenn") Van den Heuvel, Paul (Hebt ge daar nu nog altijd niks bijgeleerd in Rotterdam, Van Langenhove? Kom, 'k zal 't U nog één keer tonen") Vermeersch, Dirk ("Kunnen we de bouw nog een keer inspecteren") Stockman, Carl ("A diagnostic coronary angiogram should be performed in 8 minutes. A PTCA in 9") Convens, Stefan (My partner in "crime") Verheye, Eddy Vanagt en Marc Vaerenberg. Also the nurses (especially Carine, Jan, Koen, Linda, Jos and Inge helped me in performing some of the NOGA procedures) and the secretaries (Yes Sabine, I still love you) deserve my deepest appreciation.
Of course, a thesis cannot be written –as a life cannot be lived- without social support. Thanks to the people who make part of the juice in my life: André en Marianne for always believing in me, to Frank and Aitza for filling Sunday evening gaps, to Filip and Pascale for always being ready to lend a hand, to Tim and Patricia for being there, to Sandra and Filip for being real friends –even after the small bump in the road, to Olivier and Dominique, to Peter and Anne-Rose, to Ann and Didier, to Inge and Dirk, to Karim and Isabelle, to Nico and Ann, to Geoffroy and Nadine, to Peter and Inge, to Dirk and Annick, to Fanny and Filip, to Veerle and Bart, to Jean and Karen, to Paul and Sophie, to Annick, to Patrick, to John Paul II, together making my life complete, and also to Johan –I hope he has a good life, wherever he is: may it be as bright as the night we spend together in that sleazy bar with amazing women downtown Havana, Cuba, back in 1993, where we wanted to be like Hemingway in his young days. Thanks to Jos, Nelly, Jeanine, Charles, Inge, Bobonne. Thanks to the friends I have forgotten today, but will remember tomorrow.
Thanks to the Biosense team Geert Gijsbers, Peter Goemaere, Frank Verdonck, Gilad Glick, Céline Martin, Rita Peeters and Dirk Beelen, for their belief in this project.
Of course there is the inevitable Marianne Eicholtz whose honesty, sympathy, humor, endurance and beers made this project happen.
Thanks to Ivo, Dirk (C), Bart, Christina, Dirk (J), Roel for being friends even without the commercial aspect.
I do not know where to start to thank my parents. Although they were somewhat sceptic in the beginning, they provided me with all the opportunities necessary to pursue my goals. The love, support and understanding of my mother and my father have helped me reaching my goals. Unfortunately, during the final preparation of this thesis, my father died suddenly. Only heaven knows how much I will miss his love, his generosity, his smile, his giving me some money "to buy a beer" when I had to leave for yet another meeting, his wine, his everything. You're in my heart, wherever I go from here. Thanks papa, this one's for you.
There are those 3 –in a little while 4- diamonds in my life, Zoé, Sam, and Ben, who I hope will forgive me one day for not having spend enough time with them over the last 3 years.
It's useless to ask forgiveness to my wife, for having supported my absence, my working during holidays, my inevitable laptop wherever we went, my bad moods when I was tired, my coming home at 5 a.m. when I promised it would be 9 p.m., and so on. Sorry baby, but better times are ahead (Yes, I know I've told you that before). The only thing I can promise you is my eternal flame.

Generous sponsoring by Guidant, Medtronic, Lilly, Boston Scientific, Thermocore Diagnostics, Flux Medical Systems, VZW CardioMid, AstraZeneca, Jomed, Bolton Medical and especially Cordis and Biosense-Webster is gratefully acknowledged.

Curriculum Vitae and List of Publications

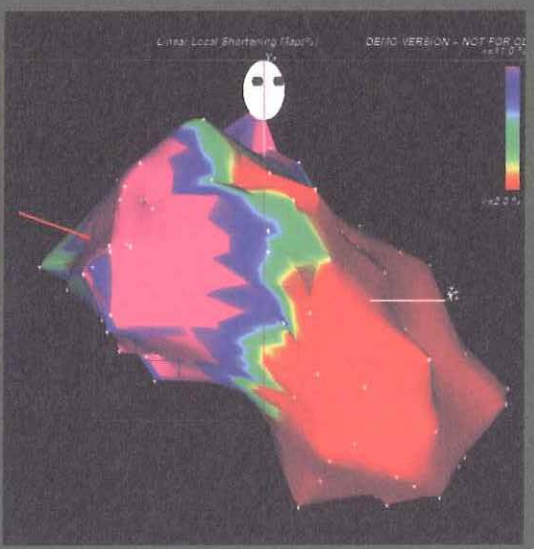

Curriculum Vitae

Personalia:
Family Name: Van Langenhove
First names: Glenn Joseph Jan
Born: Ghent, Belgium, 26th november 1965
1 brother, Tim, Civil Engineer, Major in the Belgian Army
Married to Anne Lippens, Dentist
3 children, Zoé (4 yrs), Samuel (3 yrs) and Ben (1 yr)

SCHOOL:
Koninklijk Atheneum Gent II, Latin-Mathematics

MEDICAL SCHOOL:
Doctor in Medicine, State University of Ghent, graduated in 1991 magnum cum laude
Dentistry license, State University of Ghent graduated in 1992 cum laude

ROTATION IN INTERNAL MEDICINE/INTENSIVE CARE/CARDIOLOGY:
University Hospital Antwerp, Belgium;
1/10/1992- 30/9/1996

TRAINING IN INTERVENTIONAL CARDIOLOGY:
Middelheim Hospital Antwerp, Belgium;
Head: Dr.F.Van den Branden.
1/10/1996- 30/10/1999.

CURRENT POSITION:
Fellow in Interventional Cardiology, Thoraxcenter Rotterdam, The Netherlands,
Director Prof. Patrick W. Serruys.
Part-time Interventional Cardiologist Middelheim Hospital Antwerp
Director of the NOGA corelab (ANCORE™, the Antwerp Core Lab) for the "DINO" study
Director of Flux Medical Systems BVBA and Thermocore Diagnostics NV

OTHER ACHIEVEMENTS:

*Reviewer for "Catheterization and Cardiovascular Diagnosis", an international publication with a 1997 Citation Index of 1,329.

*Special license in Electrocardiography, State University of Ghent, Belgium, Prof.D.Clement, 1991

*1997 laureate of the "Belgian Young Cardiologists Award", under auspices of the "Belgische Vereniging voor Cardiologie" (BVC).

*Special Degree in "Medical Statistics", State University of Antwerp, 1996

*License in Radiation, Protection and Radiotherapeutic Management, State University of Ghent, Belgium, 1997

*Founder and Director of "ANCORE" (Antwerp Core Lab), a recently founded corelab, focusing on nonfluoroscopic mapping analysis. ANCORE functions as the corelab for the forthcoming DINO-study (Biosense-Webster, a Johnson & Johnson company)

*Operator (together with Dr D Stockman) for live case sessions on nonfluoroscopic electromechanical mapping transmitted from the Middelheim Hospital to the Biosense training center in Hamburg, Germany)

*Operator in Animal Lab (Temperature and flow-dividing stent implantation protocols at the Laboratory of Experimental Cardiology, Erasmus University Rotterdam, The Netherlands, together with Rob Krams, MD, PhD)

*Co-founder of Flux Medical Systems BVBA and Thermocore Diagnostics NV

Full papers in NON peer-reviewed journals:

Convens C, Stockman D, Van Langenhove G, Van den Branden F; Dynamische veranderingen in een acuut coronair syndroom. Tijdschrift voor Cardiologie, Vol 7, 1995, 2 : 48-51

Oei F, Van Langenhove G, Vanagt E, Stockman D, Van den Branden F; Tachycardie-Cardiomyopathie. Tijdschrift voor Cardiologie, Vol 10, 1998, 4 : pp 49-51

Van Langenhove G, Ligthart J, Albertal M, Costa MA, Kay IP, Sabate M, Serruys PW. Intracoronair Ultrageluid. Een blik op verleden, heden en toekomst. Deel 1: Een inleiding in techniek, indikaties en complicaties van intravascular ultrasound (IVUS). Bloedvaten, Hart en Longen 1999; 4 (7): 209-214

Van Langenhove G, Ligthart J, Albertal M, Costa MA, Kay IP, Sabate M, Serruys PW. Intracoronair Ultrageluid. Een blik op verleden, heden en toekomst. Deel 2: IVUS bij coronaire interventies. Bloedvaten, Hart en Longen 1999; 4 (8): 232-236

Oei F, Van Langenhove G, Vanagt E, Stockman D, Van den Branden F; Cardiomyopathie tachycardique. Journal de Cardiologie. Vol 10, 1998, 4 : 49-51

Van Langenhove G, Carlier SG. Coronary imaging and interventions into the next millennium. Highlights from the 5th Thoraxcenter Stent Course. Cardiovascular Interventions Online, 1999; 3:17-18.

Van Langenhove G. American College of Cardiology 49th Annual Scientific Meeting Report. Stent, 2000, 3; 1:30-31.

Serrano P, Casasnovas JA, Sabate M, Ligthart JMR, Van Langenhove G, Cervinca P, Costa MA, Peleato A, Fereira Monteiro IJ. Ecografia intracoronaria : utilidad en la practica clinica y nuevas perspectivas. Revista de la Sociedad Aragonesa de Cardiologia 1999, 5 (2) : 37-43

Serrano P, Sabate M, Costa MA, Van Langenhove G, Casasnovas JA, Peleato A, Fereira Monteiro IJ, Serruys PW. Aplicaciones diagnosticas a las arterias coronarias de las nuevas tecnologias de la imagen (New diagnostic techniques for coronary artery imaging). Archivos de la Facultad de Medicina de Zaragoza 1999, 39(2) : 55-59.

Full papers in peer-reviewed journals:

Kay IP, Sabate M, Van Langenhove G, Costa MA, Wardeh AJ, Gijzel AL, Deshpande NV, Carlier SG, Coen VL, Levendag PC, Van der Giessen W, de Feyter PJ, Serruys PW. Outcome from balloon induced coronary artery dissection after intracoronary beta radiation. Heart. 2000;83:332-7.

Van Langenhove G, Van den Heuvel P, Van den Branden F. Main stem subocclusion shortly after aortic valve replacement. Heart. 1998;80:530-1.

Van Langenhove G, Convens C, Seynaeve P, Van den Heuvel P, Van den Branden F, Stockman D, Vermeersch P. Intralobar pulmonary sequestration supplied by the right coronary artery. Catheter Cardiovasc Interv. 1999;47:218-20.

Van Langenhove G, Vermeersch P, Kay IP, Vaerenberg M, Heuten H, Stockman D, Convens C, Albertal M, Vrints C, Van Den Branden F, Van Den Heuvel P. Elective Wiktor GX Stenting for Symptomatic Stenosis in Old Aortocoronary Saphenous Vein Bypass Grafts: The Antwerp Experience. J Invasive Cardiol. 1999;11:274-280.

Van Langenhove G, Vermeersch P, Serrano P, Kutryk MJ, Stockman D, Convens C, Van den Branden F, Vanagt E, Albertal M, Van den Heuvel P. Saphenous vein graft disease

treated with the Wiktor Hepamed stent: procedural outcome, in-hospital complications and six-month angiographic follow-up. Can J Cardiol. 2000;16:473-80.

Van Langenhove G, Serrano P, Serruys PW. Vineberg revisited. Long-term survival more than two decades after direct surgical myocardial revascularization [letter] [see comments]. Int J Cardiol. 2000;73:83-6.

Van Langenhove G, Daelemans R, Zachee P, Lins RL. Pasteurella multocida as a Rare Cause of Peritonitis in Peritoneal Dialysis. Nephron. 2000;85:283-284.

Van Langenhove G, Regar E, Foley DP, Hamburger JN, Smits PC, Albertal M, Serruys PW. Acute changes of global and regional left ventricular function immediately after direct myocardial revascularization. Semin Interv Cardiol. 2000;5:103-106.

Van Langenhove G, Hamburger JN, Smits PC, Foley DP, Albertal M, Serruys PW. Improved regional wall motion 6 months after direct myocardial revascularization (DMR) with the NOGA DMR system. Circulation 2000;102(7):e44-5

Carlier SG, Van Langenhove G, Lupotti F, Serruys PW. Coronary flow reserve versus geometric measurements of coronary dimensions: advantages and limitations of the functional stenosis assessment. J Interv Cardiol 1999; 12 (6):411-424

Van Langenhove G, Vermeersch P, Serruys PW. Thrombus overlying the main stem crista: a three-dimensional reconstruction. Heart 2000, In Press.

Van Langenhove G, Hamburger JN, Smits PC, Onderwater E, Albertal M, Serruys PW. Comparison of mechanical properties of the left ventricle in patients with severe coronary artery disease by nonfluoroscopic mapping versus two-dimensional echocardiograms. American Journal of Cardiology, In Press (November 2000).

Van Langenhove G, Hamburger JN, Smits PC, Onderwater E, Albertal M, Serruys PW. Evaluation of left ventricular volumes and ejection fraction using a nonfluoroscopic endoventricular three-dimensional mapping technique. A comparison with contrast ventriculography. American Heart Journal 2000, 140;4:596-602.

Van Langenhove G, Daelemans R, Zachee P, Lins RL. Omeprazole-induced acute tubulo-interstitial nephritis. Gastroenterology 2000, In Press.

Van Langenhove G, Hamburger JN, Smits PC, Onderwater E, Albertal M, Roelandt JRTC, Jordaens L, Serruys PW. Nonfluoroscopic real-time endoventricular 3-D mapping. A novel catheter-based technique to assess mechanical and electrical properties of the heart. The Thoraxcenter Journal 1999;11/4:97-103

Van Langenhove G, Wentzel JJ, Krams R, Slager CJ, Hamburger JN, Serruys PW. Helical velocity patterns in a human coronary artery. Circulation 2000;102: e22-e24

Kay IP, Sabate M, Van Langenhove G, Heyndrickx GR, Grollier G, Suryapranata H, Hoorntje JC, van der Giessen WJ, Morel MA, Disco C, Serruys PW. The ESSEX (European Scimed Stent Experience) Study. Catheterization and Cardiovascular Interventions 2000 50(4):419-25

Van Langenhove G, Vermeersch P, Convens C, Stockman D, Vaerenberg M, Vanagt E, Van den Heuvel P, Van den Branden F. Elektieve of aansluitende angioplastiek? Tijdschrift voor Geneeskunde, 2000, 56 (13):995-1001

Albertal M, Van Langenhove G, Carlier SG, Serruys PW. Angiographic and Clinical Outcome of Mild to Moderate Nonocclusive Unstented Coronary Artery Dissection and the Influence on Coronary Flow Reserve. American Journal of Cardiology 2000, 15; 86(4):375-378

Van Langenhove G, Hamburger JN, Diamantopoulos L, Smits PC, Onderwater E, Serruys PW. Validation of the local shortening function as assessed by nonfluoroscopic electromechanical mapping: a comparison with computerized left ventricular angiography. Int J Cardiology, 2000, In Press.

Van Langenhove G, Kozuma K, Serruys PW. Nonfluoroscopic Endoventricular Electromechanical Three-dimensional Mapping. Current Status and Future Perspectives. Japan Circ J, 2000, In Press

Van Langenhove G, Diamantopoulos L, Regar E, Foley DP, Tuin J, Carlier SG, Serruys PW. Distal embolization: a threat to the coronary artery? Circulation 2000;102:e95.

Thury A, Van Langenhove G, Wardeh AJ, Foley DP, Serruys PW. Further insights into coronary debulking : the EUROCARE-trial of directional atherectomy and the PACT trial of pullback atherectomy. Semin Interv Cardiol. 2000, In Press.

Thury A, Van Langenhove G, Carlier S, Albertal M, Krams R, Slager CJ, Serruys PW. A higher average shear stress is paradoxically predictive of restenosis after balloon angioplasty in human coronary arteries. Eur Heart J 2000, In Press.

Book Chapters

Van Langenhove G, Kutryk MJB, Serruys PW. Pharmacological adjuncts to coronary stenting: the case of stent thrombosis. In: Handbook of coronary stents 3rd edition, 2000, 355-402. Editors Serruys PW, Kutryk MJB. London, Martin Dunitz, 2000.

Van Langenhove G, Verheye S, Foley DP. Ablative techniques. In: Coronary Interventions, a Pragmatic approach. In Press. Editors Serruys PW, Colombo A, Leon MB, Kutryk MJB. London, Martin Dunitz, 2000, In Press.

Verheye S, Van Langenhove G. Calcified and fibrotic lesions. In: Coronary Interventions, a Pragmatic approach. In Press. Editors Serruys PW, Colombo A, Leon MB, Kutryk MJB. London, Martin Dunitz, 2000, In Press.

Van Langenhove G, Serruys PW. Intracoronary thrombus or severe spiral dissection? Make your choice, but make it fast! In: 100 Cases in Interventional Cardiology. In Press. Edited by Martin T Rothman. London, Martin Dunitz, 2000, In Press.

ABSTRACTS:

Van Langenhove G, C.Convens, P.Van den Heuvel, D.Stockman, F.Van den Branden, P.Vermeersch ; Aortic Coarctation : A rare and unexpected cause of Secondary Arterial Hypertension in the Elderly. The Journal of Invasive Cardiology, Vol.9, Suppl.C, 1997: 67C

Van Langenhove G, P.Van den Heuvel, A.Vervaet, P.Vermeersch, M.Vaerenberg, H.Heuten, F.Oei , D.Stockman, C.Vrints, F.Van den Branden ; Is Elective Wiktor Stenting After Angioplasty Versus Elective angioplasty Alone the Treatment of Choice for Severely Diseased Symptomatic Old Aortocoronary Saphenous Vein Bypass Grafts ? The Journal of Invasive Cardiology, Vol.9, Suppl.C, 1997: 56C

Van Langenhove G, P.Vermeersch, F.Oei, A.Vervaet, M.Vaerenberg, H.Heuten, D.Stockman, C.Convens, C.Vrints, F.Van den Branden, P.Van den Heuvel ; Elective stenting in old saphenous vein bypass grafts : the Antwerp experience with 38 cases. Acta Cardiologica, Vol.LII, 1997, 6, pp 8-10

Van Langenhove G, P.Vermeersch, C.Convens, M.Vaerenberg, E.Vanagt, D.Stockman, P.Van den Heuvel, F.Van den Branden ; Economics of Angioplasty : a Comparison Between Elective and On-line Angioplasty in 3500 Consecutive PTCA's. Acta Cardiologica. Vol.LII, 1997, 6, 545-46.

Van Langenhove G, M.Vaerenberg, F.Oei, F.van den Branden ; Estimating Left Ventricular Ejection Fraction : a Comparison Between Acoustic Quantification, Contrast Ventriculography and Radionuclide Ejection Fraction. Acta Cardiologica. Vol.LII, 1997, 6, 570.

Van Langenhove G, P.Vermeersch, C.Convens, M.Vaerenberg, E.Vanagt, D.Stockman, P.Van den Heuvel, F.Van den Branden ; A Comparison between elective and on-line angioplasty in 3478 Consecutive PTCA's. A retrospective analysis. Acta Cardiologica. Vol.LII, 1997, 6, 581-82.

Van Langenhove G, S.G.Carlier, M.Albertal, E.Boersma, P.W.Serruys. A higher average shear stress is paradoxically predictive of restenosis and/or MACE after balloon angioplasty in human coronary arteries. Eur Heart J 1999, 507

S.G.Carlier, Van Langenhove G, F.Mastik, R.Krams, E.I.Cespedes, A.F.W.van der Steen, N.Bom, P.W.Serruys. In vivo assessment of instantaneous wall shear stress with the IVUS flow method. Eur Heart J 1999, 406

Albertal M, Van Langenhove G, Serrano P, Carlier SG, Costa MA, Serruys PW. DEBATE II: analysis of the flow velocity profile in the stented and non-stented, optimal and suboptimal groups. Eur Heart J 1999, 372

Van Langenhove G, Hamburger JN, Smits PC, Serrano P, Onderwater E, Albertal M, Slager C, Serruys PW. Evaluation of left ventricular function using a non-fluoroscopic endoventricular three-dimensional mapping technique. A comparison with contrast ventriculography. Acta Cardiologica 2000;55:2

Albertal M, Van Langenhove G, Serrano P, Carlier SG, Serruys PW. Predictors of coronary flow reserve before and after balloon angioplasty. Eur Heart J 1999, 490.

Knook AHM, Wardeh AJ, Van Langenhove G, van der Giessen WJ, Sabate M, Serruys PW. B-energy to prevent restenosis. The Rotterdam contribution to the BERT 1.5 trial. 1 year follow-up. Acta Cardiologica 2000;55:7

Ph.Vandenbergh, P.Vermeersch, M.Vaerenberg, P.Van den Heuvel, C.Convens, D.Stockman, Van Langenhove G, F.Van den Branden. Preliminary results of transcatheter closure of patent foramen ovale and ostium secundum atrial septal defect using the Cardioseal™ occlusion device. Acta Cardiologica 2000;55:10-11

P.Van den Heuvel, Van Langenhove G, P.Vermeersch, C.Convens, D.Stockman, M.Vaerenberg, F.Van den Branden. Wiktor Heparin-coated stents for saphenous vein graft disease: procedural outcome, in-hospital complications and 6 month angiographic follow-up. Acta Cardiologica 2000;55:11

Van Langenhove G, Kay IP, Sabate M, Carlier S, Knook AHM, Wardeh AJ, van der Giessen WJ, Serruys PW. Persisting coronary artery dissection after intracoronary beta-radiation. Acta Cardiologica 2000;55:11-12

Knook AHM, Wardeh AJ, Van Langenhove G, van der Giessen WJ, Sabate M, Serruys PW. The European P-32 dose response trial. The RotterdamContribution. Acta Cardiologica 2000;55:12

Van Langenhove G, Smits PC, Albertal M, Serrano P, Kay IP, Poldermans D, Hamburger JN. NOGA mapping for the detection of viable and ischemic myocardium: a comparison with dobutamine stress echocardiography. Circulation 1999;100(18):I-23

Van Langenhove G, Smits PC, Hamburger JN, Serrano P, Serruys PW. Hibernating myocardium diagnosed with nonfluoroscopic mapping: a comparison with dobutamine stress echocardiography. J Am Coll Cardiol 2000 (feb), 81A

Van Langenhove G, Smits PC, Albertal M, Kay IP, Hamburger JN. NOGA mapping for the detection of viable and ischemic myocardium. A comparison with dobutamine echocardiography. Circulation 1999;100:18:I-23

Kay IP, Sabate M, Costa MA, Wardeh AJ, Ligthart JM, Coen VLMA, Levendag PC, Van Langenhove G, de Feyter PJ. The Edge effect after radioactive and conventional stent implantation. Circulation 1999;100:18:I-222

Van Langenhove G, Smits PC, Serrano P, Kosuma K, Serrano P, Onderwater E, Albertal M, Kay IP, Hamburger JN. Assessment of regional LV wall motion: a comparison between computerized LV angiography and nonfluoroscopic electromechanical mapping. Circulation 1999;100:18:I-725

Albertal M, Carlier SG, Van Langenhove G, Regar E, Thury A, Scianos G, Serruys PW. Value of postprocedural stenotic flow velocity acceleration in the invasive prediction of restenosis after coronary angioplasty Eur Heart J 2000, 21:34

Hagers Y, Van Langenhove G, Vandenbergh P, Van den Heuvel P, Stockman D, Convens C, Vaerenberg M, Verheye S, Van den Branden F, Vermeersch P. Biochemical predictors of events two years after coronary intervention. Eur Heart J 2000, 21:501

Van Langenhove G, Wardeh AJ, Sabate M, Albertal M, Lins M, Knook AHM, R.W.R. Simon1, P.W. Serruys, D.P. Foley. Pullback atherectomy in small coronary arteries. A pilot study. Eur Heart J 2000, 21:645

Van Langenhove G, Hamburger JN, Smits PC, Albertal M, Onderwater E, Wardeh AJ, Knook AHM, Serruys PW. NOGA™ mapping for the assessment of regional left ventricular dysfunction. Eur Heart J 2000, 21:174

Van Langenhove G, Hamburger JN, Smits PC, Albertal M, Wardeh AJ, Knook AHM, Onderwater E, Serruys PW. Nonfluoroscopic electromechanical mapping for the in-cathlab detection of ischaemia: a comparison with dobutamine stress echocardiography. Eur Heart J 2000, 21:175

Van Langenhove G, Hamburger JN, Smits PC, Albertal M, Onderwater E, Wardeh AJ, Knook AHM, Serruys PW. In-cathlab detection of hibernating but recoverable myocardium using nonfluoroscopic electromechanical (NOGA™) mapping: a comparison with dobutamine stress echocardiography. Eur Heart J 2000, 21:174

Albertal M, Carlier SG, Van Langenhove G, Kay IP, Serruys PW. Angiographic and clinical outcome of mild to moderate nonocclusive unstented coronary artery dissection and the influence on coronary flow reserve. Eur Heart J 2000, 21:516

Van Langenhove G, Regar E, Hamburger JN, Smits PC, Serruys PW. Assessment of global and regional left ventricular function before and immediately after percutaneous direct myocardial revascularization. Eur Heart J 2000, 21:288

Diamantopoulos L, Van Langenhove G, Foley DP, De Feyter PJ. Non-Invasive Heating of Implanted Arterial Stents in Vivo: A Novel New Method to Prevent Restenosis. Feasibility and Safety. Circulation 2000, In press

Van Langenhove G, Smits PC, Hamburger JN, Van der Giessen WJ. Assessment of Global and Regional Left Ventricular Function Before and Immediately after Percutaneous Direct Myocardial Revascularization. Circulation 2000, In press

Van Langenhove G, Diamantopoulos L, Hamburger JN, Smits PC, Stockman D, Van Den Heuvel P, Van Den Branden F, Bossi I, Fajadet J, Foley DP. In-Cathlab Diagnosis of Hibernating Myocardium Using NOGATM. A Comparison with Low-Dose Dobutamine Echocardiography. Circulation 2000, In press

ORAL PRESENTATIONS
at National and International Conferences:

Which Coronary Artery Disease Risk Factors Should be Treated. Presented at the « Shared Care Disease Management » Helsinki University Conference, Espoo, Finland, June 7-9, 1996.

Comparative value of 2D-echo-dobutamin and perfusion/metabolism- imaging with SPECT to detect damaged but viable myocardium post-infarction. Presented in Nice, France, February 14-15, 1997, European Society of Cardiology Symposium « Ischaemic myocardial damage : detection by functional and biochemical markers. »

Elective stenting in old saphenous vein bypass grafts : the Antwerp experience with 38 cases. Presented at the 12th Annual Scientific Sessions of the Belgian Working Group on Interventional Cardiology, Brussels, Belgium, December 5th, 1997.

A Comparison between elective and on-line angioplasty in 3478 Consecutive PTCA's. A retrospective analysis. Oral presentation at the 17th Annual Scientific Meeting of the Belgian Society of Cardiology, Brussels, Belgium, February 5-7, 1998.

The Wiktor Heparin Coated Stent for Saphenous Vein Graft Disease. Presentation held at the XIIth Practical Course In Interventional Cardiology, Madrid, Spain, July 8-10, 1998;

Left Ventricular Ejection Fraction measured with Acoustic Quantification: a Comparison with Contrast Ventriculography and Radionuclide Ventriculography. Oral Computer Demo Presentation held at the XXth Congress of the European Society of Cardiology, Vienna, Austria, August 22-26, 1998.

A Comparison Between the Wiktor GX and the Wiktor Hepamed Stent for the Treatment of Saphenous Vein Graft Disease. Oral presentation at the 18th Annual Scientific Meeting of the Belgian Society of Cardiology, Brussels, Belgium, 4-6 Feb 1999. Presentation held on February 4th 1999, at 17h00.

The Wiktor Hepamed stent for saphenous vein graft disease: procedural outcome and in-hospital complications in 49 patients. Oral presentation (category "Young Investigators") held at the 6th joint meeting of the Belgian and Dutch Working Groups on Invasive Cardiology, Maastricht, The Netherlands, 8-9 january 1999. Presentation held on January 8th 1999, at 12h15.

Ischaemic myocardial damage : detection by functional and biochemical markers. Nice, February 14-15, 1997. Symposium organized by the European Heart House.

Aortic Coarctation : A rare and unexpected cause of Secondary Arterial Hypertension in the Elderly. Presented at the 2nd International Meeting on Interventional Cardiology, Jerusalem, Israel, June 30-July 3, 1997.

Is Elective Wiktor Stenting After Angioplasty Versus Elective angioplasty Alone the Treatment of Choice for Severely Diseased Symptomatic Old Aortocoronary Saphenous Vein Bypass Grafts ? Presented at the 2nd International Meeting on Interventional Cardiology, Jerusalem, Israel, June 30-July 3, 1997.

Estimating Left Ventricular Ejection Fraction : a Comparison Between Acoustic Quantification, Contrast Ventriculography and Radionuclide Ejection Fraction. 17th Annual Scientific Meeting of the Belgian Society of Cardiology, Brussels, Belgium, February 5-7, 1998.

Economics, Safety and Feasibility of On-line Angioplasty : a Single Center Comparison Between Elective and On-line PTCA in 2777 Cases. 17th Annual Scientific Meeting of the Belgian Society of Cardiology, Brussels, Belgium, February 5-7, 1998.

A Comparison between elective and ad hoc procedures in 3478 consecutive balloon angioplasties. A retrospective analysis. XXth Congress of the European Society of Cardiology, Vienna, Austria, August 22-26, 1998.

Left ventricular function measured with acoustic quantification. XXth Congress of the European Society of Cardiology, Vienna, Austria, August 22-26, 1998.

The Wiktor Heparin Coated stent in Saphenous Vein Grafts : Procedural Outcome and In-hospital Complications. XII th Practical Course in Interventional Cardiology, Madrid, Spain, July 8-10, 1998.

A Comparison between elective and ad hoc procedures in 3478 consecutive balloon angioplasties. A retrospective analysis. XII th Practical Course in Interventional Cardiology, Madrid, Spain, July 8-10, 1998.

4 French Infinity versus 6 French Super Torque Plus for diagnostic coronary angiography. XII th Practical Course in Interventional Cardiology, Madrid, Spain, July 8-10, 1998.

Techniques for the measurement of the left ventriclar ejection fraction. Joint Meeting of the XIX Congress of the ES NI CVD and the CSDS, August 27-30, 1998, Gent, Belgium

Saphenous Vein Graft Disease treated with the Wiktor Hepamed Stent: Acute Outcome and 6 Month Angiographic Follow-up. 18th Annual Scientific Meeting of the Belgian Society of Cardiology, Brussels, Belgium, February 4-6, 1999

A Comparison Between the Wiktor GX and the Wiktor Hepamed Stent for the Treatment of Saphenous Vein Graft Disease. 18th Annual Scientific Meeting of the Belgian Society of Cardiology, Brussels, Belgium, February 4-6, 1999.

The Wiktor Hepamed Stent for Saphenous Vein Graft Disease : Procedural Outcome and In-hospital Complications in 49 patients. 18th Annual Scientific Meeting of the Belgian Society of Cardiology, Brussels, Belgium, February 4-6, 1999.

A higher average shear stress is paradoxically predictive of restenosis and/or MACE after balloon angioplasty in human coronary arteries. XXIth Congress of the European Society of Cardiology, Barcelona, Spain, August 28 - September 1, 1998.

Persisting coronary artery dissection after intracoronary beta-radiation. 7th joint meeting of the Belgian and Dutch Working Groups on Invasive Cardiology, Brussels, Belgium, December 18-19, 1999.

Evaluation of left ventricular function using a non-fluoroscopic endoventricular three-dimensional mapping technique. A comparison with contrast ventriculography. 7th joint meeting of the Belgian and Dutch Working Groups on Invasive Cardiology, Brussels, Belgium, December 18-19, 1999.

NOGA mapping. Technique and clinical experience. First Cordis symposium in Innovative techniques in Coronary Interventions. Ostend, Belgium, May 15th 2000.

Technique, feasibility and indications of NOGA mapping. 5th Symposium on Interventional Cardiology, Prague, Czech Republic, May 4th, 2000.

NOGA mapping for the detection of viable and ischemic myocardium. A comparison with dobutamine echocardiography. 72th Scientific Sessions of the AHA. Atlanta, Georgia, USA, November 7-10 1999.

Hibernating myocardium diagnosed with nonfluoroscopic mapping: a comparison with dobutamine stress echocardiography. 49th Annual scientic sessions of the American College of Cardiology, Anaheim, California, USA, March 12-15, 2000.